UNIVERSITY OF CALIFORNIA,
IRVINE

Regulation of IL-1α and Its Role in Microbial Keratitis

DISSERTATION

Submitted in partial satisfaction of the requirements
for the degree of

DOCTOR OF PHILOSOPHY

in Biomedical Sciences

by

Bridget Ratitong

Dissertation Committee:
Professor Eric Pearlman, Chair
Assistant Professor Armando Villalta
Assistant Professor Francesco Marangoni
Associate Professor Melissa B. Lodoen

2022

DEDICATION

To

My parents, Khim and Angel

My brother, Asawin

My friends

And

My teachers

“I wish I could give you more

Because that’s what you deserve

While I’m sailing around the world

Please always know

That you are who I call home”

-Courtney Peppernell

TABLE OF CONTENTS

LIST OF FIGURES

ACKNOWLEDGMENTS

I would like to express the deepest appreciation to my advisor, Dr. Eric Pearlman, who has been like a science dad to me. Without his guidance and mentorship, this dissertation would not have been possible. I am the scientist I am today thanks to the training I received from you.

I would like to thank my committee members, Armando Villalta, Francesco Marangoni, and Melissa Lodoen, who have all supported me through this journey with advice and thoughtful discussions. You all inspire me.

Thank you to the Pearlman Lab members and our collaborators for providing support throughout the years, especially to Michaela E. Marshall who has worked closely with me on all my projects and Serena Abbondante who helped tremendously with performing my experiments. Martin Minns, thank you for training me when I first joined the lab and being a great friend, colleague, and trivia buddy.

I am grateful to my friends and family for the emotional support that has helped carry me through my graduate career. You've helped me persevere and for that I am forever thankful.

Lastly, I acknowledge Elsevier and The American Association of Immunology for permission to include my publications in this thesis as well as my co-authors.

VITA

EDUCATION

University of California, Irvine — Irvine, CA

Ph.D., Biomedical Sciences, CGPA 4.000 — 2017-2022

University of California, San Diego — San Diego, CA

B.S., Molecular Biology, CGPA 3.784 — 2011- 2015

RESEARCH

Pearlman Lab, University of California Irvine — Irvine, CA

Ph.D. Candidate, Advisor: Eric Pearlman — 2018-present

Croft Lab, La Jolla Institute of Allergy and Immunology — La Jolla, CA

Research Technician I, Advisor: Michael Croft — 2016-2017

Takeda Pharmaceutical, San Diego — San Diego, CA

Analytical Chemistry Intern, Advisor: Lu Zheng — 2013-2015

PUBLICATIONS

1. **Ratitong, B.**, Marshall, M. & Pearlman, E. β-Glucan-stimulated neutrophil secretion of IL-1α is independent of GSDMD and mediated through extracellular vesicles. *Cell Reports* **35**, 109139 (2021).
2. **Ratitong, B.** & Pearlman, E. Pathogenic *Aspergillus* and *Fusarium* as important causes of blinding corneal infections — the role of neutrophils in fungal killing, tissue damage and cytokine production. *Current Opinion in Microbiology* **63**, 195–203 (2021).

3. **Ratitong, B.**, Marshall, M. E., Dragan, M. A., Anunciado, C. M., Abbondante, S. & Pearlman, E. Differential Roles for IL-1a and IL-1b in *Pseudomonas aeruginosa* infection of the cornea. Manuscript in review, *Journal of Immunology* (2022).

AWARDS AND HONORS

- NIH NRSA F31 fellowship (funded by the National Eye Institute), 2020-2023
- ARCS Foundation, Orange County chapter, Scholar award, 2020-2022
- AAI Young Investigator Award at Immunology Seminar, 3rd place *Best Poster presentation,* 2020
- UCI School of Medicine Grad Day *Best Elevator Talk award,* 2020
- NIH T32 Immunology training grant, 2019-2020
- AAI Young Investigator Award at UCI Immunology Seminar for *Best oral presentation,* 2019
- AAI Young Investigator Award at Immunology LA for *Best oral presentation,* 2019
- UC Irvine Graduate Dean's Recruitment Fellowship Award, 2017
- Provost's Honor for academic achievement at UC San Diego, 2011-2015
- Cum Laude Honor for academic achievement at UC San Diego, 2015

ABSTRACT OF THE DISSERTATION

Regulation of IL-1α and Its Role in Microbial Keratitis

By

Bridget Ratitong

Doctor of Philosophy in Biomedical Sciences

University of California, Irvine, 2022

Professor Eric Pearlman, Chair

Microbial infection of the cornea is one of the leading causes of preventable blindness world-wide. The infection results in corneal opacity, inflammation, and intense pain that could lead to permanent blindness if left untreated. Treatment involves antimicrobial agents followed by corticosteroids to suppress inflammation. However, there is a need for a more targeted treatment to regulate inflammation as steroids are non-specific.

In both human patients and our murine model of bacterial and fungal keratitis, neutrophils are the predominant infiltrating cell-type in the cornea comprising up to 90% of recruited cells. Neutrophils are essential for bacterial killing and acts as an important source of proinflammatory cytokines during microbial keratitis. Depletion of neutrophils leads to tremendously impaired bacterial clearance and decreased cytokine levels in the cornea. We previously reported that the proinflammatory cytokines IL-1α and IL-1β are highly upregulated in both human and mice during microbial keratitis. IL-1β is necessary for neutrophil recruitment to the corneas and subsequently protection from the infection. However, whether there is a role for IL-1α and what role that may be is unclear. *This*

thesis explores the production and regulation of IL-1α, and what role it is playing in the cornea during infection.

We found that while neutrophils are the predominant source of IL-1β in the cornea, both neutrophils and monocytes contribute to IL-1α production which peaked at 24hpi. To examine whether there is a role for IL-1α in the response to bacterial infection of the cornea, we compared WT*, Il1a-/-, Il1b-/-,* and *Il1a-/-Il1b-/-* mice infected with *P. aeruginosa*. In accordance with our previous studies, *Il1b-/-* and DKO mice were unable to control the infection due to delayed neutrophil and monocyte recruitment to the cornea. On the contrary, *Il1a-/-* mice had the opposite effect—showing enhanced bacteria killing compared to WT mice despite no differences in neutrophil recruitment. We found no differences in neutrophil effector functions between WT and *Il1a-/-* neutrophils. However, RNA sequencing revealed *Il1a-/-* neutrophils had a more proinflammatory transcriptomic profile than WT neutrophils with elevations in C1q expression. These findings reveal a novel role for IL-1α, that is distinct from IL-1β, in regulating the response to *P. aeruginosa* infection in the cornea.

Further, we examined the regulation of IL-1α secretion compared to IL-1β in macrophages and neutrophils. The mechanism for IL-1β secretion is well characterized in macrophages where it is tightly regulated in a two-step process mediated by inflammasomes and GSDMD. We found that IL-1α secretion by macrophages is also mediated by GSDMD, but not NLRP3 inflammasome. However, IL-1α secretion by neutrophils is independent of both NLRP3 and GSDMD in response to stimulation with β-glucan. Secretion of IL-1α by neutrophils is also independent of cell death. Instead, we found that IL-1α secretion is mediated by extracellular vesicle release.

In conclusion, we described a novel role for IL-1α that is distinct from IL-1β during bacterial infection of the corneas—where IL-1α is detrimental and IL-1β is protective. We also found that IL-1α is important for monocyte recruitment to the cornea whereas IL-1β is essential for neutrophil recruitment. Our finding adds to the increasing evidence showing non-redundant roles for the two cytokines despite sharing the same receptor, IL-1R1. Further, we found differential regulation for IL-1α and IL-1β secretion by neutrophils. While IL-1β is dependent on NLRP3 and GSDMD for secretion, IL-1α release is mediated by extracellular vesicles. Together, these studies improve our understanding of the inflammatory response during microbial keratitis and identify potential targets for therapeutics.

CHAPTER1:

INTRODUCTION

The cornea

The cornea is the exposed, transparent outer surface of the eye that acts as a barrier protecting ocular tissue. It is structurally composed of five layers: corneal epithelium, Bowman's layer, corneal stroma, Descemet's membrane, and corneal endothelium (1, **Figure 1.1**). The corneal epithelium layer is stratified with multiple layers of non-keratinized corneal epithelial cells forming tight junctions and acting as a physical barrier to prevent pathogens from entering the corneal stroma (2). New epithelial cells derives from stem cells in the limbus and can displace existing cells rapidly both centripetally and superficially (1, 3). The basal layer of corneal epithelial cells is anchored to the Bowman's layer which is an acellular layer consisting of collagen fibrils. The corneal stroma lies between Bowman's layer and Descemet's membrane. It is the thickest layer of the cornea and consists of dense connective tissues of collagenous lamellae with keratocytes in between. The layering and arrangement of collagen fibrils in the lamellae helps maintain transparency.

Descemet's membrane is a thin layer posterior to the stroma that is rich in glycoproteins, laminin, and collagen and precedes the endothelium layer. The corneal endothelium is a made up of a thin layer of endothelial cells separating the cornea from the anterior chamber. They play a crucial role in fluid transport and are responsible for maintenance of corneal hydration which is an important factor affecting cornea transparency. Cornea transparency is also dependent on the diameter and spacing of collagen fibers in the stroma. Further, to maintain transparency, the cornea is avascular and has few resident immune cells—making it an immune-privileged tissue (1, 4).

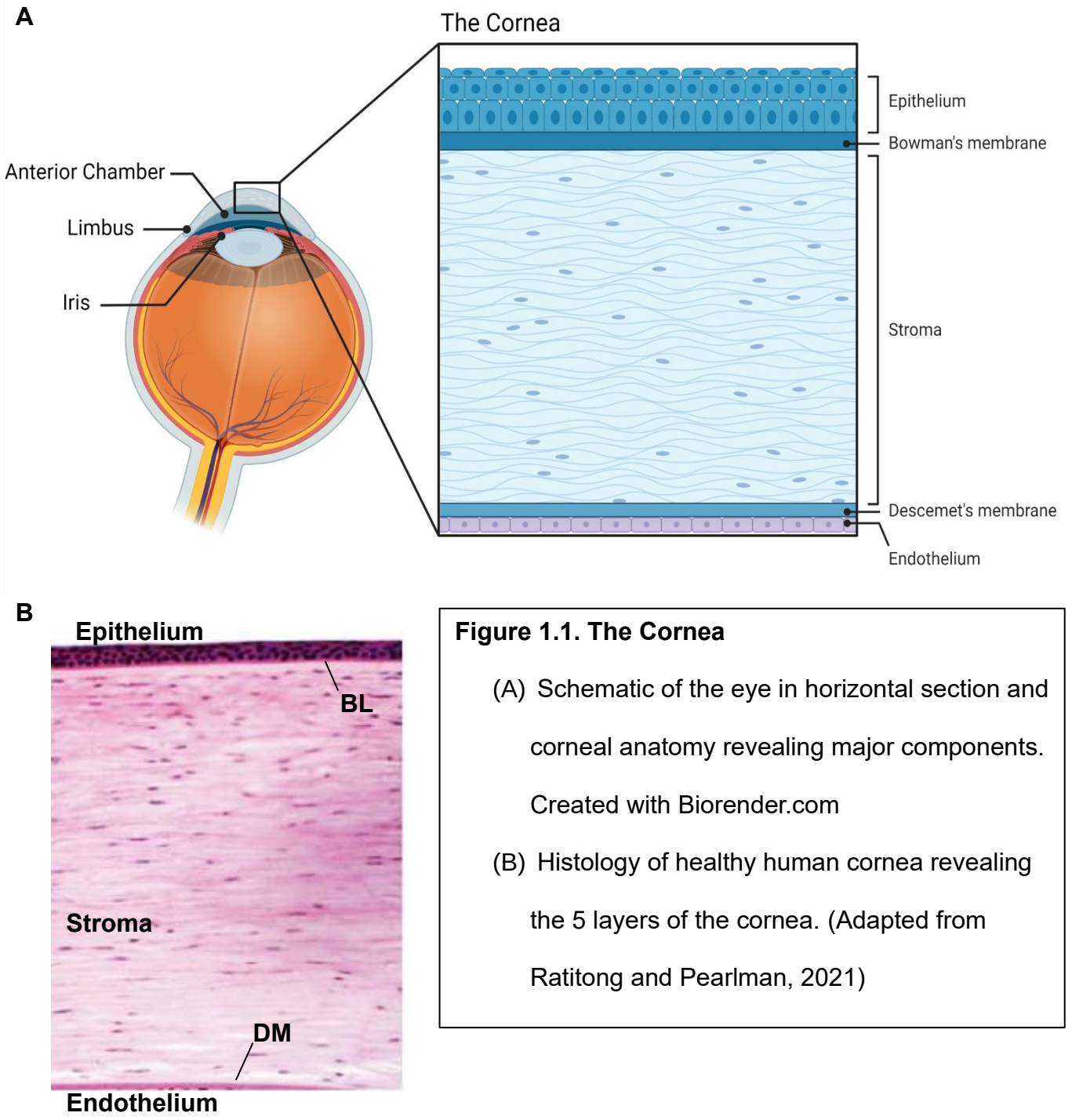

Figure 1.1. The Cornea

(A) Schematic of the eye in horizontal section and corneal anatomy revealing major components. Created with Biorender.com

(B) Histology of healthy human cornea revealing the 5 layers of the cornea. (Adapted from Ratitong and Pearlman, 2021)

Microbial Keratitis

The tight junctions formed by corneal epithelial cells as well as tear film protects the ocular tissue from infections. However, ocular trauma or contact lens use are important risk factors that allow opportunistic pathogens to cause an infection and subsequently a blinding disease called microbial keratitis (5, 6).

Fungal keratitis

Fungal infections of the cornea (keratitis) came to the attention of the public in the United States, Britain and Europe in 2005, when a lens care product failed to control the growth of the environmental mold *Fusarium* on contact lenses and lens cases, leading to an outbreak of painful and sight-threatening corneal infections in contact lens wearers (7). Although the outbreak ended after the product was removed from the market, *Fusarium* and *Aspergillus* species remain important causes of fungal keratitis in industrialized countries, especially in hotter and more humid regions. *Candida* species can also cause corneal infections, but these are relatively rare and occur mostly as a consequence of contamination of donor corneas used for transplantation, or following ocular surgery (8–10). In contrast to industrialized countries, it is in developing countries where fungal keratitis has the greatest medical and socioeconomic impact (11). Of an estimated 1 million cases occurring annually worldwide, >80% are in developing countries, leading to a call to the World Health Organization to designate microbial keratitis as a neglected tropical disease in order to obtain more resources for managing

Adapted and Reprinted from Current Opinion in Microbiology, Vol 63, Ratitong and Pearlman, ***Pathogenic* Aspergillus *and* Fusarium *as important causes of blinding corneal infections — the role of neutrophils in fungal killing, tissue damage and cytokine production****, Pg 195-203, Copyright (2021), with permission from Elsevier*

this disease (12, 13). Corneal infections are initiated following trauma to the corneal epithelium, especially by plant material containing fungal spores; hence, the incidence of fungal keratitis is higher in agricultural regions and during harvest seasons when there is an increased likelihood of ocular trauma from airborne plant material. Fungal keratitis is most prevalent in tropical and subtropical climates, with the highest rates in Asia and Africa (14). Studies in India and China reported that most culture-positive cases of microbial keratitis were of fungal rather than bacterial etiology, and that Aspergillus and Fusarium species, specifically *Aspergillus fumigatus* and *Aspergillus flavus*, and *Fusarium oxysporum* and *Fusarium solani*, were the most common causes of corneal infections (15–17).

The host response to fungal keratitis involves rapid influx of infiltrating innate immune cells with neutrophils comprising of 80-90% of total cellular infiltrate and <10% of cells being monocytes (18, 19). While neutrophil effector functions such as secretion of proteases from neutrophil granules or reactive oxygen species production are necessary for controlling the infection, they also result in tissue damage and corneal opacification that could lead to permanent blindness if left untreated.

Treatment for fungal keratitis generally begins with topical antifungal, followed by corticosteroids to suppress inflammation (20). Natamycin is the first-line antifungal medication, and the only one approved by the Food and Drug Administration (FDA) for fungal keratitis (21). However, natamycin has low water solubility and is limited in corneal penetration. Further, corticosteroid is a non-specific anti-inflammatory treatment, and incomplete clearance of fungi before administration of corticosteroids results in rapid hyphal growth in the absence of an immune response. Therefore, there

is a need for a more targeted treatment for fungal keratitis that balances fungal killing with limiting tissue damage.

Bacterial keratitis

Bacteria is the most common cause for infectious keratitis in Europe, North America, South America, and Australia (22). Much like fungal keratitis, opportunistic bacteria such as *S. aureus*, *P. aeruginosa*, and *Streptococci spp.* can gain access to the cornea following ocular trauma or contact lens usage (23); however, bacteria replicate much more rapidly compared to fungi and can cause more severe disease leading to perforated corneas.

Pseudomonas aeruginosa is a gram-negative bacteria that is the most common cause of infectious keratitis associated with contact lens usage (24). *P. aeruginosa* infection is associated with worse prognosis than other bacteria and often presents clinical features such as corneal epithelial defect and irregular infiltration beneath the epithelium that resembles a ring formation and could result in corneal perforation (25, 26). One of the key virulence factors for *P. aeruginosa* is their type III secretion system (T3SS). The T3SS is a macromolecular complex that forms a needle-like structure injecting bacterial effector proteins into host cells to interfere with the host response (27). *P. aeruginosa* expression of T3SS correlates with morbidity and mortality in patients with bacteremia (28, 29). Similarly, mutations in the T3SS complex or the effector proteins decrease disease severity and increase the rate of bacterial clearance (30, 31).

P. aeruginosa T3SS targets neutrophils, macrophages, endothelial, and epithelial cells to increase their survival while inhibiting host antimicrobial functions and inducing

death of the host cells (31–34). The secreted effector proteins include ExoS, ExoT, ExoY, and ExoU (35). However, most strains of *P. aeruginosa* express *exoS* and *exoU* in a mutually exclusive manner (36). The strain used in our experiments described in this thesis is PAO1 which has ExoT, ExoY, and ExoS.

Initial recognition of *P. aeruginosa* in the cornea is through TLR4 and TLR5 on resident macrophages that produce the chemokines necessary for neutrophil and monocyte recruitment (37). Similar to fungal keratitis, 90% of the cellular infiltrate in response to infection comprise of neutrophils and <10% monocytes (26). This phenotype is recapitulated in murine models of *P. aeruginosa* keratitis used in this thesis (37, 38). Recruitment of neutrophils is necessary for controlling infection and preventing dissemination (38). Neutrophil effector functions used to clear the infection will be later discussed in this chapter.

The Innate Immune System

The mammalian immune system comprises of two arms: innate immunity and adaptive immunity. While the adaptive immune system (lymphoid cells) requires antigen presentation to mount a highly specific response to antigens and form memory cells, the innate immune system (myeloid cells) recognizes broader patterns and danger signals (39). Neutrophils, monocytes, and macrophages are innate immune cells from the myeloid lineage that rapidly mobilize in response to inflammatory signals and pathogens—these cells will be further discussed in this chapter (**Figure 1.2**).

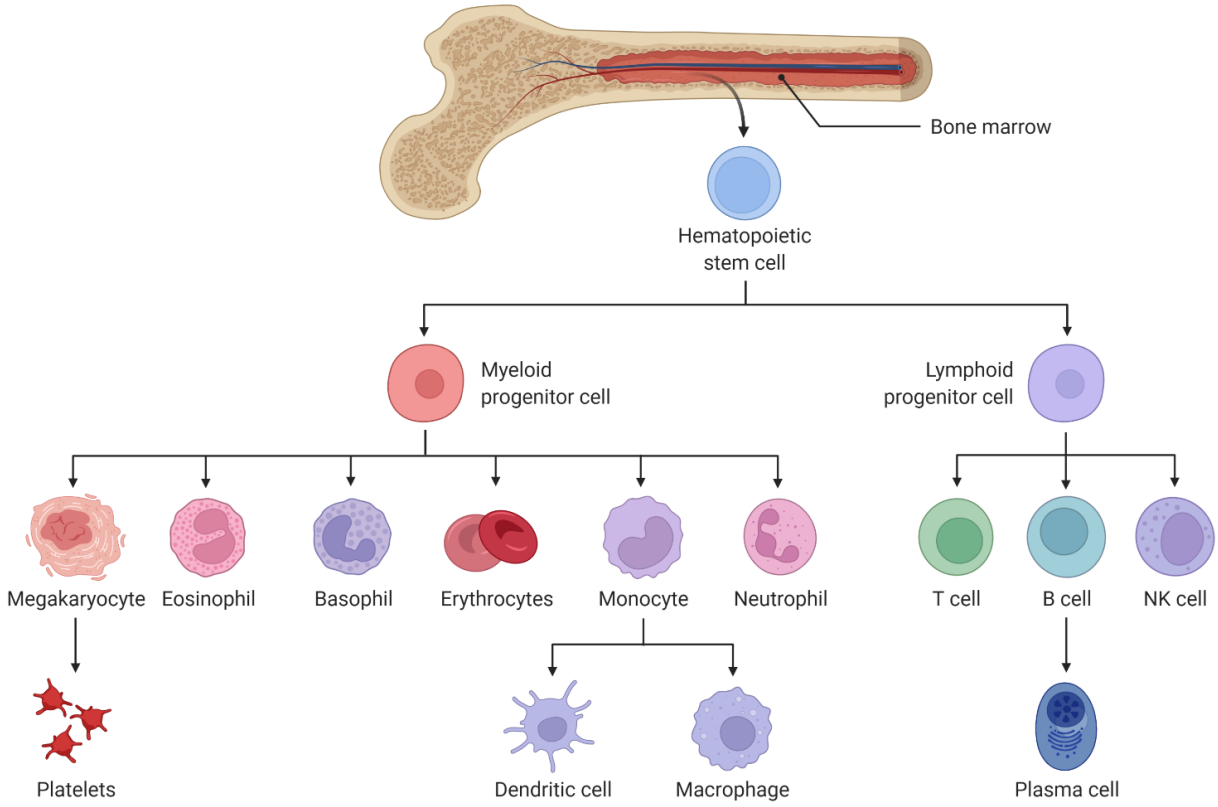

Figure 1.2. Hematopoietic cells

Myeloid and lymphoid cells originate from hematopoietic cells in the bone marrow and differentiates into effector cells. Created with Biorender.com

Pattern Recognition Receptor (PRR)

Innate immune cells are able to recognize pathogen-associated molecular patterns and danger signals rapidly through pattern recognition receptors (40). They do not express antigen-specific receptors like lymphoid cells. PRR signaling leads to non-specific inflammatory responses to aid clearance of infection. There are multiple families of PRRs; toll-like receptors (TLRs) are the most extensively studied class of PRRs (41).

TLR4 recognizes lipopolysaccharides (LPS) and is important for protection against bacterial keratitis (37, 42). TLR4, TLR2, and TLR6 are also important for protection in fungal keratitis (43–45) as well as the C-type lectin receptor (CLR), Dectin-1, that recognizes fungal cell-wall component, β-glucan (46, 47). Signaling through PRRs lead to activation and nuclear translocation of the transcription factor NF-κB which further results in proinflammatory cytokine expression (48). This process is essential for signal amplification and recruitment of immune cells necessary for clearing the infection (37, 48, 49).

Further, the cytosolic nod-like receptors (NLRs) are also essential for inflammatory mechanisms involved in infectious keratitis. NLRs, specifically the pyrin domain-containing subfamily, can oligomerize and form large, multi-protein complexes called inflammasomes (50). The NLRP3 inflammasome is most widely studied and will be further discussed later in chapter 3 in the context of IL-1β processing.

Cellular infiltration in infected corneas

The cornea is an immuno-privileged tissue. To maintain transparency, it is avascular and has few resident immune cells. However, the limbus and periphery of the cornea acts as a portal for immune cell infiltration and is rich in capillaries and lymphatic

vessels (51). Langerhans cells and macrophages comprise the majority of tissue-resident cells residing in the basal layer of corneal limbal epithelium and distributed around the limbal vessels, respectively (52). In response to an infection, these tissue-resident cells are likely the initiators of local inflammation that recruit the main effector cells: neutrophils and inflammatory monocytes. Both fungal keratitis and bacterial keratitis are characterized by a large influx of neutrophils. In patients, 90% of infiltrating cells are neutrophils. Similarly, in our murine model of infectious keratitis approximately 80% of CD45+ cells are neutrophils (**Figure 1.3**). In addition to neutrophils,

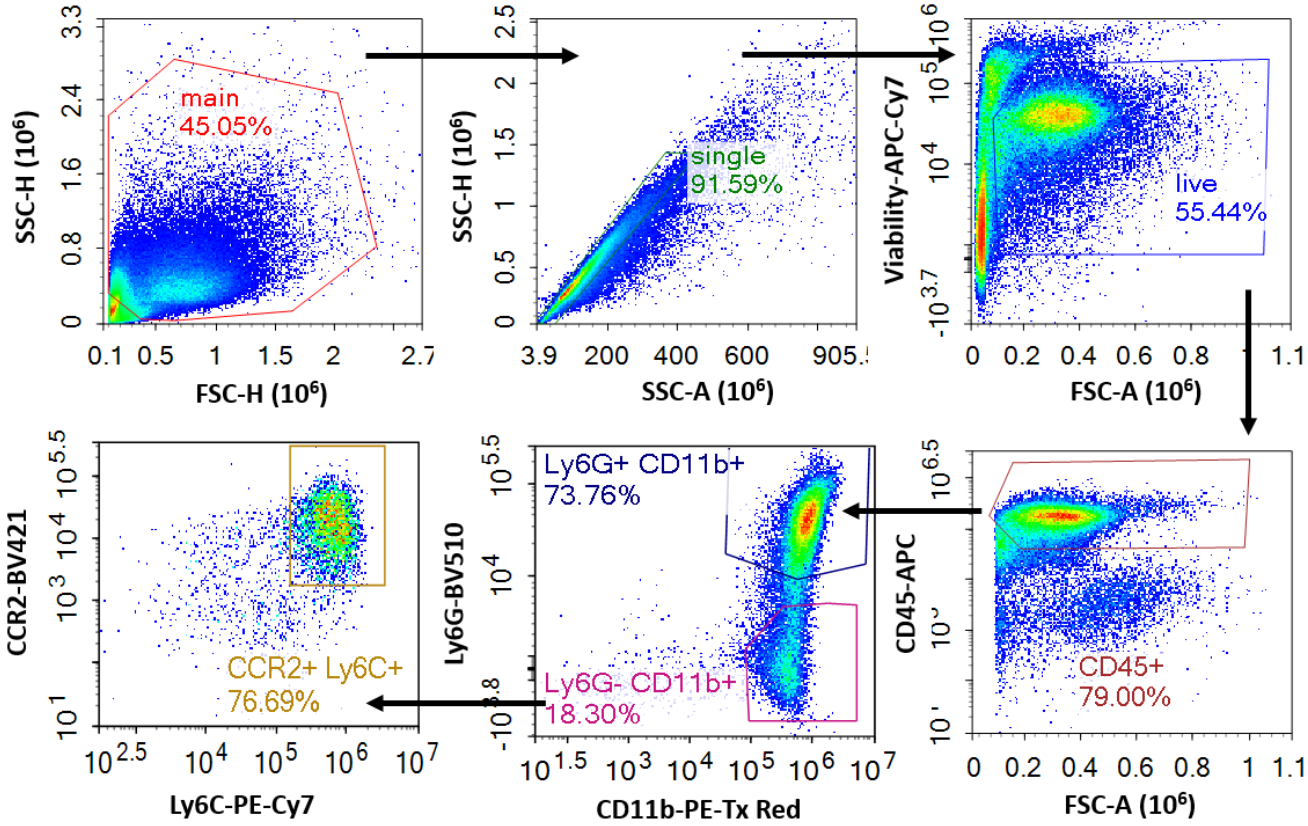

Figure 1.3. Cellular infiltration during bacterial keratitis.

Representative flow cytometry plot of cells from digested corneas of mice infected with *Pseudomonas aeruginosa* at 24hpi. Neutrophils are gated on Ly6G+ CD11b+ and monocytes are Ly6G- CCR2+ Ly6C+

approximately 20% of infiltrating cells are classical monocytes (CCR2+ Ly6C^{hi} in mice, CD14++ CD16- in human) at 24 hours-post infection (hpi, **Figure 1.3**).

Monocytes are mononuclear cells that can differentiate into macrophages and dendritic cells in the tissue (53); however, at the early time points (24- and 48-hpi) of our infection model, they have not differentiated into F4/80+ macrophages. Monocytes originate in the bone marrow and migrate into circulation where they have an average turnover of approximately 24 hours (54). These cells are highly dynamic and are divided into three main subsets with distinct roles: classical, patrolling, and non-classical monocytes (55, 56). Classical monocytes are the most prevalent. The chemokines CCL2 and CCL17 binds to the CCR2 receptor on classical monocytes to mediate their recruitment into inflamed or infected tissues (57).

Classical monocytes are pro-inflammatory and their effector functions include cytokine production, nitric oxide (NO) production, and phagocytosis (53). Monocytes also can repopulate macrophages in some tissues (58). *In vivo*, both detrimental and protective roles have been described for monocytes during *Cryptococcus neoformans* and *Candida albicans* infection, respectively (59–61). Further, monocytes are critical for early control of *Listeria monocytogenes* infection in the spleen and liver as CCR2-deficient mice have worsen infection (62, 63). However, the role of monocytes during infection of the cornea is unclear. Our studies will examine monocytes and their role in the cornea to be further discussed in Chapter 4.

Neutrophils

Neutrophils, also known as polymorphonuclear (PMN) cells, are highly proinflammatory granulocytes that are most abundant in circulation. Large numbers of neutrophils (estimated 10^{11} cells) are produced in the bone marrow daily, and enter the circulation where they migrate into tissues (64, 65). Under homeostatic conditions, neutrophils can be found in the bone marrow, spleen, liver, and lung where they patrol and act as first responders to infection (66, 67). Further, emerging evidence shows immunoregulatory roles for neutrophils in these tissues (68). Neutrophils are relatively short-lived cells that are cleared from the tissue by macrophages or return to the bone marrow for clearance, (65, 69). However, their longevity can be extended during inflammation (70).

Recruitment

A pool of neutrophils is stored in the bone marrow where it can promptly egress into circulation in response to stimuli and vastly increase the number of neutrophils in circulation (65). Once in circulation, neutrophils can rapidly mobilize in large numbers into infected or inflamed tissues in response to a chemokine gradient. Neutrophils express high levels of CXCR1 and CXCR2 chemokine receptors for trafficking to the site of inflammation or infection in response to CXCL1, CXCL2, and CXCL5 (71). They can also express CXCR4 which binds CXCL12 and retains neutrophils in the bone marrow or spleen (69, 72). To extravasate into tissue, neutrophils follow the steps of leukocyte recruitment: tethering, rolling, adhesion, crawling, and transmigration through integrin and selectin interactions with vascular endothelial cells (73–75). In the cornea specifically, neutrophils migrate from the peripheral limbal capillaries into the tissue as the central cornea is avascular (76, 77).

Effector functions

Once arriving at the site of infection, neutrophils exert multiple effector functions that can both directly and indirectly kill the pathogen. These functions include but is not limited to: reactive oxygen species (ROS) production, degranulation, and neutrophil extracellular trap (NET) formation (**Figure 1.4**).

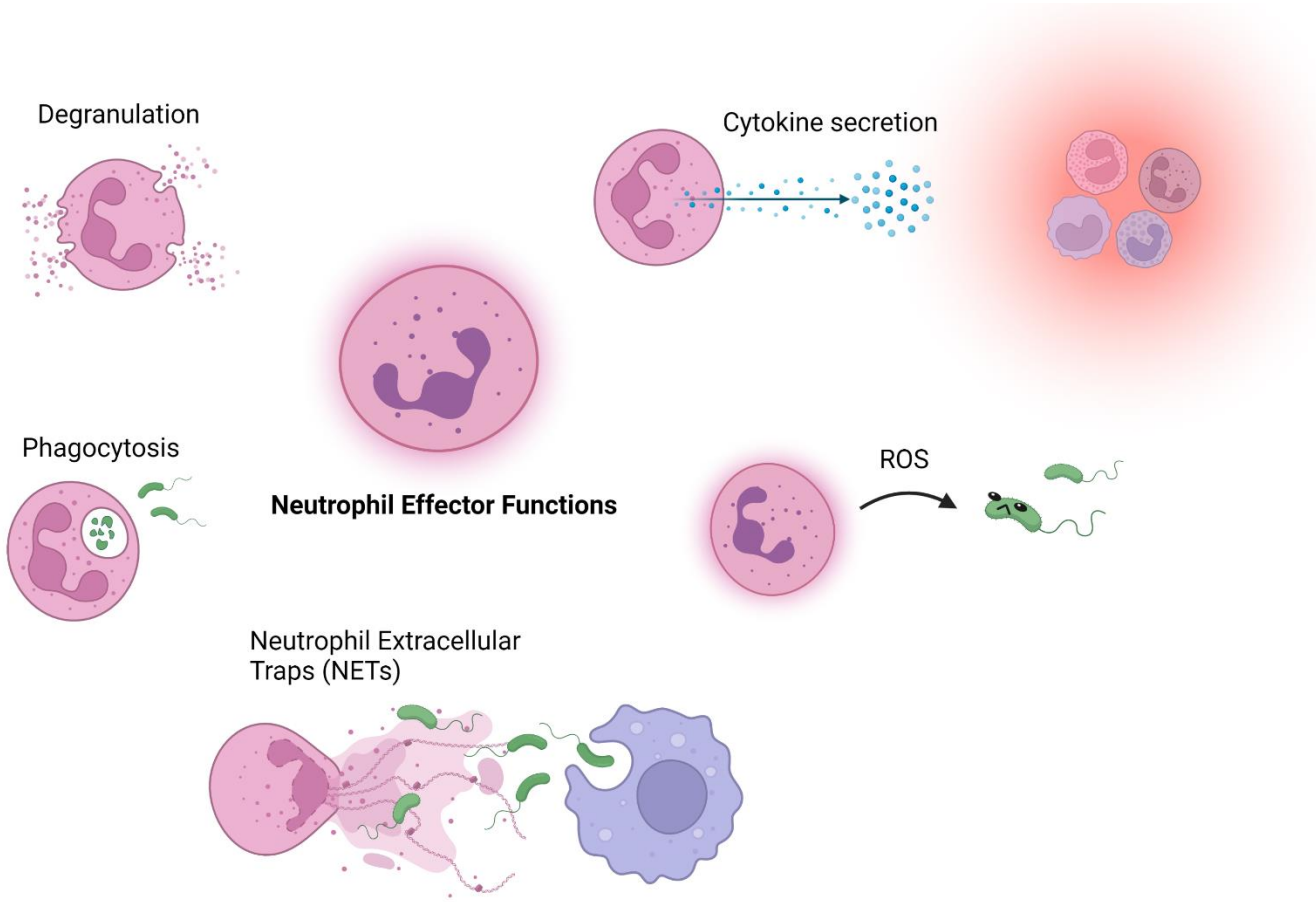

Figure 1.4. Neutrophil Effector Functions.

Neutrophils utilize reactive oxygen species (ROS), NET formation, phagocytosis, and degranulation to exert direct antimicrobial effects on pathogens. Neutrophils are also an important source of cytokines in the tissue. Created by Biorender.com

Reactive oxygen species (ROS) production is a key anti-microbial effector as well as inflammation inducer employed by neutrophils. The primary source of ROS is through NADPH oxidase complex, NOX2, which generates superoxide ($O_2^{\cdot -}$), hydrogen peroxide (H_2O_2), and hydroxyl radical ($OH^{\cdot}$) (78). Mutations in NOX2 complex results in chronic granulomatous disease (CGD) which is characterized by recurrent bacterial and fungal infections (79, 80). The degree of NOX2 impairment directly correlates to mortality in CGD patients (81). Neutrophils produce ROS in response to both fungi and bacteria where it can directly kill pathogens by reacting with organic molecules to disrupt their function (82). However, these pathogens have also evolved to inhibit ROS and promote survival. Previous studies from our lab have shown that the exotoxin Exo-S produced by *Pseudomonas aeruginosa* inhibits ROS production (83), and fungi such as *Aspergillus* express superoxide dismutase and regulate antioxidant pathways to promote survival against neutrophils (84). In addition to direct pathogen killing, ROS also plays a complex role in inducing inflammation both through inter- and intracellular signaling such as inflammasome activation and NETosis which will be later discussed in this chapter.

Degranulation: Along with eosinophils and basophils, neutrophils are granulocytes that contain antimicrobial proteases, enzymes, cationic peptides, and nutrient chelators. These antimicrobial proteins are packed in granules for regulated exocytosis (85). Neutrophil granules are divided into three distinct types: primary/azurophilic granules, secondary/specific granules, and tertiary/gelatinase granules (86). Primary granules contain neutrophil elastase (NE), cathepsin G, proteinase 3, defensins, and the serine protease myeloperoxidase (MPO). Secondary

granules contain NOX2 subunits, collagenase, and lactoferrin. And tertiary granules contain gelatinase, arginase 1, and the matrix metalloprotease MMP9. Secretion of these granules are regulated and occurs in response to stimuli and calcium signaling (86).

Neutrophil extracellular traps (NETs) are web-like extracellular structures made of decondensed chromatin and granule proteins (87, 88). NETs trap, neutralize, and kill bacteria and fungi (89, 90). Protein arginine deiminase 4 (PAD4) is responsible for citrullination of histone H3 (H3Cit) that decondenses the chromatin and mediate NETosis (91, 92). Many studies have reported that NET formation is dependent on NOX2-induced ROS. However, recent findings have implicated that there are ROS-independent NETosis as well (93–96). For ROS-dependent NETosis, Metzler et al. reported that NE translocation to the nucleus for histone degradation is required, and this process depends on both ROS and MPO activity (97). NETosis occurs *in vivo* following infection with *Pseudomonas aeruginosa* and *Aspergillus fumigatus* (90, 92, 98). However, we found that PAD4 and NE is individually not necessary for pathogen clearance during fungal and bacterial infection.

Neutrophils as a source of cytokines

Although neutrophils are relatively short-lived effector cells, they are now recognized as an important source of cytokines and chemokines in the inflammatory response. Despite producing less cytokines than macrophages or monocytes on a per cell basis, neutrophils constitute the majority of infiltrating cells during an infection or

inflammation that greatly outnumbers other cells. Therefore, neutrophils are a major source of cytokines under these circumstances.

Neutrophils have been shown to express a wide variety of cytokines and chemokines either constitutively or in response to stimuli (99). In the cornea specifically, studies from the Aravind Eye Hospital in southern India showed elevated transcripts for IL-1α, IL-1β, IL-8, and IL-17A from corneal ulcers of microbial keratitis patients compared to healthy controls (18, 26). We previously reported that depletion of neutrophils in a murine model of *Pseudomonas* keratitis fully ablated IL-1β levels indicating neutrophils are the primary source of this cytokine in the cornea (38). Further, neutrophil production of IL-1α will be discussed in chapter 2 and 3.

Interleukin-1

IL-1α and IL-1β are highly pro-inflammatory cytokines of the interleukin-1 family. Most of the IL-1 family members are in a cluster on human chromosome 2 where they likely formed as a duplication event (100). Unlike other cytokines, IL-1 family members are not secreted through canonical ER and Golgi-dependent exocytosis (101). While IL-1α and IL-1β share similarities with other IL-1 family members such as IL-18 and IL-33, they (along with their receptor antagonist, IL-1Ra) are the only ones that bind the same receptor—IL-1R1, for signaling (102). Both IL-1α and IL-1β are produced in a pro-form (30kDa) that can be cleaved into their mature 17-kDa form (103); however, IL-1α does not require cleavage for activity while pro-IL-1β cleavage into mature IL-1β is necessary for its bioactivity (104). Further, a key difference between IL-1α and IL-1β, is that IL-1α contains a nuclear localization sequence in its N-terminal half which allows for

translocation to the nucleus (105). While much of IL-1α regulation by myeloid cells is still unclear, IL-1β processing and secretion by macrophages is well characterized in the literature.

IL-1β

Analysis of evolutionary ancestry by sequence homology identified IL-1β as the proto-IL-1 gene emerging in the vertebrate subphylum (106). Its role as an inflammatory cytokine has been implicated in many diseases including autoinflammation, diabetes, rheumatic diseases, and infections (107–111). During infectious keratitis, IL-1β is necessary for recruitment of neutrophils and subsequently clearance of infection (37, 38, 112). Secretion of IL-1β is tightly regulated and well characterized in macrophages. It involves a two-step process: i) priming of cells through PRRs which results in NF-κB activation and production of pro-IL-1β, and ii) activation of the inflammasome and caspase-1 which cleaves pro-IL-1β and Gasdermin D (**Figure 1.5**).

PRR signaling such as LPS recognition by TLR4 or β-glucan recognition by Dectin-1, leads to activation and nuclear translocation of the transcription factor NF-κB (113, 114). This process which leads to NF-κB-mediated transcription and translation of pro-IL-1β and pro-IL-1α is called priming (48). As pro-IL-1β is not bioactive, it requires a second signal to induce inflammasome activation (115, 116). NLRs, the adaptor ASC, and caspase-1 oligomerizes upon activation to form a large multi-protein complex called the inflammasome (117). Inflammasome formation autoactivates caspase-1 that cleaves pro-IL-1β into its mature bioactive form (118). Many diverse inflammasome activators have been described such as extracellular ATP, monosodium urate (MSU),

and bacterial toxins (119); however, it is not entirely clear how live pathogens such as *Aspergillus fumigatus* or *P. aeruginosa* are sensed by NLRs for inflammasome activation.

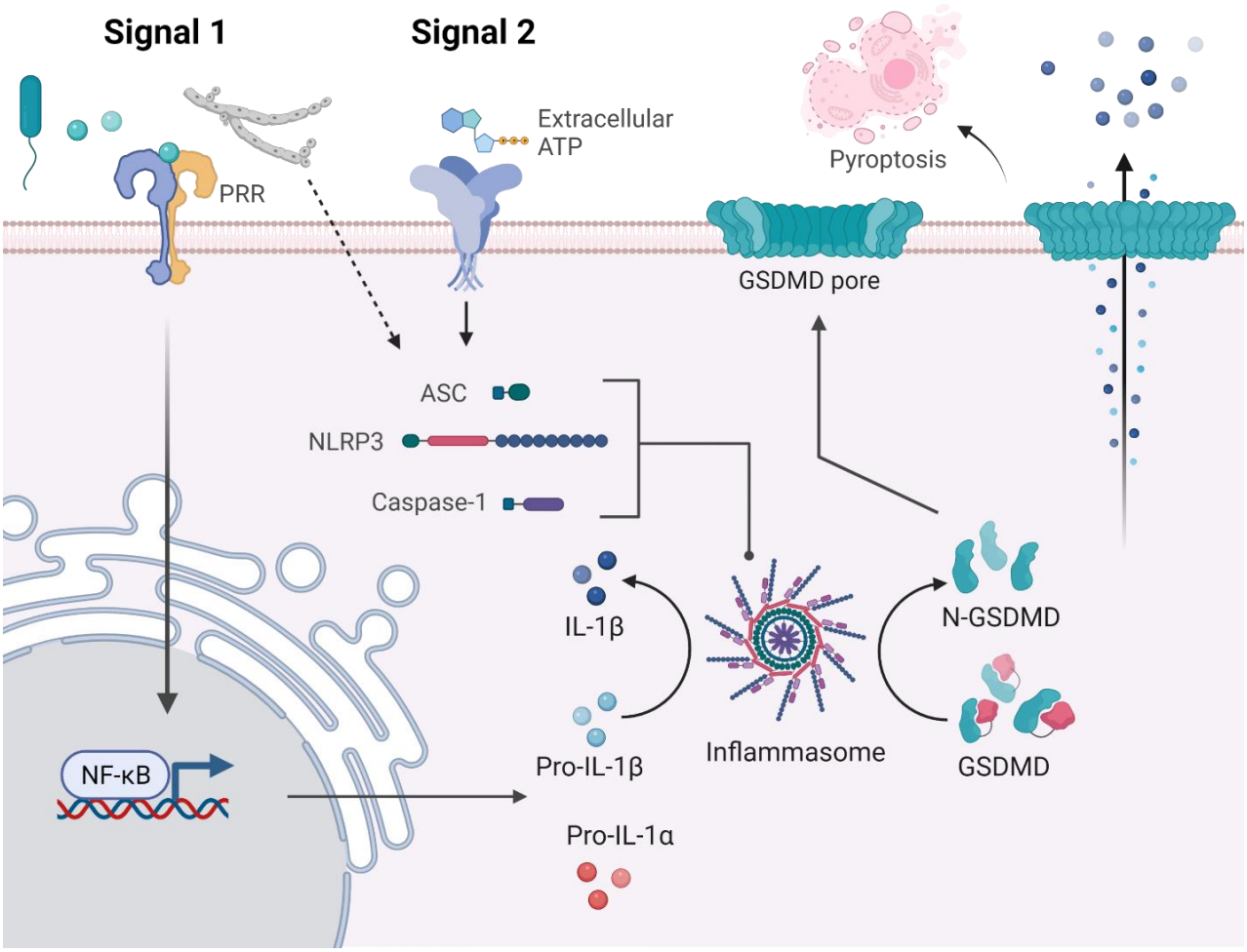

Figure 1.5. GSDMD-mediated IL-1β Secretion by Macrophages

IL-1β regulation and secretion is tightly regulated in a two-step process involving priming and subsequent activation of the inflammasome. This process leads to GSDMD-dependent IL-1β release and pyroptotic cell death. Created with Biorender.com

In addition to cleavage of pro-IL-1β, caspase-1 also cleaves the pore forming protein gasdermin D (GSDMD). The cleaved 28-kDa N-GSDMD inserts into the inner

leaflet of the plasma membrane where it oligomerizes to form pores that allows for IL-1β release (120, 121). Secretion of IL-1β through GSDMD pores is followed by pyroptotic cell death from osmotic lysis in macrophages (122). Pyroptosis is a caspase-1 dependent, necrotic cell death characterized by GSDMD-cleavage, membrane rupture, and release of proinflammatory intracellular contents (123, 124). After inflammasome activation, pyroptosis occurs rapidly in macrophages; however, we and others have found that neutrophils do not undergo pyroptosis (125–127).

Although canonical IL-1β secretion from macrophages involves the two-step process shown in **Figure 1.5**, neutrophil secretion of IL-1β is only dependent on GSDMD at early time points (128, 129). Previous work from our lab revealed that, unlike macrophages, N-GSDMD do not localize to the plasma membrane of neutrophils. Instead, they localize to primary granules and autophagosomes where IL-1β secretion is dependent on ATG-7-dependent secretory autophagy (125). In our model of microbial keratitis, GSDMD is not necessary for IL-1β release in the cornea and do not play a role in clearance of bacteria or in limiting hyphae formation during fungal keratitis (data not shown). The mechanism of IL-1β secretion *in vivo* in response to live pathogens is of great interest to the lab and remains an area of active research.

IL-1α

While IL-1α shares a similar protein structure to IL-1β and binds to the same receptor (102), there are a few key differences between the two. First, IL-1α does not require cleavage for bioactivity (130). Pro-IL-1α is expressed constitutively in many non-hematopoietic cells where it acts as an alarmin and danger-associated molecular

pattern (131). In myeloid cells, IL-1α production is induced following stimuli and can be cleaved by calpain (104). Another key difference between IL-1α and IL-1β is the nuclear localization sequence in the N-terminal domain of IL-1α which allows nuclear translocation of pro-IL-1α (105). IL-1α nuclear transport mechanism has not been described; however, this process requires binding of pro-IL-1α to HAX-1 (132–134). Nuclear localization of IL-1α is normally observed in non-hematopoietic cells under homeostatic conditions to prevent its release (104). It is also observed in macrophages and microglia after stimulation (135). However, nuclear localization of IL-1α in neutrophils has not been reported.

While IL-1β processing and secretion has been a hot topic of research, not much is known about IL-1α regulation and secretion. In non-hematopoietic cells, IL-1α is passively released through cell death where it acts as an alarmin (136). Whether IL-1α has a regulated secretion mechanism from non-hematopoietic cells is unclear. Recent studies utilizing *Gsdmd-/-* animals have now shown that IL-1α can be secreted from macrophages in a GSDMD-dependent matter (137, 138); however, GSDMD- and inflammasome-dependency is contingent on the signal activator (139). There are very few studies in the literature on neutrophil production of IL-1α. A novel mechanism for neutrophil secretion of IL-1α will be addressed in chapter 3 of this thesis.

Although our previous studies have revealed a critical role for IL-1β in both bacterial and fungal keratitis, whether there is a role for IL-1α is unknown. During pulmonary infection with *Aspergillus fumigatus*, IL-1α is necessary for neutrophil recruitment and plays a protective role in the lungs (140, 141). In a separate study, Rider et al. also reported that IL-1α recruits neutrophils while IL-1β recruits

macrophages during sterile inflammation, and this differential recruitment is temporally regulated (142). IL-1α recruitment of neutrophils is likely indirect following activation of IL-1R1 and subsequent CXCL2 production. In a chronic inflammation model induced by hydrocarbon oil, IL-1α recruitment of neutrophils to the peritoneal cavity was shown to be CXCR2-dependent (143). Given the importance of IL-1α in recruiting neutrophils in other tissues, we hypothesized that the same is true for the cornea. We address the role of IL-1α during bacterial keratitis in chapter 2 and how neutrophils regulate IL-1α secretion in response to bacterial and fungal stimuli in chapter 3.

CHAPTER 2:

Differential roles for IL-1α and IL-1β in *Pseudomonas aeruginosa* corneal infection

In press in The Journal of Immunology. *Bridget Ratitong, Michaela E. Marshall, Morgan A. Dragan, Charissa M. Anunciado, Serena Abbondante, Eric Pearlman*. *2022.* ***Differential roles for IL-1α and IL-1β in Pseudomonas aeruginosa corneal infection***. *J. Immunol.*

ABSTRACT

Pseudomonas aeruginosa is an important cause of dermal, pulmonary and ocular disease. Our studies have focused on *P. aeruginosa* infections of the cornea (keratitis) as a major cause of blinding microbial infections. The infection leads to an influx of innate immune cells with neutrophils making up to 90% of recruited cells during early stages. We previously reported that the proinflammatory cytokines IL-1α and IL-1β were elevated during infection. Compared to wild-type, infected *Il1b-/-* mice developed more severe corneal disease that is associated with impaired bacterial killing as a result of defective neutrophil recruitment. We also reported that neutrophils are an important source of IL-1α and IL-1β which peaked at 24 hours post infection. To examine the role of IL-1α compared to IL-1β in *Pseudomonas aeruginosa* keratitis, we inoculated corneas of C57BL/6 (WT), *Il1a-/-*, *Il1b-/-,* and *Il1a-/-Il1b-/-* (DKO) mice with $5x10^4$ ExoS expressing *P. aeruginosa*. *Il1b-/-* and DKO mice have significantly higher bacterial burden that was consistent with delayed neutrophil and monocyte recruitment to the corneas. Surprisingly, *Il1a-/-* mice had the opposite phenotype with enhanced bacteria clearance compared to WT mice. While there were no significant differences in neutrophil recruitment, *Il1a-/-* neutrophils displayed a more pro-inflammatory transcriptomic profile compared to WT with elevations in C1q expression that likely caused the phenotypic differences observed. These findings reveal a novel role for IL-1α, that is distinct from IL-1β, in impairing bacterial clearance.

INTRODUCTION

Pseudomonas aeruginosa is an opportunistic gram-negative bacterium that causes serious illnesses following infection of the skin or lungs. It is also a major cause of blinding corneal infections (keratitis) worldwide (11). Intact corneas are typically resistant to infection due to antimicrobial peptides in tear film and tight junctions of epithelial cells that form a physical barrier (19). However, ocular trauma and poor contact lens hygiene are predisposing factors that facilitate bacterial penetration to the corneal stroma where they rapidly replicate. *Pseudomonas* keratitis can lead to tissue damage that manifests as severe ocular pain, visual impairment, and can cause permanent blindness if left untreated (6). During the early stages of infection, neutrophils comprise the majority of infiltrating cells in patient corneal ulcers and is associated with elevated gene expression of IL-1a and IL-1b (26). Depletion of neutrophils in murine models of microbial keratitis results in significant impairment of bacterial killing, leading to more severe disease (38). We and others reported that the pro-inflammatory cytokines interleukin-1β (IL-1β) and IL-1α are highly elevated in *P. aeruginosa* corneal infections (18, 144). Further, we showed that neutrophils are the main source of IL-1β, and that IL-1β-deficient or IL-1R1-deficient mice have significantly higher bacterial burden (37, 38). However, the role of IL-1α in *P. aeruginosa* keratitis remains unclear.

IL-1α is an alarmin and danger-associated molecular pattern (DAMP) that is constitutively expressed by non-hematopoietic cells such as epithelial cells to amplify inflammation (104, 145, 146). It can also be produced by immune cells in response to stimulation. Recently, we identified neutrophils as an important source of IL-1α during

inflammatory conditions (126). Similar to IL-1β, IL-1α is first produced as a pro-form and can be cleaved by calpain into a 17-kDa mature-form. Although both IL-1α and IL-1β signal through IL-1R1, IL-1β bioactivity requires inflammasome activation and cleavage by caspase-1 while IL-1α does not (118, 139). Another key difference between these two cytokines is that proIL-1α contains a nuclear localization sequence in its N-terminal region that allows for nuclear translocation (105). IL-1α in non-hematopoietic cells localizes to the nucleus during homeostatic conditions and rapidly translocate to the cytosol for release following infection or inflammation (131). However, the role of nuclear IL-1α in hematopoietic cells is not well understood.

In the current study, we examined the role of IL-1α using a well-defined murine model of *Pseudomonas* keratitis during early-stage infection (37, 38). We demonstrate that IL-1α peaks at 24 hours post-infection (hpi) in infected corneas and is produced by neutrophils and monocytes. In contrast to *Il1b-/-* and *Il1a-/-Il1b-/-* double knock-out (DKO) mice, IL-1α-deficient mice has significantly less bacteria compared to WT mice despite no differences in neutrophil recruitment. RNA-sequencing of neutrophils isolated from infected corneas revealed a more proinflammatory transcriptomic profile in *Il1a-/-* compared to WT neutrophils that likely contributes to the phenotype observed.

MATERIALS AND METHODS

Mice

C57BL/6 mice were purchased from The Jackson Laboratory (Bar Harbor, ME) and bred inhouse. All gene knock-out mice are on C57BL/6 background. *Il1a-/-, Il1b-/-, and Il1a-/-Il1b-/-* (DKO) mice were originally generated by Dr. Iwakura (University of Tokyo, Japan) as described by Horai et al. (147). *Il1a-/-* and DKO mice were graciously provided by Dr. Joshua Obar (Dartmouth, New Hampshire), and *Il1b-/-* were obtained from Dr. Gabriel Núñez (University of Michigan). *Pad4-/-* were originally provided by Dr. Kerri Mowen at Scripps Research Institute. Mice were bred and housed in the University of California, Irvine vivarium. Age-matched 6-8 weeks old, male and female mice were used for all experiments. All protocols were approved by UC Irvine IACUC.

Bacterial strains and culture conditions

P. aeruginosa ExoS-expressing strains PAO1 and PAO1-GFP were obtained from Dr. Arne Rietsch (Case Western Reserve University). Bacteria were grown to mid-log phase (~$1x10^8$ bacteria/mL) in high-salt LB, which enhances expression of the Type III secretion system at 37°C with 5% CO_2, 200rpm. Bacteria were then washed and resuspended in sterile PBS to $5x10^4$ bacteria/ 2 µL for all *in vivo* infections.

Murine model of Pseudomonas keratitis

3x 10mm corneal epithelial abrasion was performed using a sterile 30-gauge needle followed by topical infection of $5x10^4$ PAO1 or PAO1-GFP in 2uL PBS as described (38). CFU was quantified at 2-hpi to verify the inoculum. At 24, 48, or 72hpi, mice were euthanized, and corneal opacity and GFP fluorescence were imaged and quantified.

CFU quantification

At 2- (inoculum), 24-, 48-, or 72-hours post infection (hpi), whole eyes were collected and homogenized in 1mL PBS. Serial log dilutions of homogenate were plated on LB plates and incubated at 37°C with 5% CO_2 overnight. Colonies were counted manually and CFUs were calculated by [number of colonies x dilution factor x 100 (10uL out of the 1mL was used for plating and dilution)].

Bone Marrow Transplantation

6-7 weeks old WT or *Il1a-/-* recipient mice were irradiated at a lethal, single dose of 850-cGy (X-rad 320). Donor bone marrow cells were isolated from hind leg femurs and tibias of WT or *Il1a-/-* mice. Cells were treated with 1X RBC lysis (eBioscience) for 2-minutes and then washed with sterile PBS. Cells were counted and resuspended at $1x10^7$ cells/mL of PBS. Irradiated recipient mice were anesthetized with isoflurane and transplanted with 100uL ($1x10^6$ cells) of bone marrow donor cells by retro-orbital injection. Transplanted mice were kept on an antibiotic chow diet (UNIPRIM) for 3 weeks before returning to regular chow for 1-2 weeks prior to infection.

Cytokine detection

Corneas were dissected and homogenized in 500µL of PBS with TissueLyser II (Qiagen) for 3 minutes at frequency/1 of 30. IL-1α, IL-1β, TNFα, IL-6, CXCL-2, CXCL-1, CCL2, and IL-1Ra were measured using Duoset ELISA kits (R&D Systems) according to manufacturer's protocol. Cytokine concentrations were calculated and plotted as pg/cornea.

Flow cytometry

Dissected corneas were incubated with 3mg/mL collagenase (Sigma Aldrich, C0130) in RPMI (Gibco), with 1% HEPES (Gibco), 1% penicillin-streptomycin (Gibco), and 0.5%

BSA (Fisher Bioreagents) for 1 hour and 15 minutes at 37°C. Cells were incubated for 5 minutes with anti-mouse CD16/32 antibody (Biolegend) to block Fc receptors. Then, cells were incubated 20 minutes at 4°C with anti-mouse CD45-APC, Ly6G-BV510, Ly6C-PECy7, CD11b-PETxRed, CCR2-BV421, and F4/80-FitC (BioLegend) and fixable viability dye (BD Biosciences). Cells were washed with FACS buffer and fixed with Cytofix/cytoperm (BD Biosciences) for 20 min at 4°C. Cells were washed with PBS.

For intracellular staining, BD perm/wash (BD Biosciences) was used to permeabilize cells and anti-mouse IL-1a-PE (BioLegend), H3Cit (Abcam), and C1q (courtesy of Dr. Feng Lin, Cleveland Clinic) primary antibodies was added to cells and incubated at 4°C for 30 minutes (IL-1α) or overnight for unconjugated primary antibodies. Cells were washed with BD perm/wash and suspended in 100μL perm/wash. For unconjugated H3Cit and C1q antibodies, secondary antibody donkey anti-rabbit 647 (Invitrogen) was added and incubated for 1 hour at 4°C. Cells were washed with BD perm/wash and suspended in 100μL perm/wash.

An ACEA Novocyte was used for flow cytometric analysis of neutrophils (CD45+ CD11b+ Ly6G+ Ly6C+) and monocytes (CD45+ CD11b+ Ly6G- Ly6Chi CCR2+). NovoExpress software was used for data analysis, calculation of mean fluorescent intensity, cell frequency and cell count. Amnis ImageStream™ was used for imaging flow cytometry and analysis was performed on Amnis IDEAS software.

Histology

At 24 or 48hpi, the back of eyes was punctured with a 23-gauge needle and placed in 4% PFA for at least 48 hours. Eyes were then paraffin embedded and 8 μM sections were examined by hematoxylin and eosin staining. Briefly, slides were stained with

hematoxylin (Sigma Aldrich) and rinsed in running water before dipping in bluing reagent (Fisher Scientific) and counterstaining with eosin (Sigma Aldrich). Slides were then dehydrated in an ethanol series and staining concluded with two final xylene incubations. Slides were then mounted with Permount (Fisher Scientific) and were imaged with the color brightfield.

Immunofluorescence staining of whole corneas

At 24hpi, whole eyes were embedded in OCT (Sakura) and slowly frozen with dry ice. Blocks were sectioned at 8uM for subsequent IF staining. Briefly, slides were thawed and placed in 100% acetone at -20°C for 10 minutes. Sections were then fixed with 4% PFA (ThermoScientific) and washed in 1X PBS (Gibco). 1X Normal donkey serum (Jackson ImmunoResearch) and FC block (BioLegend) were diluted in 1% BSA (Fisher Bioreagents) for use as blocking buffer. After 1 hour of blocking, primary antibodies: Ly-6G/Ly-6C Monoclonal Antibody NIMP-R14 (Invitrogen) and Rabbit anti-H3Cit (Abcam) were diluted 1:50 and 1:100, respectively, in blocking buffer and were stained overnight at 4°C. Slides were washed 3x for 10 minutes with 1X PBS. Secondary antibodies goat anti-Rat 647 (Invitrogen) and goat anti-Rabbit 488 (Invitrogen) were diluted 1:1000 and 1:500, respectively, in blocking buffer and added to sections for 1 hour at RT. Slides were then washed 4x for 10 minutes in 1x PBS and were briefly incubated with DAPI. Finally, slides were mounted using Vectashield® Antifade Mounting Medium (Vector Laboratories) and were imaged on the Keyence All-in-One Fluorescence Imager, BZ-X series (Keyence). Image contrast and brightness were adjusted to the same setting on all images.

RNA sequencing and analysis

Corneas were digested as previously described and pooled (4 pooled corneas = 1 n). Live CD45+ Ly6G+ Ly6C+ corneal neutrophils were FACS isolated with BD FACSAria II sorter (UCI flow cytometry core). RNA was isolated from sorted samples with RNeasy Micro kit (Qiagen) and submitted to UCI Genomics core for QC, library building, and sequencing. Briefly, RNA was quantified using the NanoDrop ND-1000 spectrophotometer (ThermoFisher) and quality checked using the Agilent Bioanalyzer 2100 (Agilent). Library construction was performed according to the Clontech SMART-Seq v4 Ultra Low Input RNA/Nextera XT Library Preparation Guide. One µg of total RNA was used and mRNA was enriched using oligo dT magnetic beads. The enriched mRNA was chemically fragmented for three minutes, followed by reverse transcription to make cDNA. The resulting cDNA was cleaned using AMPure XP beads, end repaired, and the 3' ends were adenylated. Illumina barcoded adapters were ligated on the ends and the adapter-ligated fragments were enriched by nine cycles of PCR. The resulting libraries were validated by qPCR and sized by Agilent Bioanalyzer DNA high sensitivity chip. The barcoded cDNA libraries were multiplexed on the Novaseq6000 platform to yield 100-bp paired-end reads. FASTQ files were trimmed using Trimmomatic version 0.39 (Bolger et al. 2014) and aligned to the mm10 genome and counted using STAR version 2.7.8a (Dobin et al. 2013). Differential expression analysis was performed using DESeq2 version 1.24.0 (Love et al. 2014) on R version 3.6.0.

Western blot

At 24hpi, corneas were dissected and homogenized in 1X cell lysis buffer (Cell Signaling) containing 5mM of diisopropyl fluorophosphate (DFP, Sigma Aldrich) to inactivate neutrophil proteases. Lysates were cleared by centrifugation at 10,000xg for

10 minutes. Protein concentration was calculated using a BCA protein assay kit (Thermo Fisher). 50ug protein from lysates, 1X SDS (from 5X stock), and ultrapure water (Invitrogen) were mixed and boiled for 10 minutes at 95°C on a heating block. Samples were loaded into 4-20% mini-PROTEAN, 10-well, 50ul TGX precast protein gels (Bio-rad). Proteins were transferred to a nitrocellulose membrane using a Bio-rad Trans-blot Turbo transfer system. The membrane was blocked with 5% milk in TBS-T for 1 hour at RT. Primary antibodies (sources listed in Supplemental Table 1) rabbit anti-C1q clone 1151 (Dr. Tenner, UCI), mouse anti-β-actin (Santa Cruz Biotechnology), hamster anti-IL-1α (eBioscience), rabbit anti-Lamin B1 (Abcam), mouse anti-IL-1R2 (Santa Cruz Biotechnology), and rabbit anti-GAPDH (Biolegend) were diluted in 5% milk and incubated at 4°C overnight on a rocker. Membranes were washed with 1X TBST buffer 3 times for 10 minutes. HRP-conjugated secondary antibodies against rabbit (Cell Signaling), mouse (Cell Signaling), or hamster (Santa Cruz Biotechnology) were diluted in 5% milk and incubated at RT for 1 hour. West Femto Maximum Supersignal (Thermo Fisher) was used to enhance the signal before the membrane was imaged with ChemiDoc™ MP Imaging System (BioRad). Band intensity was quantified using Image Lab software.

In vitro neutrophil functional analysis

Casein (9%) Sigma Aldrich) was injected intraperitoneally 16- and 3-hours prior to peritoneal lavage to induce sterile inflammation. The peritoneal cavity was lavaged with cold 10-mL sterile PBS and cells were pelleted. Negative selection (STEMCELL Technologies) beads were used to enrich for neutrophils according to manufacturer's

guidelines and generated >97% neutrophils. Neutrophils were plated at $2x10^6$ cells/mL RPMI (Gibco) for functional analysis.

Neutrophil extracellular trap formation (NETosis) – Neutrophils were pre-incubated with SYTOX (Invitrogen) for 30 minutes at 37°C before addition of 25ng phorbol myristate acetate (PMA, Sigma) or PAO1 at a multiplicity of infection (MOI) of 30. Fluorescent signal was read over 16h using a Cytation5 imaging plate reader (Agilent). The area under the curve (AUC) was calculated from the average of the curves of technical replicates.

Reactive oxygen species (ROS) – Neutrophils were pre-incubated with Luminol (Sigma) for 30 minutes prior to stimulation. 25ng PMA (Sigma) or PAO1 at MOI of 30 were added and immediately read on the Cytation5 for 90 minutes. AUC was calculated from the average of the curves of technical replicates.

In vitro neutrophil bacterial killing – $2x10^5$ cells were plated per well in a 96-well plate (CytoOne). PAO1 was added at MOI of 30 in duplicates except for the negative control wells and incubated at 37°C with 5% CO_2. After 15 minutes, 400ug/mL gentamycin (Sigma) was added to kill extracellular bacteria. After an additional 30-minute incubation with gentamycin, cells were centrifuged at 300xg for 5 minutes and washed twice with PBS. 0.1% TritonX (Fisher Scientific) in PBS was used to lyse the cells and bacteria were serially diluted and plated on LB plates. CFU was counted after an overnight incubation at 37°C, 5% CO_2.

Statistical Analysis

Statistical analysis was determined by unpaired T-tests, ordinary one-way ANOVA with Dunnett's multiple comparisons test, Brown-Forsythe and Welch ANOVA with Dunnett's

T3 multiple comparisons test, or 2way ANOVA with Tukey's multiple comparisons test (detailed in Figure legends) using GraphPad Prism software. Outliers were removed with ROUT method (Q=1%) using GraphPad Prism software. Error bars indicate mean ± SEM and p values less than 0.05 are considered significant. The number of biological replicates for each experiment can be found in the figure legends. Asterisks denotes p-values as follows: *p<0.05, **p<0.01, ***p<0.001, ****p<0.0001 in each figure and 'ns' denotes not significant.

RESULTS

Neutrophils and monocytes are the major sources of IL-1α during *P. aeruginosa* keratitis

We first measured IL-1α and IL-1β concentrations in the corneas of C57BL/6 (WT) mice after infection with $5x10^4$ *Pseudomonas aeruginosa* (PAO1 strain) by ELISA. Consistent with previous reports, IL-1α and IL-1β levels peaked at 24 hours post-infection (hpi), coinciding with infiltration of neutrophils and monocytes (**Fig 2.1A, B**). IL-1α and IL-1β were undetectable in PBS mock infected corneas (data not shown).

Previous studies identified neutrophils as the primary source of IL-1β in bacterial infected corneas (38). To identify the cellular source of IL-1α, we examined intracellular IL-1α in infiltrating myeloid cells at 24hpi by flow cytometry. Cells were gated on live, single CD45+ CD11b+ cells and neutrophils were defined by Ly6G+ Ly6C+ events while monocytes were Ly6G- Ly6C+ and CCR2+ (**Fig 2.1C,** gating strategy in **Fig S2.1B**). Consistent with previous studies from our lab (38), we found that 80-90% of CD45+ infiltrating cells at early-stage infection were neutrophils and < 10% were monocytes. Intracellular cytokine staining revealed that IL-1α was produced by neutrophils and monocytes recruited to infected corneas (**Fig 2.1D**). *Il1a-/-* cells were used as fluorescence minus one (FMO) control. Mean fluorescent intensity (MFI) levels were significantly higher than the control indicating that both cell-types are major sources of IL-1α. IL-1α-PE MFI levels were higher in monocytes than in neutrophils, indicative of higher production on a per cell basis. However, neutrophils greatly outnumber monocytes in infected corneas and therefore, are a major source of IL-1α in the cornea.

While corneal epithelial cells release IL-1α during necrotic cell death (146), we found that IL-1α and IL-1β were undetectable at 4hpi and in PBS mock infection, suggesting that infiltrating myeloid cells rather than resident corneal cells are the primary source of IL-1α during infection. In support of this, western blot analysis of whole cornea homogenates from mock-infected corneas at 24hpi revealed no detectable IL-1α compared with PAO1 infected corneas (**Fig S2.1A**). Further, there was no significant increase in IL-1α release by human corneal epithelial cells in response to incubation with LPS or PAO1. Taken together, we conclude that epithelial cells are not an important source of IL-1α or IL-1b during *P. aeruginosa* keratitis (**Fig S2.1B, C**).

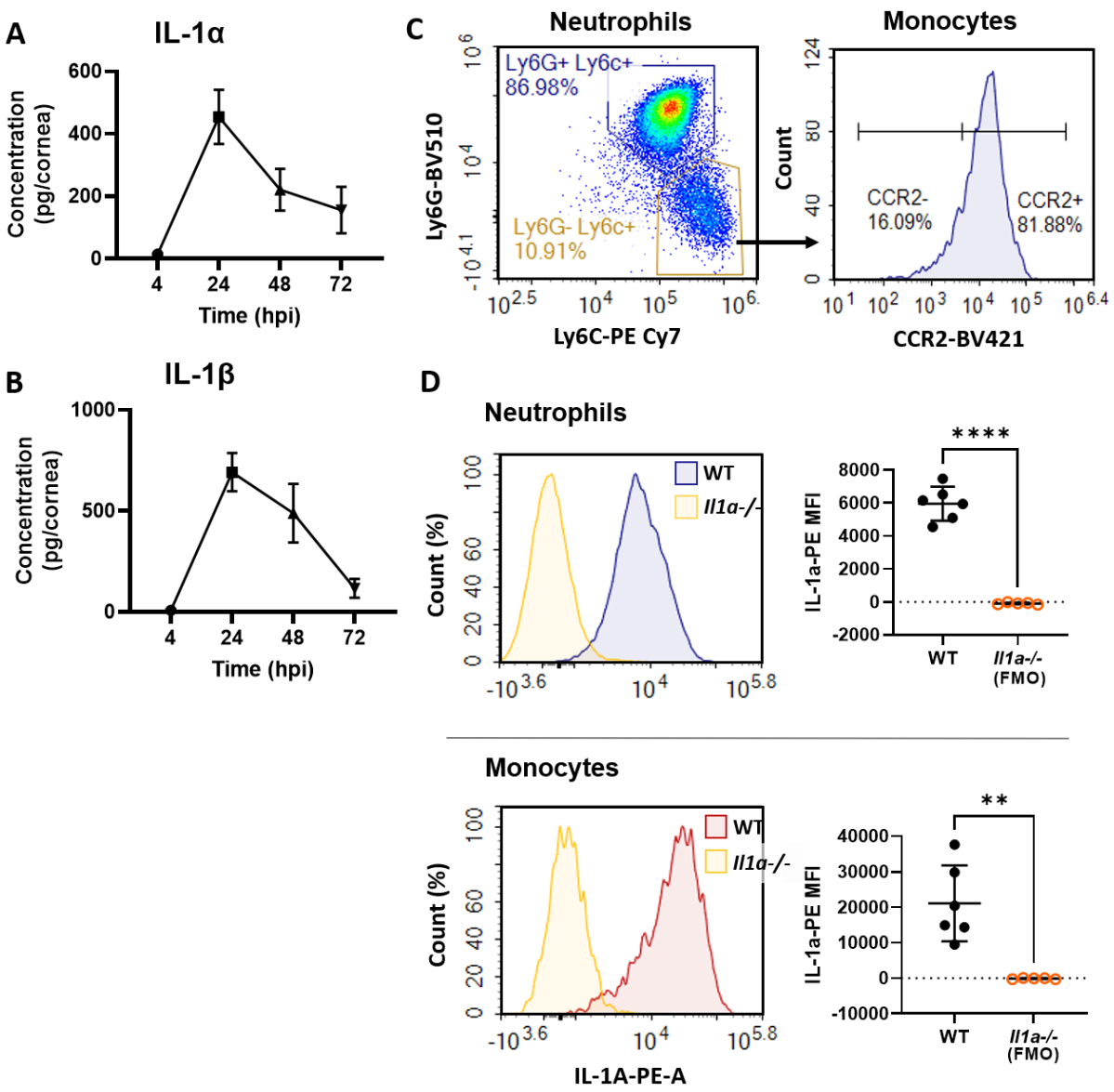

Figure 2.1: IL-1α production in *P. aeruginosa* keratitis.

(A, B) Time course of IL-1α and IL-1β production in *P. aeruginosa* (PAO1) infected corneas quantified by ELISA (n=8). (**C)** Flow cytometry of live, single CD45+ CD11b+ cells at 24hpi showing neutrophils (Ly6G+ Ly6C+) and monocytes (Ly6G- Ly6C^{hi} CCR2+). (**D**) Intracellular IL-1α+ (PE) neutrophils and monocytes shown as representative histograms (left). MFI was quantified using *Il1a-/-* cells as the FMO control (right).

Differential roles for IL-1α and IL-1β in *P. aeruginosa* keratitis

Previous studies from our lab showed impaired bacterial clearance in *Il1b-/-* mice that was associated with impaired recruitment of neutrophils to infected corneas (38). To determine if there is a role for IL-1α during *P. aeruginosa* keratitis, we infected WT, *Il1a-/-*, *Il1b-/-*, and DKO mice with $5x10^4$ PAO1-GFP and examined corneal opacity, GFP fluorescence, and bacterial burden. At 24hpi, there were no significant differences in corneal opacity among the 4 genotypes despite GFP levels seemingly higher in the *Il1b-/-* and DKO mice, and lower in *Il1a-/-* compared to WT mice. However, by 48hpi *Il1b-/-* and DKO mice had noticeably higher corneal opacity compared to WT (**Fig 2.2A, B**). Surprisingly, *Il1a-/-* mice had the opposite phenotype with significantly lower corneal opacity at 48hpi compared to WT, suggesting that IL-1α plays a distinct role from IL-1β by contributing to disease exacerbation. While not statistically significant, the DKO mice had slightly more disease and bacterial burden than *Il1b-/-* mice. However, when both IL-1α and IL-1β are absent, the *Il1b-/-* phenotype appears to be dominant, indicating that there are redundant and non-redundant roles for IL-1α and IL-1β.

Consistent with corneal opacity and GFP levels, bacterial burden was higher in *Il1b-/-* and DKO compared to WT corneas at both 24- and 48-hpi. In marked contrast, there was a log fold lower CFU in *Il1a-/-* compared to WT mice at 48- and 72-hpi (**Fig 2.2C, D**). Since *Il1b-/-* and DKO mice were at risk of corneal perforation at 48hpi, we did not extend the experiment to 72hpi for these genotypes.

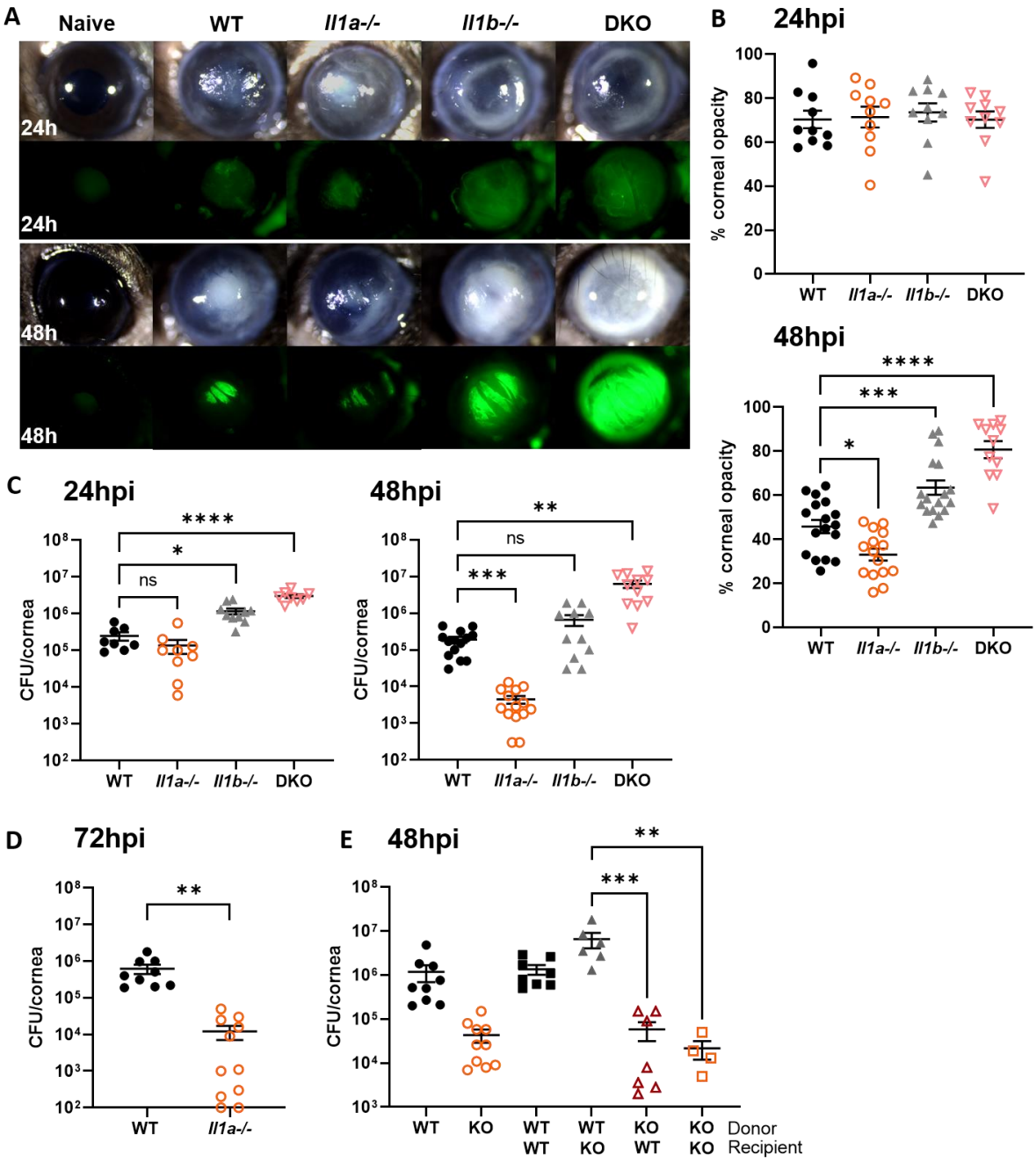

Figure 2.2: The role of IL-1α and IL-1β in *P. aeruginosa* keratitis

Corneas of WT, *Il1a-/-, Il1b-/-,* and DKO mice infected with 5x10^4 PAO1 expressing green fluorescence protein (GFP) and examined at 24- and 48-hpi. (**A**) Representative images of corneal opacity (brightfield) and GFP (bacteria) in infected WT, *Il1a-/-, Il1b-/-,* and DKO mice. (**B**) Quantification of percent corneal opacity by ImageJ. (**C, D**) Live

bacteria from infected corneas quantified by CFU at (**C**) 24-, 48-, and (**D**) 72-hpi. (**E**) CFU in bone marrow transplant mice at 48-hpi. N=8-10 corneas for 24hpi and 72hpi time points, experiment repeated 3 times, and n=10-20 corneas for 48hpi time point repeated 4 times. N=5-10 corneas for BMT, experiments were repeated 3 times.

Next, to determine whether it is IL-1α-deficiency in infiltrating immune cells or resident cells of the cornea that are causing enhanced bacterial killing, we performed bone marrow transplant experiments. WT or *Il1a-/-* donor bone marrow cells were injected intravenously into irradiated WT (WT-WT, KO-WT) or *Il1a-/-* (WT-KO, KO-KO) recipient mice. After 5 weeks, mice were infected with $5x10^4$ PAO1 and CFU was quantified at 48hpi. We found no differences between the WT-WT and WT-KO group compared to non-transplanted WT mice, but we did find significantly lower CFU in the KO-WT and KO-KO group, indicating that IL-1α-deficiency in immune cells and not resident cells mediate enhanced bacterial clearance (**Fig 2.2E**). Collectively, these findings demonstrate that IL-1α, in contrast to IL-1β, impairs rather than enhances bacterial killing.

Myeloid cell recruitment is delayed in infected *Il1b-/-* but not *Il1a-/-* corneas

Previous studies from our lab and others reported that neutrophils are critical for bacterial clearance in infected corneas (4, 38, 90). To address whether the differences observed in bacterial burden between WT, *Il1a-/-, Il1b-/-,* and DKO mice are due to changes in cellular infiltration, *P. aeruginosa*-infected eyes were examined by histology and by flow cytometry at 24- and 48hpi. Histological examination of corneal sections revealed pronounced cellular infiltration in WT and *Il1a-/-* central corneas at 24hpi compared to healthy corneas (**Fig 2.3A, S2.2A**). In contrast, cellular infiltration was

detected in the periphery, but not the central corneas of *Il1b-/-* and DKO, reflecting the ring-like pattern of corneal opacity shown in **Fig 2.2A**. By 48hpi, *Il1b-/-* and DKO exhibited a marked increase in recruited cells compared to WT and *Il1a-/-* corneas.

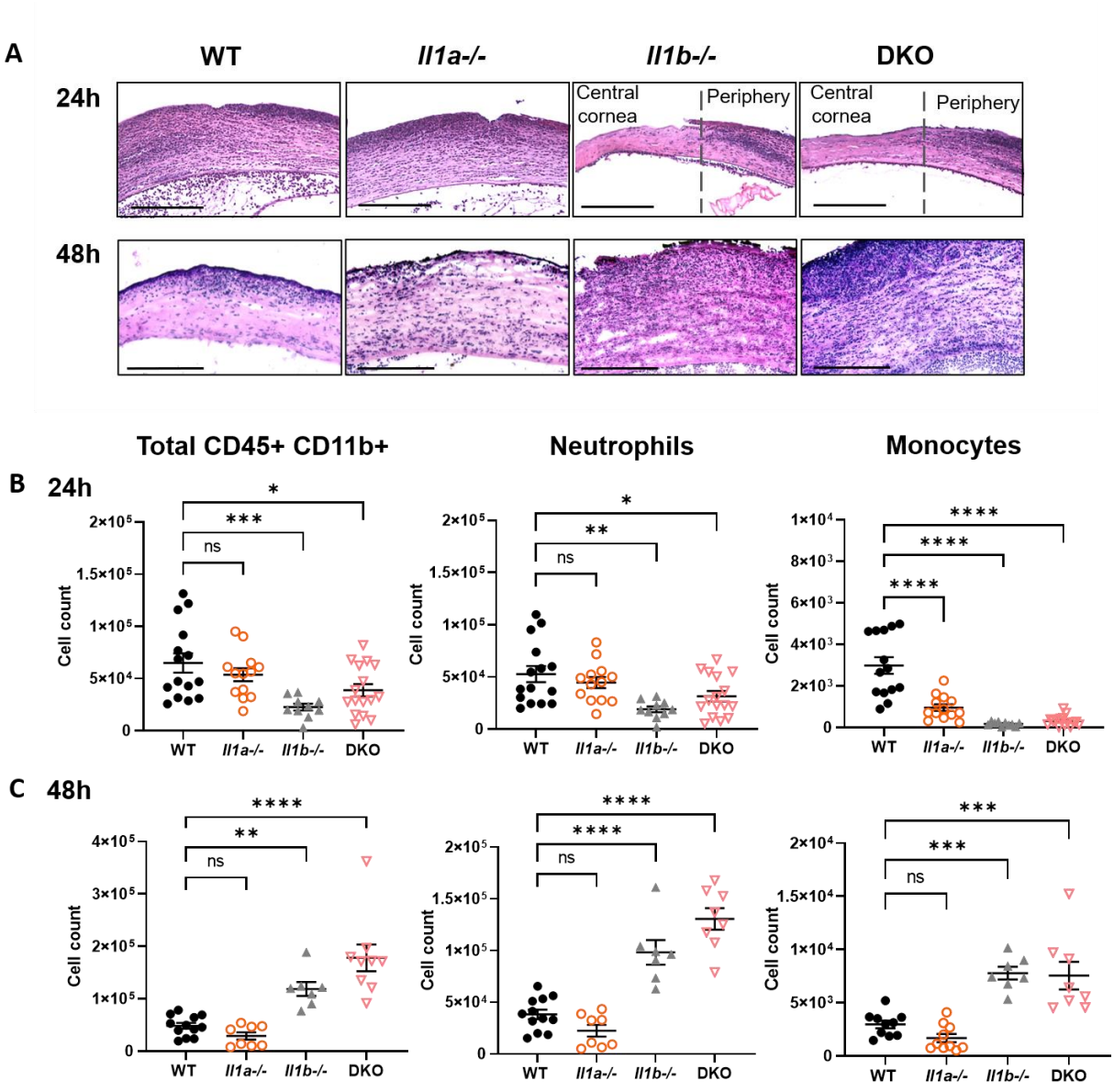

Figure 2.3. Neutrophil and monocyte recruitment to infected corneas

(**A**) Representative images from H&E-stained corneal sections of infected WT, *Il1a-/-*, *Il1b-/-,* and DKO corneas; scale bar represents 200uM. Cellular recruitment was quantified by flow cytometry at (**B**) 24- and (**C**) 48-hpi; neutrophils were gated on

CD45+CD11b+/ Ly6G+ Ly6C+ and monocytes were gated on Ly6G- Ly6Chi CCR2+ (**Fig S2.2B**).

Infiltrating cells were identified and quantified by flow cytometry as total CD45+CD11b+ cells, Ly6G+ neutrophils, and Ly6G- Ly6C+ CCR2+ monocytes (gating strategy shown in **Fig S2.2B**). Consistent with the histology, we found significantly less neutrophils and monocytes in *Il1b-/-* and DKO mice at 24hpi (**Fig 2.3B, C**). Although *Il1a-/-* corneas showed no significant differences in total CD45+CD11b+ and neutrophil cell counts compared to WT, there were significantly fewer monocytes at 24hpi (**Fig 2.3B, C**).

Cytokine production in infected corneas

To address whether the lower monocyte numbers in *Il1a-/-* compared to WT mice is due to differences in cytokine production, cytokines and chemokines in infected corneas were quantified by ELISA. For IL-1 family members, we found no differences in IL-1β production between infected WT and *Il1a-/-* corneas (**Fig 2.4A**). However, *Il1b-/-* corneas had less IL-1α, which correlates with the lower numbers of neutrophils and monocytes in the cornea at 24hpi (**Fig 2.4B**). There were no significant differences in IL-1Ra (**Fig 2.4C**). For chemokines, CXCL2 production was elevated in *Il1b-/-* and DKO compared to *Il1a-/-* and WT corneas (**Fig 2.4D**) which reflects the delayed recruitment of neutrophils migrating into central cornea (**Fig 2.3A, C**). There were no differences in CXCL1 or CCL2 among the groups (**Fig 2.4E, F**). Lastly, *Il1b-/-* had significantly higher levels of TNFα compared to WT (**Fig 2.4G**), however, the low concentration per cornea suggests it this might not be physiologically relevant. We also found significantly less IL-

6 in *Il1a-/-* and DKO corneas compared to WT that was not apparent in *Il1b-/-,* indicating that IL-6 secretion is partially IL-1α-dependent and IL-1β-independent (**Fig 2.4H**). IFNβ, IFNγ, IL-10, and GM-CSF were below the threshold of detection (data not shown).

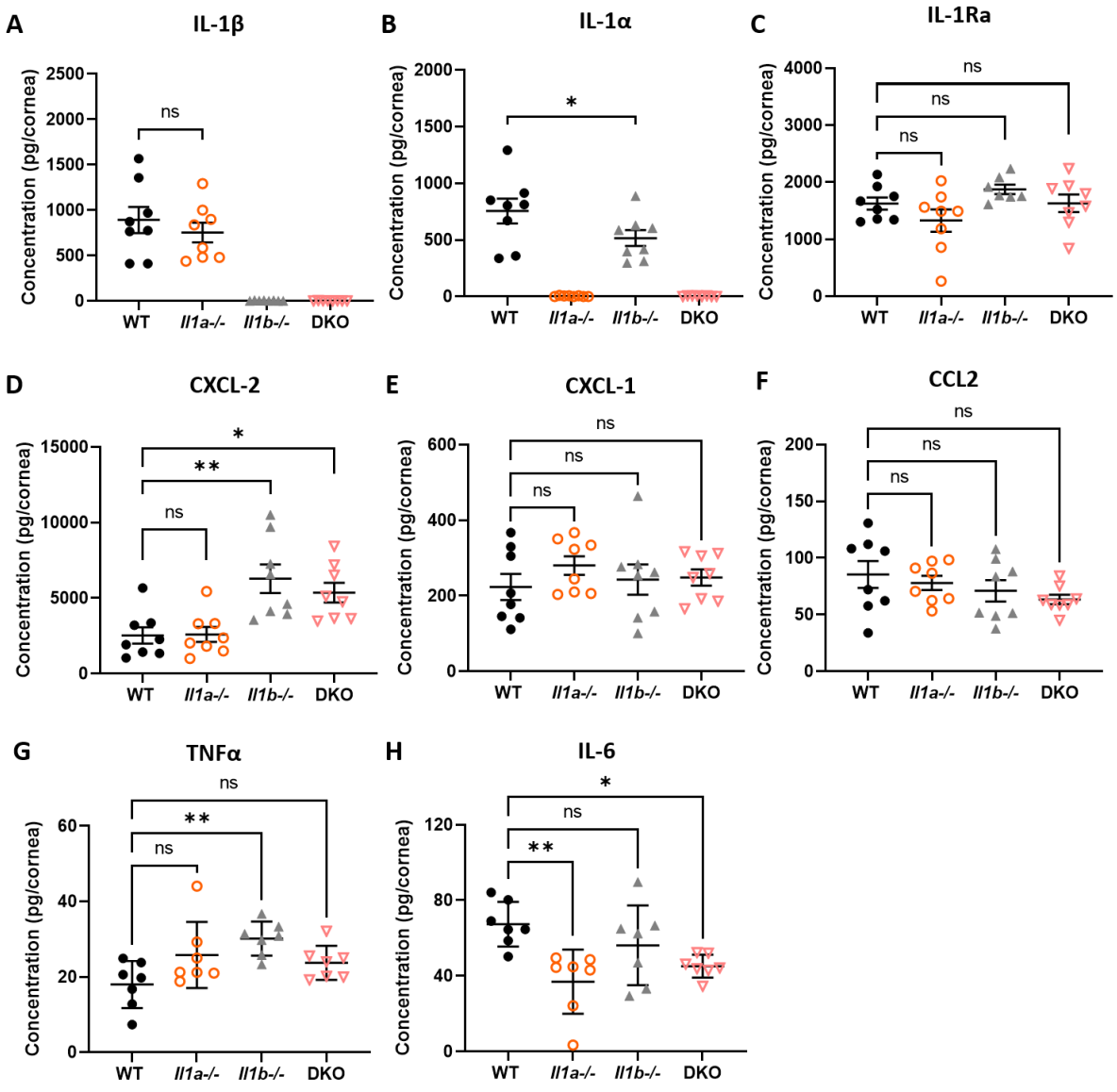

Figure 2.4: Cytokine production in infected WT, *Il1a-/-*, and *Il1b-/-* corneas.

PAO1-infected corneas from WT, *Il1a-/-, Il1b-/-,* and DKO mice were homogenized at 24hpi and cytokines were quantified by ELISA. Concentration was calculated as pg/cornea (3 repeated experiments).

As IL-6 levels in all groups was <100pg/ml compared to ng/ml levels of IL-1 cytokines and CXCL2, the major conclusion from these data is that differences in cytokine production do not appear to explain the lower monocyte numbers or the clinical phenotype of *Il1a-/-* mice. However, the increased CXCL2 production in *Il1b-/* and DKO mice at 24hpi may account for the increased recruitment of neutrophils in infected corneas 48hpi.

IL-1α-deficiency does not affect neutrophil effector functions

Although there were no differences in neutrophil recruitment to the corneas between WT and *Il1a-/-*mice, we examined whether there were functional differences. To analyze neutrophil extracellular trap formation (NETosis) in infected corneas, frozen sections of infected WT and *Il1a-/-* corneas were used for immunofluorescence of citrullinated histone 3 (H3Cit) and the neutrophil marker NIMP-R14. We found no defects in histone citrullination in *Il1a-/-* compared to WT corneas *in vivo* (**Fig 2.5A**). Additionally, we quantified intracellular H3Cit+ neutrophils *ex vivo* from infected corneas by flow cytometry using infected *Pad4-/-* corneas as a negative control and found no significant difference between WT and *Il1a-/-* (**Fig 2.5B, C, S2.3A**).

In vitro, neutrophils were isolated from the peritoneal cavity after inducing sterile inflammation, enriched by negative bead selection, and stimulated with PMA or PAO1 at MOI30 for analysis of NETosis, reactive oxygen species (ROS), and bacterial killing. Neutrophil extracellular traps (NETs) were quantified by SYTOX Green, which binds to extracellular DNA and is quantified by fluorescence. While extracellular DNA was elevated in PMA and PAO-1 infected neutrophils compared with unstimulated media

control, we found no significant differences between WT and *Il1a-/-* neutrophils under any conditions (**Fig 2.5D,** time course graphs in **Fig S2.3B**).

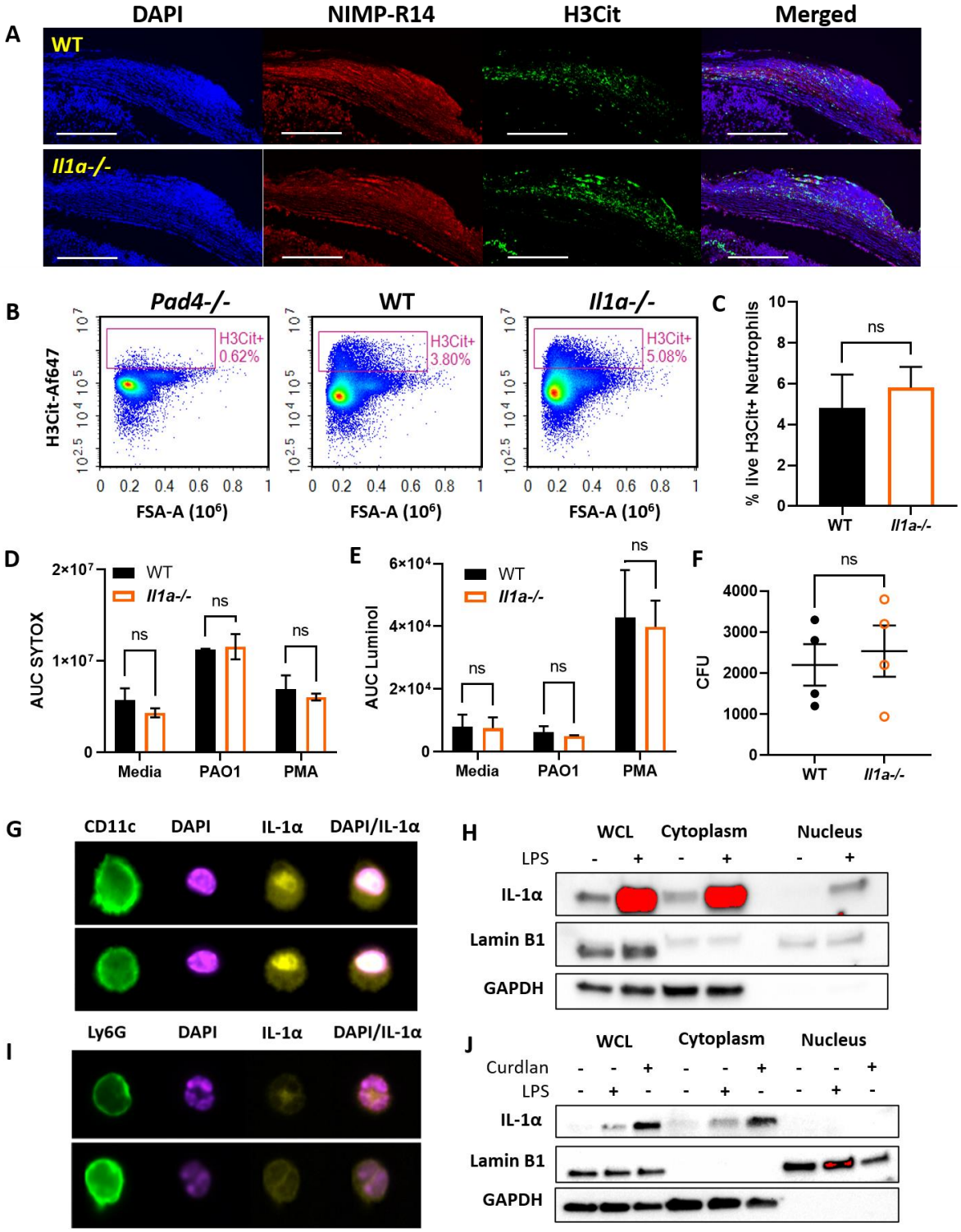

Figure 2.5: Neutrophil effector functions and IL-1α nuclear localization

(**A**) Representative images of WT and *Il1a-/-* corneal sections at 24-hpi with NIMP-R14 (neutrophils), and H3Cit as an indicator of NETosis (Representative of n=6 mice, 3 repeat experiments). (**B**) Flow cytometry of intracellular H3Cit in *ex-vivo* neutrophils from infected WT, *Pad4-/-*, and *Il1a-/-.* (**C**) Quantification of % H3Cit+ Ly6G+ neutrophils (n=4). (**D-F**) *In vitro* functional analysis of peritoneal neutrophils from WT and *Il1a-/-* mice stimulated with PMA or PAO1 (n=3 repeated experiments). (**D**) Extracellular DNA quantified by area under the curve (AUC). (**E**) Total ROS quantified as AUC of luminol fluorescence. (**F**) Neutrophil killing of phagocytosed PAO1 quantified by CFU. **(G, H)** Nuclear localization in LPS-stimulated bone marrow-derived dendritic cells (BMDCs) LPS. (**G)** Imaging flow cytometry of IL-1α (yellow) and nuclei (DAPI). (**H**) Cytoplasmic and nuclear extracts analyzed by western blot for IL-1α, Lamin B1 (nuclei) and GAPDH (cytosol). (**I**) Localization of IL-1α in β-glucan-stimulated neutrophils (curdlan) examined by Imageing flow cytometry. (**J**) Neutrophil cytoplasmic and nuclear extract analyzed by western blot for IL-1α.

To determine if there is a difference in reactive oxygen species (ROS) production, peritoneal neutrophils from WT and *Il1a-/-* mice were incubated 90 minutes with PMA or PAO1 in the presence of Luminol. PMA was used as a positive control for ROS production as PAO1 is known to inhibit ROS (83). Again, there were no differences observed between WT and *Il1a-/-* neutrophils with either stimulus (**Fig 2.5E,** time course shown in **Fig S2.3C**).

Further, we assessed if there is a difference between WT and *Il1a-/-* neutrophils in bacterial killing *in vitro* (83). Neutrophils were incubated with PAO1 for 15 minutes and extracellular bacteria were killed with gentamycin. Antibiotics were removed, and neutrophils were lysed in a mild detergent to quantify the CFU of phagocytosed bacteria. We observed no differences in CFU between WT and *Il1a-/- in vitro* (**Fig 2.5F**). Taken together, results from these studies indicate that these neutrophil effector activities are not affected by the absence of IL-1α.

Nuclear localization of IL-1α occurs in dendritic cells but not neutrophils

IL-1α and IL-1β play distinct roles in bacterial clearance from infected corneas (**Fig 2.2**) despite both signal through IL-1R1. One major difference between the two cytokines is that full-length IL-1α contains a highly conserved nuclear localization sequence while IL-1β does not (106). Nuclear translocation of IL-1α has been reported in macrophages and microglia without a clear function (135, 148). Therefore, we next addressed whether IL-1α localizes to the nucleus in neutrophils. Bone marrow-derived dendritic cells (BMDCs) were used as a positive control as they produce high levels of IL-1α in response to stimuli such as LPS (126, 139). IL-1α localization was first examined by ImageStream imaging flow cytometry where we found nuclear localization of IL-1α in approximately 35% of BMDC-stimulated with LPS (**Fig 2.5G,** quantification shown in **Fig S2.3D**). As a second approach, nuclear and cytoplasmic extracts from stimulated-BMDC were analyzed by Western blot, confirming the presence of IL-1α in the nucleus (**Fig 2.5H**). In contrast, we found that IL-1α is localized in the cytoplasm but not the nucleus of *in vitro* stimulated-neutrophils and *ex-vivo* neutrophils isolated from infected corneas (**Fig 2.5I-J, S2.3D**). These findings indicate that the distinct roles for

IL-1α and IL-1β in bacterial keratitis is not a consequence of IL-1α nuclear localization in neutrophils.

Neutrophils from infected *Il1a-/-* corneas have a more proinflammatory transcriptomic profile compared to WT neutrophils

While there was no difference in neutrophil recruitment to infected WT and *Il1a-/-* corneas and no differences in *in vitro* functional analyses, we sought to determine whether there are gene expression differences between WT and *Il1a-/-* neutrophils *in vivo* by RNA sequencing. WT and *Il1a-/-* mice were infected with $5x10^4$ PAO1 and at 24hpi, live Ly6G+ Ly6C+ neutrophils were sorted from the corneas for bulk RNA sequencing. Four infected corneas were pooled for each sample. From our sequencing data, we observed differences in gene expression between neutrophils from infected WT and *Il1a-/-* corneas. Most notably inflammatory genes including *C1qb, Msr1, Tnfsf9,* and *Pf4* were upregulated in *Il1a-/-* neutrophils (**Fig 2.6A-B**). To identify differences in biological processes and pathways, we annotated differentially expressed genes using Metascape analysis (149). Gene Ontology (GO) terms for “Regulation of leukocyte activation”, “Regulation of adaptive immune response”, and “Cytokine activity” were enriched in the *Il1a-/-* neutrophils compared with WT (**Fig 2.6C**).

C1qb is one of the genes of interest that is upregulated in *Il1a-/-*. C1qb along with C1qa and C1qc chains form the C1q molecule that regulates phagocytosis and cytokine production (150). C1q is part of the classical complement pathway initiation complex that cleaves C4 and C2 to generate C4b2b, which leads to cleavage of C3 and C5 (150). We therefore analyzed our RNAseq data for expression of additional complement genes. We found that *C3*, *Hc* (C5), and *C5ar1* gene expression was high in neutrophils;

however, *C1qb* was the only complement gene that was elevated in neutrophils from infected *Il1a-/-* corneas (**Fig 2.6D**).

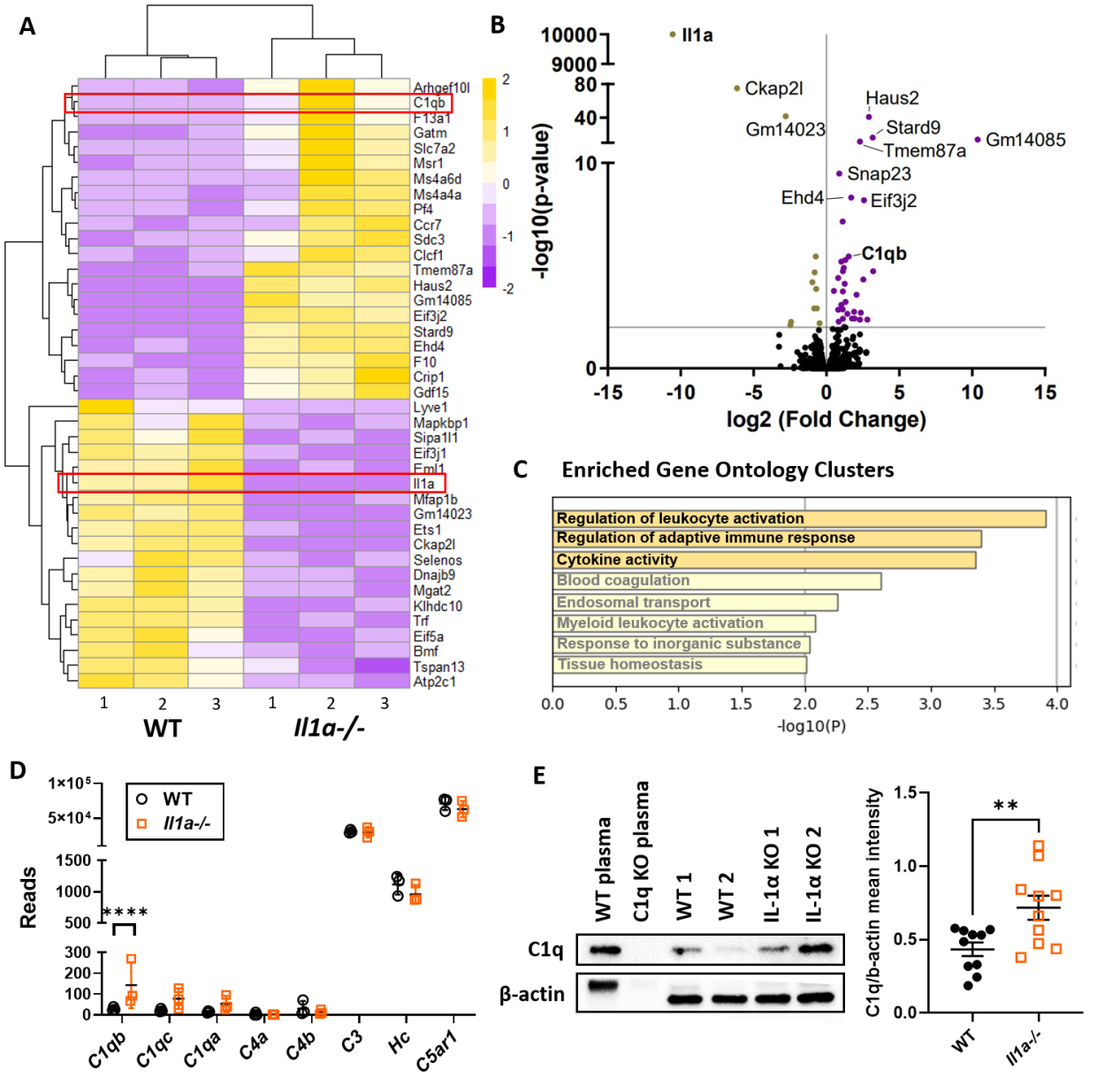

Figure 2.6: Transcriptomic analysis of WT and *Il1a-/-* neutrophils

Bulk RNA sequencing of live Ly6G+ Ly6C+ CD45+ CD11b+ neutrophils sorted from infected WT and *Il1a-/-* corneas at 24hpi (n=3). (**A**) Heatmap showing the top 30 differentially expressed genes with yellow indicative of upregulation and purple showing

downregulated genes. (**B**) Volcano plot of DE genes. Genes were filtered for subsequent analysis using the following cut-off: fold change > 2; adjusted P-value < 0.05. (**C**) Gene ontology (GO) terms associated with genes that are upregulated in *Il1a-/-* corneal neutrophils (https://metascape.org). (**D**) Complement gene reads expressed by neutrophils from infected WT and *Il1a-/-* corneas. (**E**) Representative western blot of C1q in infected corneas from WT and *Il1a-/-* mice (left) and quantification of band intensity normalized to b-actin loading control (right).

To verify that there were elevated C1q in *Il1a-/-* neutrophils, infected corneas were dissected and homogenized at 24hpi for detection of C1q protein by western blot (WT and C1q-/- plasma were used as controls). While C1q was detectable in WT mouse corneas, quantification of C1q over β-actin bands (loading control) showed that there was significantly more C1q protein in *Il1a-/-* corneas (**Fig 2.6E**). Further, immunofluorescence staining of C1q in infected corneas showed higher levels in *Il1a-/-* compared to WT and *Il1b-/-* in the central cornea (**Fig S2.4A-C**). Neutrophil-specific production of C1q in infected corneas was also quantified by flow cytometry. Although C1q+ neutrophils were <3%, we found higher frequency of C1q+ neutrophils in infected *Il1a-/-* compared with WT corneas (**Fig S2.4D, E**). Overall, these data show that infected corneas of IL-1α-deficient mice have a more pro-inflammatory transcriptomic profile, including elevated C1q, which may contribute to enhanced bacterial clearance.

DISCUSSION

IL-1α and IL-1β are pro-inflammatory cytokines that are highly upregulated during infection or sterile inflammation. We and others have identified IL-1β as a critical regulator of immune cell recruitment and subsequently bacterial clearance in a well-defined model of *Pseudomonas aeruginosa* keratitis (38, 151). Additionally, we reported that neutrophils comprise >80% of infiltrating cells during early-stage infection and are the main source of IL-1β in bacterial and fungal keratitis (38, 112). Recently, we reported that neutrophils are also an important source of IL-1α with an exosome-mediated secretion mechanism that is distinct from Gasdermin D-mediated IL-1α secretion by dendritic cells and macrophages (126). We further demonstrate in the current study that neutrophils and monocytes are the main source of IL-1α *in vivo* during *P. aeruginosa* keratitis, and that IL-1α and IL-1β play non-redundant roles in cellular recruitment and bacterial killing in the cornea.

Pseudomonas aeruginosa is a gram-negative bacterium that expresses a type III secretion system (T3SS) used to inject T3SS effector proteins into host cells (35). The effector protein ExoS inhibits ROS production by neutrophils and disrupts actin cytoskeleton to prevent phagocytosis (83, 152). *P. aeruginosa* strains expressing both ExoS and ExoU are rare, and the majority of clinical isolates are ExoS expressing strains (26). Distinct from other effector proteins, ExoU is a highly cytotoxic phospholipase that causes rapid cell death akin to necrosis (34, 35). ExoU-expressing strains are more virulent that the ExoS-expressing strain PAO1 used in the current study (37).

It is important to note that there are differences in responses to ExoS- or ExoU-expressing strains. We reported that neither IL-1α nor IL-1β were sufficient to provide protection during corneal infection with an ExoU-expressing *P. aeruginosa* strain, 19660, while *Il1r1-/-* and *Il1a-/-Il1b-/-* (DKO) had impaired bacterial clearance and more severe disease (37). These observations indicate that during infection with an ExoU-expressing strain, IL-1α and IL-1β play redundant roles. Conversely, IL-1β was sufficient for protection in an infection with the ExoS-expressing PAO1 (38), which we replicated in the current study. We now find that IL-1α has a distinct role from IL-1β by exacerbating disease and impairing bacterial killing. As *Il1b-/-* mice display delayed cellular recruitment and impaired bacterial clearance that is mirrored in the DKO mice, we conclude that the *Il1b-/-* phenotype is dominant in this model. Together, these studies indicate that there is a differential requirement of IL-1α and IL-1β for protection against ExoS compared to ExoU expressing strains of *P. aeruginosa*.

Further, in a lung infection model with a different ExoU-expressing *P. aeruginosa* strain, PA103, neutrophil recruitment was IL-1α-dependent and IL-1β-independent. This finding was based on ExoU activity as infection with ΔExoU PA103 displayed the opposite phenotype where IL-1β, instead of IL-1α, is required for neutrophil recruitment to the lungs (153), further illustrating that IL-1α and IL-1β can play distinct roles in response to T3SS effectors produced by *P. aeruginosa*.

A selective role for IL-1α was also reported during infections with *Legionella pneumophilia, Streptococcus pneumoniae,* and *Aspergillus fumigatus*. In an *in vivo* murine model of *Legionella pneumophilia* infection, only IL-1α but not IL-1β is essential for neutrophil recruitment to the lungs (154). Further, IL-1α and IL-1β was shown to

have non-redundant roles during *S. pneumoniae* infection that is based on spatial restriction *in vivo* (155). Pulmonary infection with a virulent strain of *Aspergillus fumigatus* also showed that IL-1α rather than IL-1β is critical for neutrophil recruitment and was required for survival of infected animals (140, 141). However, IL-1α is not necessary in *A. fumigatus* corneal infection (data not shown) while IL-1β is important for this model (112). Taken together, these findings indicate that the relative contributions of IL-1α and IL-1β to disease severity and microbial killing is dependent on the sites of infection and the infectious agents.

The conflicting effects of IL-1α and IL-1β on bacterial burden during corneal infection with PAO1 point to differing roles played by these cytokines despite binding to the same receptor. As IL-1α was found only in the cytoplasm, there is no evidence of a nuclear role for IL-1α in neutrophils. We also found that there were no intrinsic differences in neutrophil ROS production, NETosis or bacterial killing *in vitro* between WT and *Il1a-/- in vitro* suggesting an indirect, but selective, role for IL-1α signaling. As IL-1α and IL-1β share similar protein structures and signal through the same receptor, IL-1R1, their roles were often considered redundant (102). However, accumulating evidence now suggest they each play distinct roles during different pathological conditions (156). For instance, in a dextran sulfate sodium (DSS)-induced model of intestinal inflammation, IL-1α plays a key role in driving inflammation while IL-1β promotes repair and reconstitution of the epithelial barrier (157). Similarly, in the tumor microenvironment, IL-1α stimulates anti-tumor cell immunity whereas IL-1β produced by myeloid-derived suppressor cells (MDSCs) induces immunosuppression (158, 159). Moreover, IL-1α is the predominant IL-1R1 determinant of mortality in a neonatal sepsis

model while IL-1β was detected but unnecessary for lethality (160). Our current study adds to the accumulating evidence supporting the paradoxical, non-redundant roles of IL-1α and IL-1β.

One possible mechanism for the differential roles of IL-1α and IL-1β observed *in vivo* could be the spatial and temporal expression of IL-1R1 and IL-1R2. A recent study suggests that the bioavailability of IL-1α and IL-1β in different tissues as a possible mechanism for their nonredundant roles (155). Although we found no differences in IL-1β levels in *Il1a-/-* corneas, we examined expression of IL-1R2, the IL-1 decoy receptor, and found it highly expressed in the corneas of both WT and *Il1a-/-* mice (**Fig S4F, G**). IL-1R2 has a higher affinity for IL-1β at 10^{-10} M which is 100 times higher than its affinity for IL-1α (161, 162). As we found high levels of IL-1R2 in the corneas, it is likely that IL-1β signaling is dampened by the decoy receptor in WT animals, allowing IL-1α signaling to be dominant. In *Il1a-/-*, signaling is solely induced by IL-1β which has a protective role in *P. aeruginosa* keratitis. However, the bioavailability of IL-1α versus IL-1β to signal IL-1R1 *in vivo* requires further investigation.

In this study, we examined the transcriptomic profile of neutrophils from WT and IL-1α-deficient corneas to identify genes that are selectively expressed in the absence of IL-1α. C1qb was one of the genes that's upregulated in *Il1a-/-* neutrophils. Complement proteins are present at low levels in healthy corneas ; however, serum complement and complement components secreted by infiltrating cells lead to activation of the complement cascade that contributes to disease pathology during infection or inflammatory conditions (163). C1q is part of the classical complement pathway initiator that cleaves C4 and C2 resulting in activated C3 convertase (150). Cleaved C3

components lead to i) activation of the membrane attack complex (MAC, C5b-9) and ii) exerts direct effector function to directly kill bacteria (164). While we did not find differences in neutrophil C3 expression in the corneas, it is likely that the increased production of C1q would lead to more C3 cleavage and facilitate bacterial killing. In addition, novel roles of C1q that is independent from the classical complement pathway has been described; this includes: antibody-independent activation of C1 by direct binding to bacteria and enhancing FcyR-mediated phagocytosis (165). Future studies will examine these functions of C1q in the cornea and determine if they have a role in bacterial killing.

In summary, our current study revealed an unexpected role for IL-1α during *Pseudomonas* keratitis that is distinct from IL-1β, and identified monocytes and neutrophils as the primary sources of IL-1α. Our observations raise several questions that will require further studies including: identifying differences in IL-1 signaling, the relative concentration of bioactive forms of IL-1α and IL-1β under different infectious and inflammatory conditions, and signal outcome in different IL-1R1-expressing cells (156). It is also unclear how IL-1α-deficiency contributes to upregulation of C1q and if it is due to IL-1β signaling. IL-10 and IL-17 were shown to indirectly regulated chemokine mRNA stability in neutrophils (166, 167); therefore, it is possible that the increased C1qb expression in *Il1a-/-* neutrophils is a consequence of IL-1α regulating C1qb mRNA stability. Overall, further studies in this area will increase our understanding of host-pathogen interactions in infected corneas and may identify novel targets for therapeutic intervention.

Supplementary Figures

Supplementary Figure 1

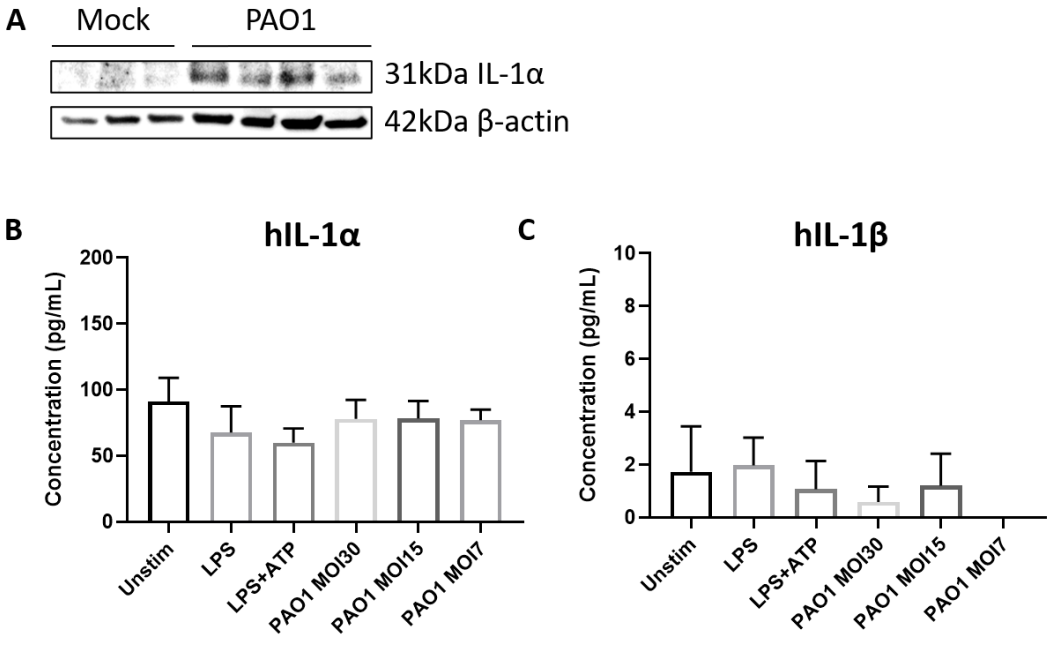

Supplementary Figure 1. IL-1α production by corneal epithelial cells. (**A**) *P. aeruginosa* infected and PBS-mock infected cornea analyzed for IL-1α production by western blot. (**B**) IL-1α and (**C**) IL-1β secretion quantified from stimulated human corneal epithelial cells.

Supplementary Figure 2

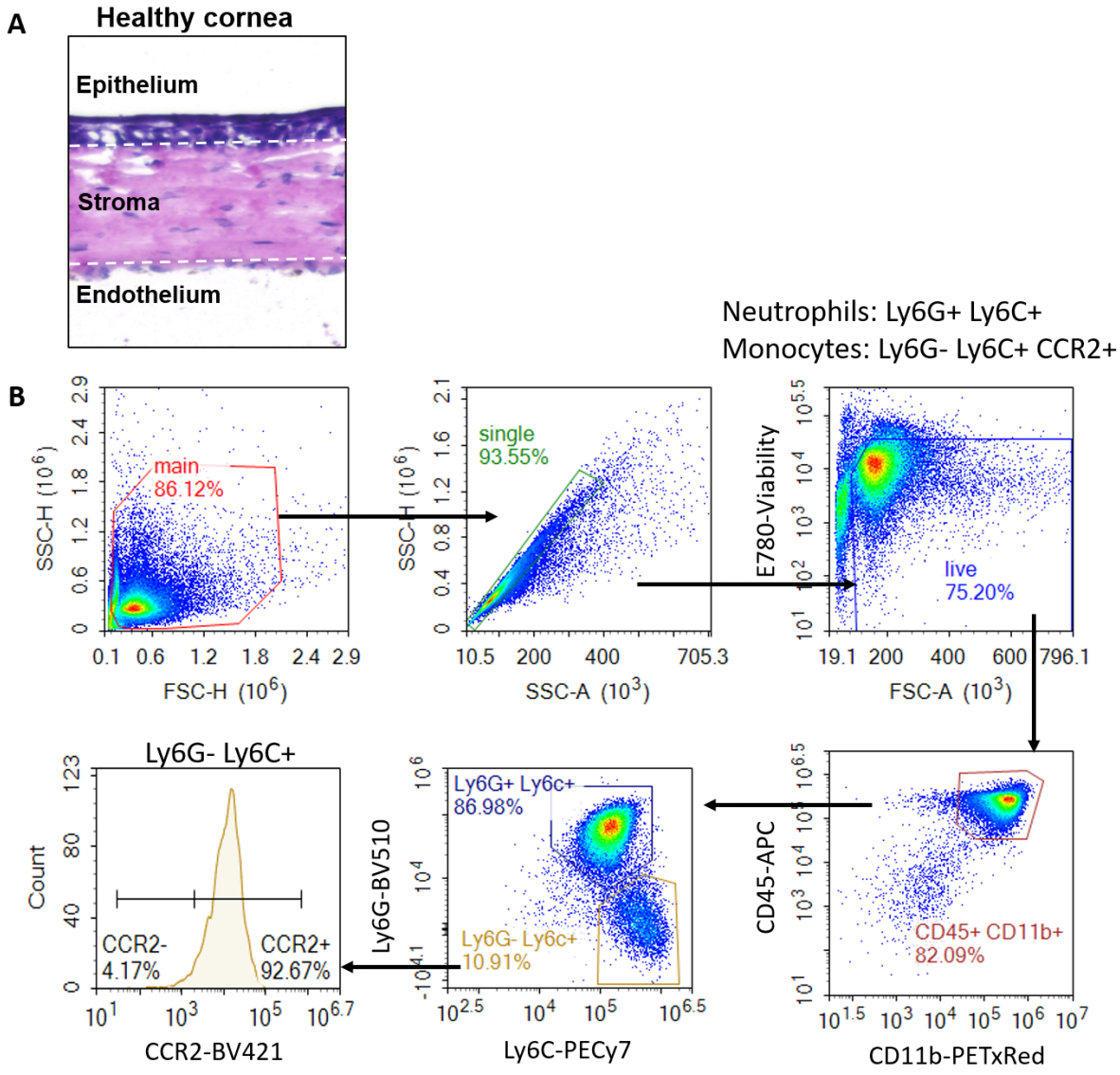

Supplementary Figure 2. Gating strategy. (**A**) Representative H&E image of healthy cornea showing the major layers of the cornea. (**B**) Gating strategy for neutrophils and monocytes from digested whole cornea samples.

Supplementary Figure 3

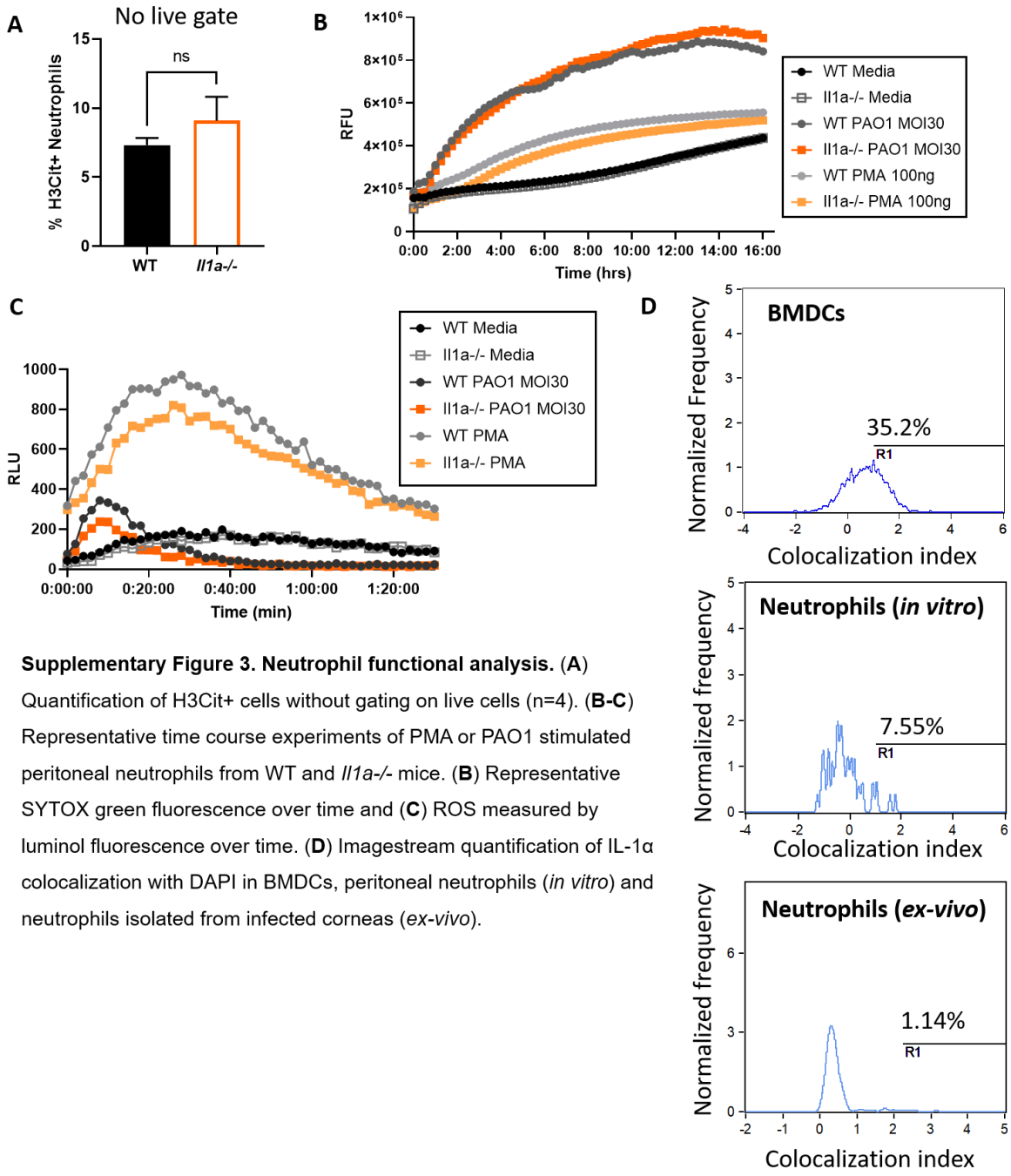

Supplementary Figure 3. Neutrophil functional analysis. (**A**) Quantification of H3Cit+ cells without gating on live cells (n=4). (**B-C**) Representative time course experiments of PMA or PAO1 stimulated peritoneal neutrophils from WT and *Il1a-/-* mice. (**B**) Representative SYTOX green fluorescence over time and (**C**) ROS measured by luminol fluorescence over time. (**D**) Imagestream quantification of IL-1α colocalization with DAPI in BMDCs, peritoneal neutrophils (*in vitro*) and neutrophils isolated from infected corneas (*ex-vivo*).

Supplemental Figure 4

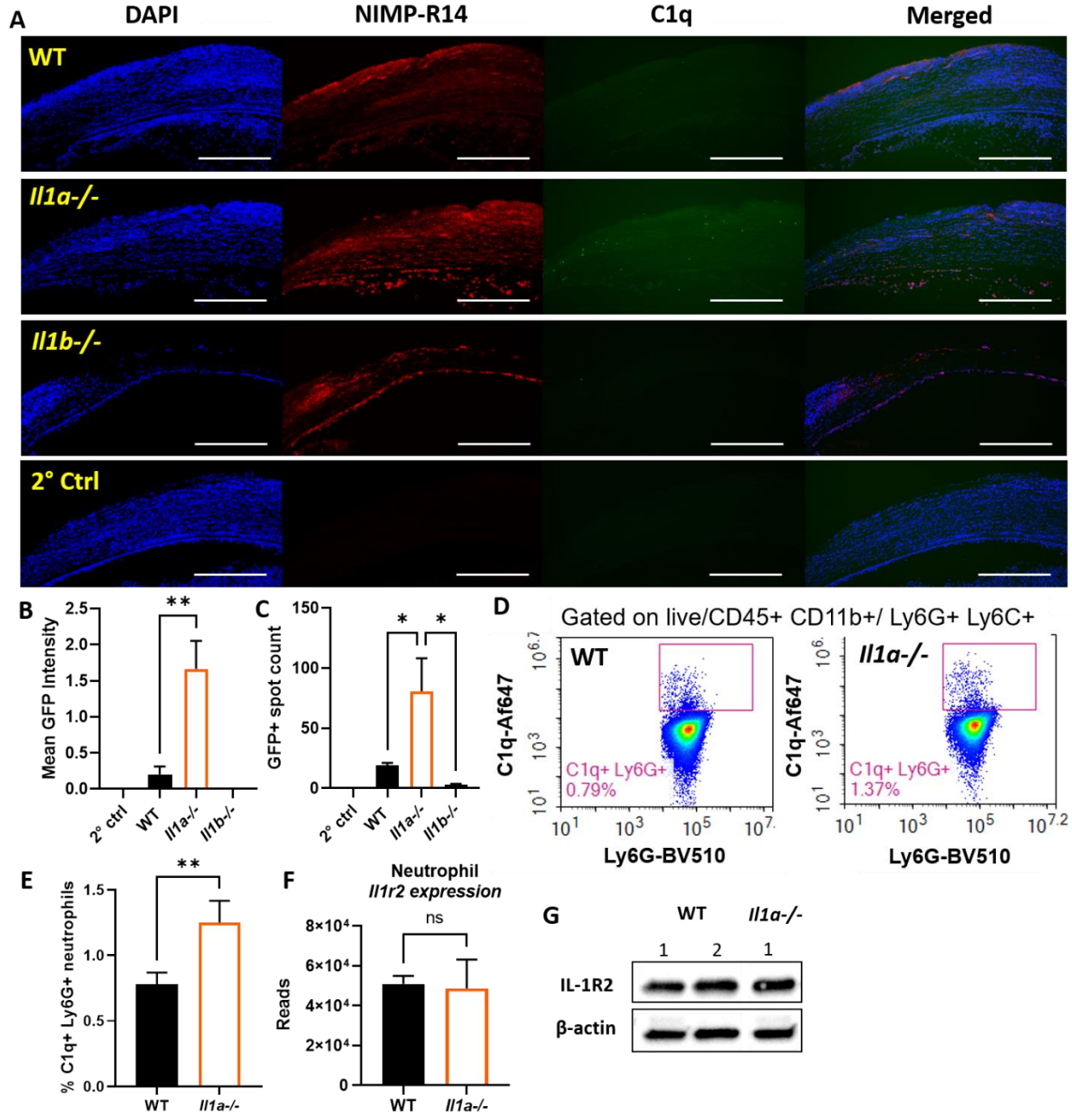

Supplementary Figure 4. C1q and IL-1R2 in the cornea. (**A**) Representative images and (**B**) GFP mean fluorescence intensity of WT, *Il1a-/-*, and *Il1b-/-* corneal sections at 24hpi. (**C**) Spot analysis of GFP+ puncta analyzed by ImageJ. N=4, experiment was repeated 2 times. (**D**) Representative flow cytometry plot and **(B)** quantification of % C1q+ Ly6G+ cells gated on live/CD45+ CD11b+ neutrophils (n=4, experiment repeated 2 times). **(F)** Il1r2 reads from bulk RNA sequencing. **(G)** Whole cornea western blot analysis of IL-1R2.

CHAPTER 3:

β-glucan stimulated neutrophil secretion of IL-1α is independent of GSDMD and mediated through extracellular vesicles

ABSTRACT

Neutrophils are an important source of IL-1β and other cytokines as they are recruited to sites of infection and inflammation in high numbers. Although secretion of processed, bioactive IL-1β by neutrophils is dependent on NLRP3 and Gasdermin D (GSDMD), IL-1α secretion by neutrophils has not been reported. In this study, we demonstrate that neutrophils produce IL-1α following injection of *Aspergillus fumigatus* spores that express cell surface β-glucan. While IL-1α secretion by LPS/ATP activated macrophages and dendritic cells is GSDMD dependent, IL-1α secretion by β-glucan-stimulated neutrophils occurs independently of GSDMD. Instead, we found that bioactive IL-1α is in exosomes that were isolated from cell free media of β-glucan-stimulated neutrophils. Further, the exosome inhibitor GW4869 significantly reduces IL-1α in EVs and total cell-free supernatant. Together, these findings identify neutrophils as a source of IL-1α, and demonstrate a role for extracellular vesicles, specifically exosomes, in neutrophil secretion of bioactive IL-1α.

INTRODUCTION

IL-1α and IL-1β are pro-inflammatory cytokines that lack the signal peptide for ER/Golgi-dependent secretion, and are released by non-canonical pathways (101). Canonical IL-1β secretion by murine macrophages is tightly regulated in a two-step process: signal 1 is induced through pathogen recognition receptors leading to transcription of pro-IL-1α and pro-IL-1β. For IL-1β, a second signal, such as ATP activation of the P2X7 receptor, is required for assembly of the multi-protein NLRP3 inflammasome complex, which mediates caspase-1 processing of proIL-1β to its bioactive form. Caspase-1 also cleaves pro-Gasdermin D (GSDMD) to N-GSDMD subunits that rapidly assemble and form pores in the plasma membrane, leading to passive IL-1β release and pyroptotic cell death (122, 137, 168). While secretion through GSDMD pores appears to be the most rapid means of IL-1β release, GSDMD-independent mechanisms of IL-1β secretion have been reported, including trafficking to the plasma membrane and release through PIP2-rich membrane microdomains (128), and secretory autophagy in which autophagosomes containing mature IL-1β are trafficked to the plasma membrane instead of lysosomes (169, 170).

Neutrophils are also an important source of IL-1β as they are recruited in large numbers to sites of infection and inflammation. Although neutrophils have functional NLRP3 and NLRC4 inflammasomes, unlike macrophages, inflammasome activation in neutrophils does not result in pyroptosis (171–173). Further, while GSDMD is required for IL-1β secretion by neutrophils, N-GSDMD does not localize to the plasma membrane; instead, it is detected in the membrane of primary granules and autophagosomes, and autophagy-related proteins are required for IL-1β secretion (125).

In contrast to IL-1β, there are relatively few studies on IL-1α in infection or inflammation. Gross et al. reported that in a murine model of monosodium urate (MSU)-induced peritonitis, neutrophil recruitment to the peritoneal cavity was significantly impaired in *Il1a*$^{-/-}$ mice (139). Similarly, Caffrey et al. demonstrated impaired neutrophil recruitment to the lungs of *Il1a*$^{-/-}$ mice in a model of pulmonary aspergillosis (140, 174).

In the current study, we found an important role for IL-1α in neutrophil recruitment in a fungal peritonitis model where *A. fumigatus* conidia (spores) are injected into the peritoneal cavity. Further, we show that neutrophils are a source of IL-1α during inflammation. We found that whereas IL-1α secretion by bone marrow-derived dendritic cells (BMDCs) and macrophages is dependent on GSDMD, IL-1α secretion by β-glucan-stimulated neutrophils is mediated through extracellular vesicles, primarily exosomes. Together, these findings identify neutrophils as a source of IL-1α, and define a non-canonical pathway for IL-1α secretion.

MATERIALS AND METHODS

Mice

Male and female C57BL/6J mice aged 6-8 weeks were purchased from The Jackson Laboratory (Bar Harbor, ME). All gene knock-out mice are on a C57BL/6 background. *Gsdmd*$^{-/-}$ mice were provided by Dr. Russell Vance (University of California, Berkeley). *Nlrp3*$^{-/-}$ mice were generated by Millennium pharmaceuticals (Cambridge, MA). *Il1a*$^{-/-}$, *Il1b*$^{-/-}$ and *Il1a*$^{-/-}$*Il1b*$^{-/-}$ mice were originally generated by Dr. Iwakura (University of Tokyo) as described (147) and were graciously provided by Dr. Obar (Dartmouth, New Hampshire; *Il1a*$^{-/-}$, and *Il1a*$^{-/-}$*Il1b*$^{-/-}$), and Dr. Núñez (University of Michigan Medical School; *Il1b*$^{-/-}$). Mice were bred under IACUC approved conditions, and all animals were housed in the University of California, Irvine vivarium. Age-matched, male and female mice were used for all experiments.

Fungal Strains

Virulent *Aspergillus fumigatus* strain CEA10 was provided by Dr. Cramer (Dartmouth, New Hampshire), generated as previously described (174). Frozen glycerol stocks were maintained at -80°C and were grown on Sabouraud Dextrose agar plates (Fisher Scientific) at 37°C with 5% CO_2.

Aspergillus fumigatus peritoneal inflammation model

Conidia from *A. fumigatus* strain CEA10 were incubated in SD broth until they germinated and expressed cell surface b-glucan. Conidia were then heat-killed, and $1x10^7$ were resuspended in 500uL, then injected into the peritoneal cavity of 6- to 10-week-old age- and sex-matched mice. After 4, 6, 8, 12, or 20 hours, total peritoneal cells were collected by intraperitoneal lavage. Cells were kept on ice until processed.

Cell Lines

The HEK-blue IL-1R1 cell-line used in this study is a commercially made cell line by InvivoGen (Cat# hkb-il1r). No sex of the cells is reported and cell authentication can be viewed under the “Data” PDF provided on the manufacturer’s website. Cell vials were stored in a liquid nitrogen chamber until use. For experiments, cells were transferred to a T-75 TC treated flask (Olympus) with 10 mL of warm media supplemented with 1X HEK-Blue Selection (InvivoGen). Flasks were then incubated at 37°C with 5% CO_2. Media was replaced twice a week and cells were passaged once 70-80% confluency was reached. Sterile PBS was used to lift cells for passaging or prepping for assays.

Source Materials for *in vitro* Studies

Bone marrow-derived dendritic cells, peritoneal neutrophils, and peritoneal macrophages used for *in vitro* experiments in this study were all isolated from mice described above. Both female and male animals were used and were 6-10 weeks of age.

METHOD DETAILS

Preparation of Conidia

Aspergillus fumigatus was incubated on SD agar plates at 37°C for 3-5 days. To harvest conidia, 10 mL of PBS containing 0.00025% Tween-20 were added to each plate, and plastic sterile scrapers were used to collect the conidia. Conidia suspensions were then filtered and centrifuged at 500x g. Supernatant was decanted and conidia were resuspended in 5 mL sterile 1x PBS (Corning), and counted using a hemocytometer. To facilitate germination, $1x10^7$/mL conidia were incubated in 200 mL of sterile Sabouraud Dextrose broth (Fisher Scientific) at 37°C with agitation for 3-4hr until ~80% showed

germination by light microscopy (seen as budding of conidia and loss of spherical shape), indicating that they express cell wall b-glucan on the surface. Germinating conidia were centrifuged at 500x g for 5 minutes. Supernatant was decanted and swollen conidia were resuspended in 1x PBS at $1x10^7$ per 500 µL. Conidia were placed in a 50 mL centrifuge tube and were heat killed by submerging tubes in boiling water for 5 minutes. Heat-killed swollen conidia were stored at 4°C until in vivo injections.

Flow Cytometry

Total cell numbers were counted, and cells were stained using mouse Ly6G-BV510 (clone 1A8, BioLegend), Ly6C-PE-Cy7 (clone HK1.4, BioLegend), and F4/80-FitC (clone BM8, BioLegend), IL-1α-PE (clone ALF-161, BioLegend), IL-1β-APC antibodies (clone NJTEN3, Thermo Fisher), and amine-reactive fixable viability dye e780 (Invitrogen, Thermofisher). Cell surface staining was performed at 4°C for 20 minutes. Cells were fixed for 15 minutes at 4°C and then permeabilized for intracellular stain (30 minutes) with Cytofix/Cytoperm kit (BD Biosciences). Flow cytometry and analysis was conducted on ACEA Novocyte instrument and Novoexpress software, respectively. The frequency of Ly6G+ neutrophils, F4/80+ macrophages, and F4/80- Ly6G- $Ly6C^{hi}$ monocytes were multiplied by total cell count to get cell numbers of each cell type.

Bone Marrow-Derived Dendritic Cells

Hind leg femurs and tibias were dissected from mice and were cleaned of tissue. The bones were clipped to expose the bone marrow. Up to four bones were placed in a 0.6 mL microcentrifuge tube (Genesee Scientific) which had a hole pierced through the bottom of it by an 18-gauge needle (Fisher Scientific). This 0.6 mL microcentrifuge tube with bones was capped and placed in a 1.5 mL microcentrifuge tube (Genesee

Scientific) and was centrifuged at 10,000x g for approximately 10 seconds (just enough time for centrifuge to get up to speed, and immediately stopped). Bone marrow was then present in 1.5 mL microcentrifuge tube while the emptied bones remained in the 0.6 mL microcentrifuge tube. The 0.6 mL microcentrifuge tube was discarded, and bone marrow cells were resuspended in 1 mL of warmed RPMI (Gibco). Cells were then placed in T-75 TC culture flasks with 10 mL of RPMI (Gibco) supplemented with 10% FBS (Corning), 1% penicillin-streptomycin (Gibco), 1% non-essential amino acids (Gibco), 1% sodium pyruvate (Gibco), and 10 ng/mL granulocyte-macrophage colony-stimulating factor (StemCell Technologies). Cells were incubated at 37°C with 5% CO_2 for 7 days. Media was replaced every other day. On day 7, semi-adherent cells were gently washed with PBS to lift, and cells were stained for CD11c, Ly6G, F4/80, and viability dye. CD11c+ Ly6G- F4/80- dendritic cells were isolated by BD FACS Aria Fusion flow cytometer.

Peritoneal Neutrophils and Macrophages

Neutrophils: Intraperitoneal injection of 1 mL 9% casein (Sigma Aldrich) was used to induce sterile inflammation in 6- to 10-week-old mice 16 hours prior to collection, and boosted again 3 hours prior to lavage. To collect cells, the peritoneal cavity was flushed with 10 mL PBS and the lavage fluid was centrifuged at 300x g for 5 minutes. Neutrophils were isolated using a negative bead selection kit (StemCell Technologies), which routinely yields >95% neutrophils. Cells were diluted to 2.5 x 10^6 neutrophils/mL and were plated in RPMI (Gibco) supplemented with 10% FBS (Corning), 1% penicillin-streptomycin (Gibco), 1% non-essential amino acids (Gibco), 1% sodium pyruvate

(Gibco), and 10 ng/mL granulocyte-macrophage colony-stimulating factor (StemCell Technologies).

Macrophages: Intraperitoneal injection of 1 mL 9% casein (Sigma Aldrich) was used to induce sterile inflammation in 6- to 10-week-old mice 4 days prior to collection of peritoneal cells. The peritoneal cavity was flushed with 10 mL PBS and the lavage fluid was centrifuged at 300x g for 5 minutes to collect peritoneal cells. Cells were plated overnight at $1x10^6$ cells/mL in DMEM (Gibco) with 10% FBS (Corning), 1% penicillin-streptomycin (Gibco, Life Technologies), 1% non-essential amino acids (Gibco), 1% sodium pyruvate (Gibco), and 10 ng/mL granulocyte-macrophage colony-stimulating factor (StemCell Technologies) for adherence. Non-adherent cells were aspirated the next day, and each well was washed with PBS before adding fresh media. Adherent macrophages were lifted using Cell Stripper (Corning, NY).

In Vitro Stimulation

BMDCs and macrophages were incubated at 5×10^5/mL (neutrophils at 2.5×10^6/mL) with either 100 µg/mL curdlan (Sigma Aldrich), 500 ng/mL ultrapure E. coli LPS (Invivogen), or LPS + 3 mM extracellular ATP (Sigma Aldrich) added in the last hour of incubation. All cells were incubated at 37°C with 5% CO_2.

Flow Cytometry and ImageStream^{TM} Flow Cytometry

Cells were stained using the following fluorophore conjugated anti-mouse antibodies: WGA-488 (Invitrogen), Ly6G-FitC (clone 1A8, BioLegend), Ly6G-BV510 (clone 1A8, BioLegend), Ly6G-PE (clone 1A8, BioLegend), CD11c-BV605 (clone N418, BioLegend), F4/80-FitC (clone BM8, BioLegend), F4/80-PE (clone BM8, BioLegend), CD11b-PE (clone M1/70, BioLegend), Ly6C-PE Cy7 (clone HK1.4, BioLegend), CD63-

APC (clone NVG-2, BioLegend), CD9-APC (clone MZ3, BioLegend), IL-1α-PE (clone ALF-161, BioLegend), and IL-1β-APC (clone NJTEN3, ThermoFisher Scientific). Antibodies were diluted in wash buffer (PBS with 1% BSA and 2 mM EDTA). Cells were stained for 20 minutes at 4°C, washed with wash buffer, fixed for 15 minutes in BD Biosciences cytofix/cytoperm, and permeabilization prior to intracellular staining. ACEA Novocyte was used for flow cytometry, and Novoexpress software was used for subsequent analysis. AMNIS ImageStream™ was used for imaging flow cytometry and the AMNIS IDEAS software was used to calculate the colocalization coefficient.

Western Blot

BMDCs, peritoneal macrophages, or peritoneal neutrophils were lysed with 1X CST lysis buffer (Cell Signaling). For neutrophils, DFP (Sigma Aldrich) was added to the lysis buffer to inhibit any protease activity. BCA assay kit (Thermo Fisher) was used to determine protein concentration from lysates. Twenty µg of protein from lysates mixed with 1X SDS (from 5X stock), and Ultrapure water (Invitrogen) were boiled for 10 minutes at 95°C on a heating block. Samples were loaded into 4-20% mini-PROTEAN, 10-well, 50 µl TGX precast SDS-PAGE gels (Bio-rad). Gels were run in 1X TAE buffer at a constant 110V. Proteins were transferred onto a nitrocellulose membrane using Bio-rad Trans-blot Turbo transfer system. The membrane was blocked with 5% milk for 1 hour at RT, and incubated with rabbit anti-mouse GSDMD (EPR20859, Abcam) or mouse anti-β-actin (Santa Cruz Biotechnology) diluted in 5% milk and incubated at 4°C overnight on a rocker. Membranes were washed with 1X TBST buffer 3x for 10 minutes. HRP-conjugated secondary antibodies against rabbit or mouse IgG (Cell Signaling) were diluted in 5% milk and incubated at RT for 1 hour. West Femto Maximum

Supersignal (Thermo Fisher) was used to enhance signal before the membrane was imaged by the Chemidoc (BioRad) instrument.

Immunofluorescence and Confocal Microscopy

Stimulated neutrophils were collected after 6 hours and stained with Ly6G-FITC antibody (clone 1A8, BioLegend) for 20 minutes. Cells were washed and fixed with 4% PFA (BD Biosciences) overnight. To permeabilize fixed cells, 0.1% TritonX (Fisher Scientific) was used. Cells were incubated with 10% normal donkey serum (NDS, Jackson ImmunoResearch) for 1 hour before addition of primary antibodies: ALF-161 Armenian hamster anti-mouse IL-1α (Fisher Scientific), and rabbit anti-mouse CD63 (clone EPR21151, Abcam). Primary antibodies were incubated overnight at 4°C. Cells were washed twice with FACS buffer (PBS with 1% BSA and 2 mM EDTA). AF546 goat anti-hamster IgG (ThermoFisher Scientific) and AF647 donkey anti-rabbit IgG (ThermoFisher Scientific) secondary antibodies were added and incubated at room temperature for 30 minutes. 4 µL of cells were mixed with 4 µL of Vectashield® antifade mounting media with DAPI (Vector Laboratories) and plated on a coverslip. Imaging was done using an LSM700 confocal microscopy (Optical Biology Core, UCI, Leica LSM700) and analyzed with Zen software.

Cytokine analysis

ELISA was used for quantification of cytokines in cell-free supernatant and lavage fluid. Cells were centrifuged at 300x g for 5 minutes and the supernatant was collected and stored at -80°C. Murine IL-1α and IL-1β ELISA kits were purchased from R&D Systems. A Biotek Cytation-5 plate reader was used to quantify concentrations.

HEK-blue IL-1R1 cell-line used to measure IL-1a and IL-1β bioactivity was purchased from InvivoGen. For each experiment, $2.8x10^5$ HEK IL-1R1 reporter cells/mL in DMEM (Gibco) complete media were seeded in 180 µL per well. Twenty µL of each sample was added in duplicates without neutralizing antibodies, with anti-IL-1α neutralizing antibodies (Fisher Scientific), anti-IL-1β neutralizing antibodies (R&D Systems), or both and incubated overnight at 37°C with 5% CO_2. The supernatant was collected and incubated with QUANTI-Blue (InvivoGen) for 30 minutes. SEAP detection and concentration calculations were measured on the Biotek Cytation-5 instrument. IL-1a and IL-1β concentrations were calculated based on a set of standards of known bioactive IL-1a and IL-1β concentrations and presented as pg/mL.

Lactate Dehydrogenase (LDH) Assay for Cell Death

Promega CytoTox 96® Non-radioactive Cytotoxicity Assay was used to measure LDH release in cell-free supernatant. Released LDH in culture supernatants was measured with a 30-minute coupled enzymatic assay, which results in conversion of a tetrazolium salt (INT) into a red formazan product. Maximum LDH control was prepared by lysing the same concentration of cells in each experiment with lysis buffer from the Promega kit for 15 minutes prior to collection. LDH read was measured at 490nm with a Biotek Cytation-5 instrument. The % of max LDH release was calculated by dividing the LDH read from each sample by the maximum LDH control read. The maximum LDH control was prepared for each individual experiment.

Propidium Iodide (PI) Uptake Assay for Plasma Membrane Permeability

Cells were plated in a black-sided, optically clear flat bottom 96-well plate (Corning). PI (Alfa Aesar) was added to each well at 1:10,000 dilution in PBS. Cells were incubated

in the Biotek Cytation-5 instrument at 37°C with 5% CO_2. Red fluorescence reads at 590/640nm were measured every 1 minute for 5 minutes for background measurement before adding stimulation. Duplicate wells of cells were primed with 500 ng/mL E. coli LPS (Invivogen) or 100 µg/mL curdlan (Sigma Aldrich) for 6 hours. Three mM extracellular ATP (Sigma Aldrich) was added to LPS primed cells in the last hour of incubation in the LPS+ATP conditions. Fluorescence measurements were taken at 1-minute intervals throughout stimulation.

Extracellular Vesicle Isolation

Peritoneal neutrophils were cultured in RPMI (Gibco) supplemented with 10% exosome-depleted FBS (Systems Biosciences, SBI) containing 1% penicillin-streptomycin, 1% non-essential amino acids, 1% sodium pyruvate, and 10 ng/mL granulocyte-macrophage colony-stimulating factor (StemCell Technologies). After 6 hours of stimulation, 200 µL of ExoQuick-TC reagent (System Biosciences, SBI) was added to 1 mL of cell-free supernatant from cultured neutrophils and was inverted to mix. The supernatant was incubated overnight at 4°C, and extracellular vesicles were recovered after centrifugation (1500x g for 30 minutes at 4°C). Supernatant was aspirated and dry pellets were resuspended in 1 mL PBS and frozen at -20°C for short-term storage.

Nanoparticle Tracking Analysis and flow cytometry of EVs

A Malvern Nanosight NS300 was used for nanoparticle tracking analysis of isolated EVs. EVs suspended in PBS (700uL) was used to measure 3 technical replicates, measuring size distribution and concentration from 60-seconds video (approximately 10^7-10^8 particles/mL concentration) with constant syringe flow. For flow cytometry analysis, EVs were stained and detection threshold on the ACEA Novocyte instrument

was lowered to 1000 on the FSC. For ELISA, resuspended EV pellets were lysed with 1% Triton X (Fisher Scientific) and loaded into a 96-well plate followed by the standard ELISA protocol from R&D Systems.

Exosome Isolation by Differential Ultracentrifugation

Neutrophils stimulated for 6 hours with LPS, LPS/ATP, or curdlan were pelleted at 300x g, 4°C for 5 minutes. The cell-free supernatant was then centrifuged at 2000x g, 4°C for 10 minutes to pellet dead cells and debris. Next, the supernatant was centrifuged at 10,000x g and the pellet (microvesicles and cell debris) was discarded. The remaining supernatant was ultracentrifuged at 100,000x g, 4°C for 70 minutes and the pellet was washed three times with PBS before resuspension in PBS for further analysis.

QUANTIFICATION AND STATISTICAL ANALYSIS

Statistical analysis was determined by ordinary one-way ANOVA with Dunnett's multiple comparisons test, or by 2-way ANOVA with Tukey's multiple comparisons test (detailed in figure legends) using GraphPad Prism software. Error bars indicate mean ± SEM and p values less than 0.05 were considered significant.

RESULTS

Neutrophil recruitment is dependent on IL-1α, and neutrophils are a source of IL-1α in *A. fumigatus*-induced peritonitis

To examine the role of IL-1α in neutrophil recruitment, we repeated the experiments by Gross et al., and also found impaired neutrophil recruitment in *Il1a*$^{-/-}$ and *Il1a/b*$^{-/-}$ mice compared with C57BL/6 wild-type (**WT**) mice following intraperitoneal (**ip**) injection of MSU (2 mg/mouse); there was no difference in monocyte numbers (**Figure S1A,B)**. As we are interested in the response against fungal infection, we repeated the experiment using a model of peritonitis where 1x10^{7} *Aspergillus fumigatus* germinating conidia (spores) expressing cell surface β-glucan were heat killed and injected into the peritoneal cavity of WT, *Il1a*$^{-/-}$, *Il1b*$^{-/-}$, and *Il1a*$^{-/-}$/ *Il1b*$^{-/-}$ double knock-out (DKO) mice. Neutrophils, monocytes, and macrophages were quantified by flow cytometry after 4 hours (gating strategy is shown in **Figure S1C**). We found that *A. fumigatus* conidia induced infiltration of 7x10^{6} neutrophils compared with 4x10^{5} monocytes, and that *Il1a*$^{-/-}$, *Il1b*$^{-/-}$, and DKO mice had significantly fewer neutrophils than WT mice (**Figure 1A, B**). In contrast to neutrophils, there were no significant differences in the number of monocytes and macrophages recruited to the peritoneal cavity of *Il1a*$^{-/-}$, *Il1b*$^{-/}$, or DKO mice compared to WT (**Figure 1B, S1D**).

We next examined if neutrophils were a source of IL-1α by examining intracellular IL-1α and IL-1β following ip injection of *A. fumigatus* conidia. IL-1α and IL-1β MFI levels peaked at 6 hours post injection (**Figure 1C, D**), and secreted IL-1α in the peritoneal lavage was highest at earlier time points (**Figure S1E**). Representative MFI

of intracellular IL-1α and IL-1β in neutrophils at 6 hours showed increased production of both cytokines over fluorescent minus one (FMO) control (**Figure 1E**).

Collectively, these data identify neutrophils as a source of IL-1α. Though IL-1β production was 10-fold higher than IL-1α, elimination of IL-1α yields a similar phenotype as IL-1β, indicating that even the relatively low levels of IL-1α are important in this model of inflammation.

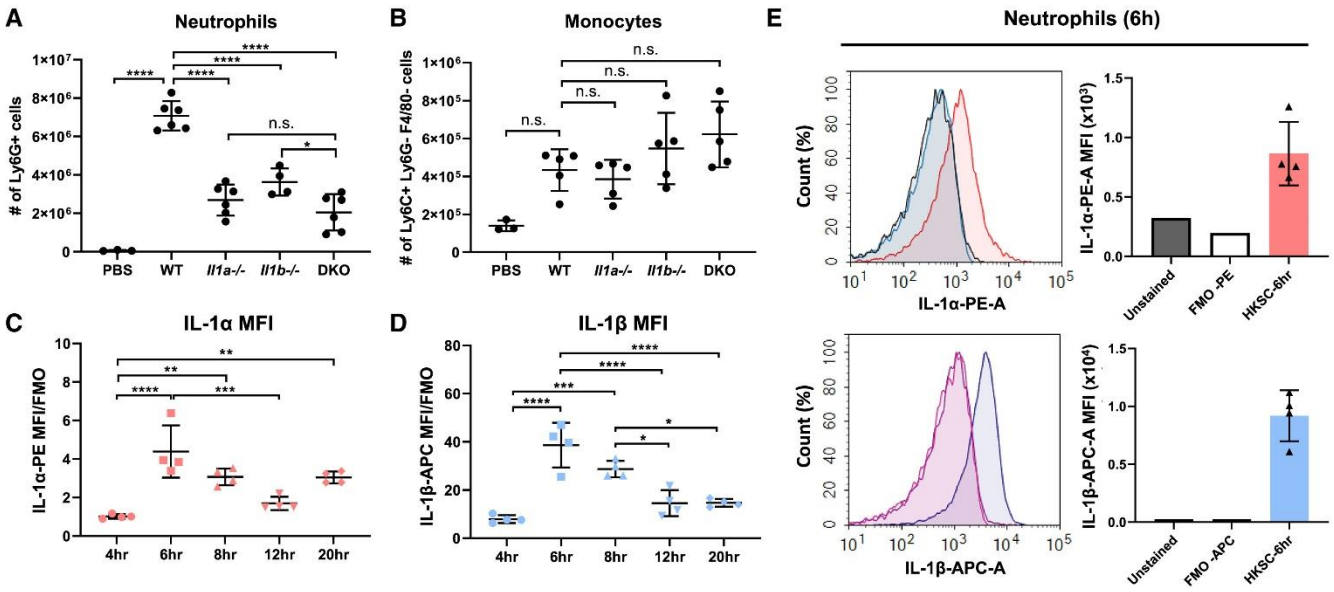

Figure 3.1: Neutrophils are a source of IL-1α in *A. fumigatus*-induced peritonitis

(**A** and **B**) Neutrophils (**A**) and monocytes (**B**) were quantified by flow cytometry 24 h after i.p. injection of heat-killed *A. fumigatus* conidia into WT, IL-1α$^{-/-}$, IL-1β$^{-/-}$, or IL-1α$^{-/-}$/IL-1β$^{-/-}$ DKO mice. Cell numbers shown are percentage of each cell type × total cell count.

(**C** and **D**) MFI of intracellular IL-1α (**C**) and IL-1β (**D**) in neutrophils from the peritoneal cavity at multiple time points after injection of *A. fumigatus* conidia. IL-1α MFI and IL-1β MFI were normalized to FMO control (n = 4).

(**E**) Representative histogram and corresponding MFI levels after 6-h incubation (n = 4). Each data point represents an individual mouse. Experiments were repeated twice with similar results.

Significance was calculated by one-way ANOVA followed by Dunnett's multiple comparisons test. $^{*}p < 0.05$, $^{**}p < 0.01$, $^{***}p < 0.001$, $^{****}p < 0.0001$.

Distinct roles for GSDMD in IL-1α secretion by dendritic cells, macrophages, and neutrophils

As secretion of IL-1α is not well defined, we examined IL-1α production by neutrophils compared to macrophages and BMDCs. Cells were incubated for 6h with LPS or insoluble β-glucan (curdlan). LPS and curdlan induced IL-1α+IL-1β+ populations of macrophages, BMDCs, and neutrophils, although curdlan was more effective at activating neutrophils (**Figure 2A, B**). MFI levels in neutrophils were lower than macrophages and BMDCs, indicating that neutrophils produce less IL-1α on a per cell basis (**Figure 2C**). However, neutrophils are the majority of infiltrating cells in inflamed tissues and are therefore an important source of IL-1α under these conditions.

As IL-1α is co-expressed with IL-1β in BMDCs, macrophages, and neutrophils (**Figure 2A-C**), we next addressed whether IL-1α secretion follows the same mechanism as IL-1β. To examine the role of GSDMD in IL-1α secretion, we quantified IL-1α secreted by WT, *Gsdmd*$^{-/-}$, and *Nlrp3*$^{-/-}$ cells following stimulation with LPS, LPS/ATP or curdlan. FACS isolated BMDCs (≥99% CD11c+ F4/80- Ly6G-) and ip macrophages (≥95% F4/80+) primed with LPS and stimulated with ATP induced high levels of IL-1α and IL-1β secretion in WT, but not *Gsdmd-/-* and *Nlrp3-/-* cells (**Figure 2D-G**). BMDCs and macrophages secreted relatively low levels of IL-1α and IL-1β in response to curdlan compared to LPS+ATP stimulation.

In contrast to BMDCs and macrophages, enriched ip neutrophils (≥97% Ly6G+) secreted the highest levels of IL-1α in response to curdlan. Further, while IL-1β secretion by neutrophils was dependent on GSDMD and NLRP3, there was no significant difference in IL-1α secretion between WT, *Gsdmd*$^{-/-}$, and *Nlrp3*$^{-/-}$ cells (**Figure**

2H, I). Surprisingly, we found IL-1β production in the absence of additional stimulation (**Figure 2I**), which is likely a consequence of NLRP3 activation of neutrophils isolated from the peritoneal cavity following casein injection.

In contrast to IP neutrophils, stimulated bone marrow (BM) neutrophils had <15% intracellular IL-1α+IL-1β+, and secreted <80 pg/mL IL-1α in response to LPS+ATP (**Figure S2A, B**). IL-1α secretion by BM neutrophils is GSDMD dependent, however, they are not responsive to curdlan. Consistent with reports that neutrophils recognize b-glucan via the lectin binding domain of CR3 (CD18/CD11b) (45, 175), we found that BM neutrophils do not express plasma membrane CD18, and have lower levels of CD11b than ip neutrophils **(Figure S2C, D)**. Consequently, BM neutrophils did not secrete IL-1α when stimulated with depleted zymosan or *A. fumigatus* hyphal extracts (**Figure S2E**).

Together, these data show that IL-1α secretion by LPS/ATP stimulated BMDCs and macrophages is dependent on NLRP3 and GSDMD. In contrast, β-glucan-induced IL-1α secretion by CR3 expressing neutrophils is GSDMD independent.

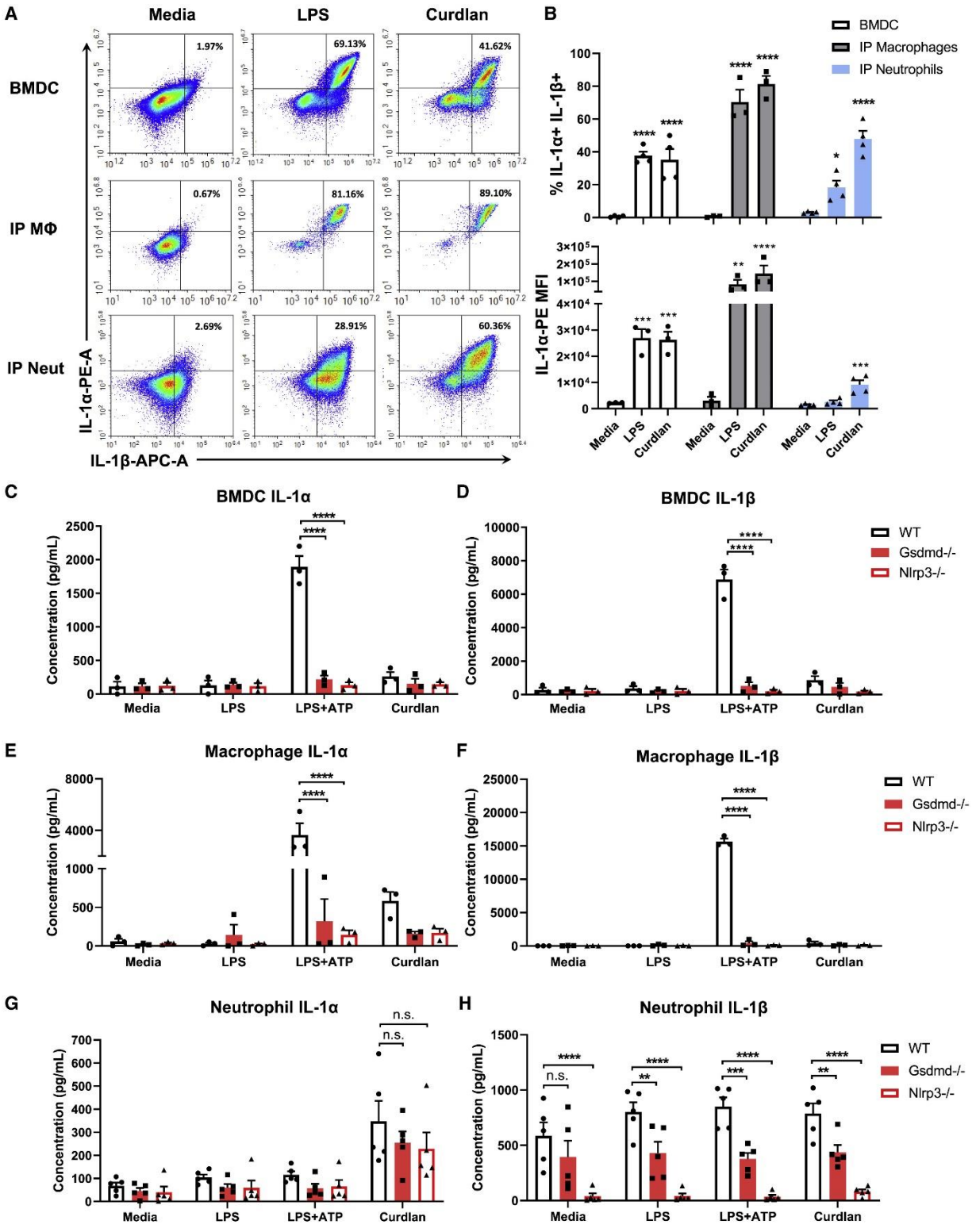

Figure 3.2: IL-1α secretion by bone-marrow-derived dendritic cells, peritoneal macrophages, and neutrophils

(**A**) Representative flow cytometry plots of intracellular IL-1α and IL-1β in BMDCs, macrophages, and neutrophils following 6-h stimulation with LPS or β-glucan (curdlan). (**B**) Quantification of percent IL-1α^{+}/IL-1β^{+} cells (B) and IL-1α MFI (C) (n = mean of total cells in 3 independent experiments).

(**C–H**) IL-1α and IL-1β secretion by BMDCs, macrophages, and neutrophils from WT, *Gsdmd*$^{-/-}$, and *Nlrp3*$^{-/-}$ mice. (**C** and **D**) FACS-isolated CD11c^{+} Ly6G^{-} F4/80^{-} BMDCs (n = 3), (**E** and **F**) peritoneal macrophages (≥95% F4/80^{+}, n = 3), and (**G** and **H**) neutrophils (≥98% Ly6G^{+}, n = 5).

Significance was calculated by two-way ANOVA with Tukey's multiple comparisons test. $^{*}p < 0.05$, $^{**}p < 0.01$, $^{***}p < 0.001$, $^{****}p < 0.0001$.

β-glucan induces pro-GSDMD cleavage and increased membrane permeability, but not cell death

IL-1α is passively released through cell death in non-hematopoietic cells (136, 145), and GSDMD-dependent IL-1β secretion by macrophages results in pyroptotic cell death (123). Therefore, we next examined GSDMD cleavage, membrane permeability, and pyroptotic cell death.

BMDCs, ip macrophages, and ip neutrophils were examined by western blot for pro- and N-GSDMD. We found that in all cell types incubated with LPS+ATP or curdlan, pro-GSDMD was cleaved to the 31kDa N-GSDMD (**Figure 3A-C**). Consistent with GSDMD cleavage, propidium iodide (PI) uptake, indicative of plasma membrane permeability, was observed following ATP activation of LPS-primed BMDCs and macrophages, but not neutrophils (**Figure 3D-F**). Although curdlan did not induce PI uptake in BMDCs, we observed a gradual increase in PI uptake in macrophages and neutrophils. Lactate dehydrogenase (LDH) release (indicative of cell lysis) was elevated in LPS/ATP but not β-glucan stimulated DCs or macrophages (**Figure 3G,H**). However, there was no significant increase in LDH release by neutrophils under any of these conditions (**Figure 3I**).

Collectively, these findings demonstrate that β-glucan induces GSDMD cleavage in each of these cell types, and increased plasma membrane permeability in macrophages and neutrophils, but does not lead to LDH release, indicating that β-glucan mediated IL-1α and IL-1β secretion occurs in the absence of pyroptotic cell death.

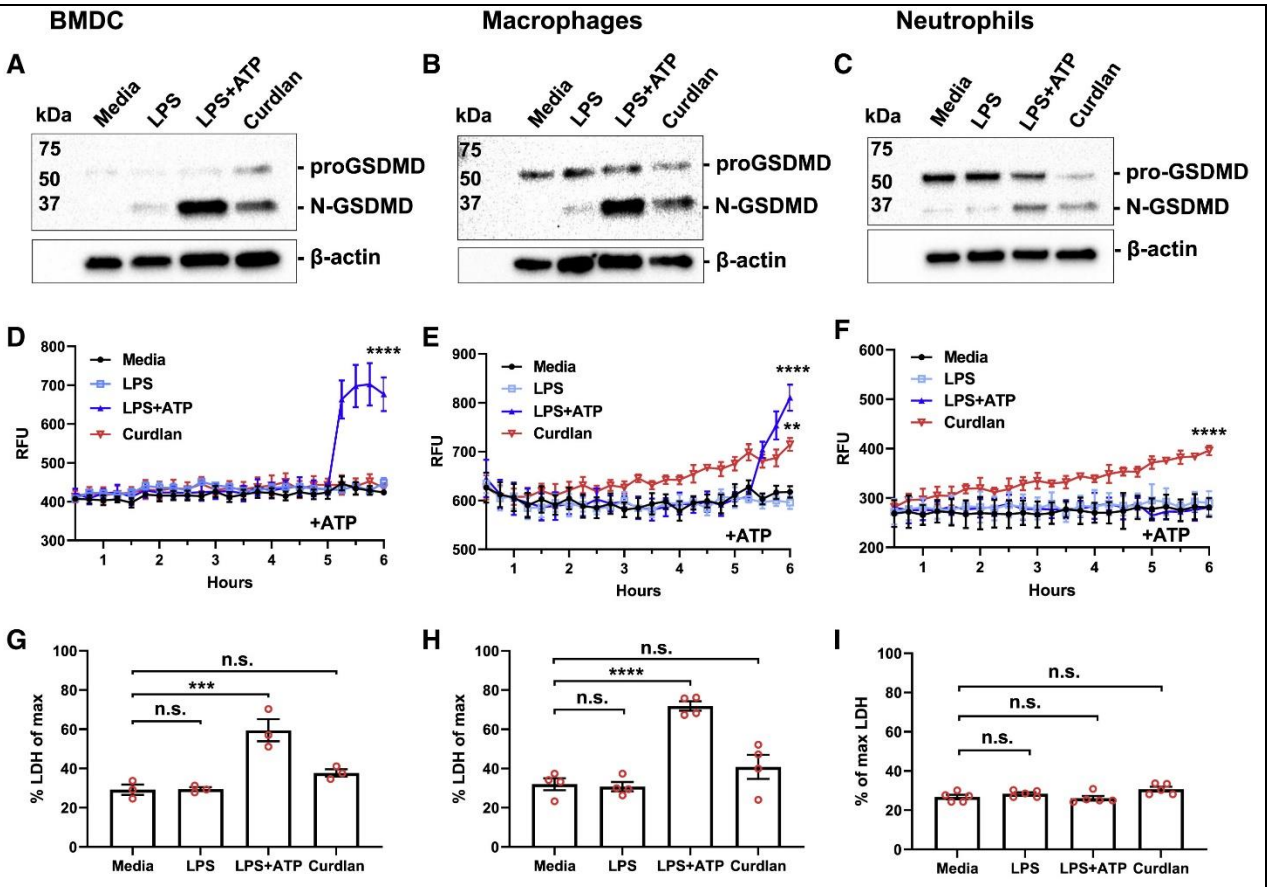

Figure 3.3: β-Glucan induced GSDMD cleavage and increased membrane permeability, but not cell death

(**A–C**) Western blot analysis of GSDMD cleavage following 6-h stimulation with LPS, LPS/ATP, or curdlan in BMDCs (**A**), macrophages (**B**), and neutrophils (**C**).

(**D–F**) Propidium iodide (PI) uptake measured over 6 h in each cell type.

(**G–I**) Lactate dehydrogenase (LDH) release after 6-h incubation as a measure of cell death was calculated as percent of maximum (lysed cells). Two-way ANOVA with Tukey's multiple comparisons test was used for PI uptake, and one-way ANOVA with Dunnett's multiple comparisons test for LDH release.

$^{*}p < 0.05$, $^{**}p < 0.01$, $^{***}p < 0.001$, $^{****}p < 0.0001$. Western blots are representative of three repeat experiments; PI and LDH data points represent 3–5 biological replicates.

Neutrophil IL-1α is released through extracellular vesicles

Given that IL-1α release by stimulated neutrophils is independent of GSDMD and cell death, we examined other unconventional secretion pathways. Extracellular vesicles (EVs) have emerged as an important mechanism for inter-cellular communication. While most cells secrete EVs at steady state, their cargo and number depends on the stimulus (176–178). EV-mediated cytokine release has been described in multiple cells and tissues (179). However, the role of EVs in mediating IL-1α secretion has not been clearly defined.

To determine if IL-1α is secreted in EVs, and specifically in exosomes, we first examined if IL-1α localizes with the exosome marker CD63 in stimulated neutrophils. Representative confocal microscopy images and quantification using ImageJ showed colocalization of IL-1α and CD63, most notably in curdlan-stimulated neutrophils (**Figure 4A, B, S3A**). Imaging flow cytometry also revealed co-localization of IL-1α with CD63 in 17-24% of stimulated neutrophils (**Figure S3B**).

Second, we examined isolated EVs using the ExoQuick-TC^{TM} kit, which enriches for exosomes by co-precipitation with polymers. EVs were characterized by Nanoparticle tracking analysis (NTA), surface expression of CD63, CD9, and CD81, and inhibition with GW4869. NTA has been used extensively to characterize and quantify EVs (180–182). NTA showed that most neutrophil-isolated EVs were within the size range of exosomes and small microvesicles (100-200nm, **Figure 4C**). Flow cytometry also showed that exosome markers CD63, CD9, and CD81 were each expressed on isolated EVs from unstimulated and stimulated neutrophils, indicating that exosomes are a major component of this EV population (**Figure 4D, S3C**). However, IL-1α was not

detected on the surface of EVs (**Figure S3D**). As a third approach, neutrophils were incubated with GW4869, a neutral sphingomyelinase inhibitor that effectively inhibits exosome release (Essandoh et al., 2015; Jiang et al., 2019; Sitrin et al., 2011, **Figure 4E**). These findings indicate that exosomes are a major component of EVs secreted by neutrophils.

To determine whether EVs contain IL-1α and IL-1β, neutrophil EVs from LPS, LPS/ATP or curdlan-stimulated neutrophils were lysed, and IL-1α and IL-1β were quantified by ELISA. We found both cytokines in lysed EVs and in total cell-free supernatant (containing intact EVs; **Figure 4F-I**). EVs from curdlan-stimulated neutrophils had significantly higher levels of IL-1α and IL-1β compared to unstimulated neutrophils (**Figure 4F,H**). We also isolated EVs by ultracentrifugation (100,000xg), and detected IL-1α and IL-1β in exosomes from curdlan-stimulated neutrophils (**Figure S4A**).

Pre-incubation with GW4869 resulted in significantly reduced IL-1α, but not IL-1β, secretion by curdlan-stimulated neutrophils, indicating that IL-1α is secreted in exosomes (**Figure 4F-I**). IL-1α secretion in total supernatants and EVs of curdlan-stimulated neutrophils increased over 24h, although there was also a small increase in neutrophil cell death at later time points (**Figure S4B,C**). We also found that neutrophils incubated with GW4869 exhibited no difference in intracellular IL-1α and IL-1β, indicating that this inhibitor selectively blocks IL-1α secretion but not production (**Figure S4D-F**). Although we expected to find an increase in IL-1α, it is likely that the increase on a per cell basis is minor and not reflected well by MFI.

Given that pro-IL-1α is bioactive whereas IL-1β bioactivity requires processing, we next determined whether IL-1α and IL-1β in intact EVs are bioactive. Isolated EVs from stimulated neutrophils were incubated with HEK293T IL-1R1 reporter cells in the presence of neutralizing antibodies to IL-1α, IL-1β, or both. The concentration of bioactive IL-1 was calculated based on a standard curve using recombinant cytokines. We found that EV-encapsulated IL-1 can signal its surface receptor (**Figure 4J**). IL-1R1 activation by LPS/ATP-stimulated neutrophils was mediated by IL-1α and IL-1β, but curdlan-stimulated neutrophil EVs was primarily mediated by IL-1α. This finding implies that the IL-1β detected in curdlan-stimulated neutrophil EVs by ELISA was not bioactive.

Finally, we found that cytokines CXCL1 and TNF-α that follow the canonical Golgi/ER secretion pathway were not detected in isolated EVs, and that GW4869 had no inhibitory effect on their secretion (**Figure S4G, H**). Collectively, these findings identify a selective role for exosomes in secreting bioactive IL-1α.

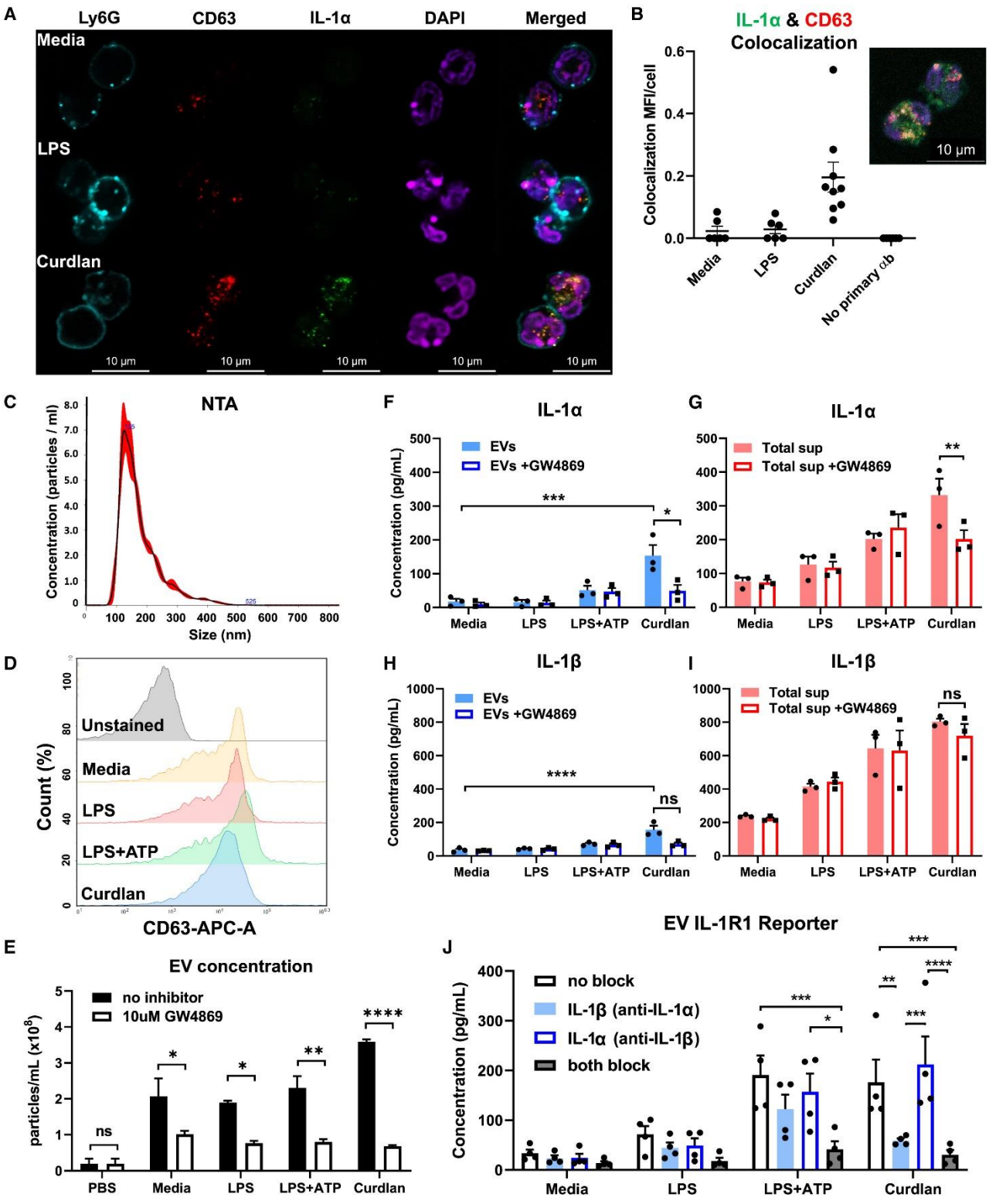

Figure 3.4: Exosomal release of IL-1α by neutrophils

(**A**) Representative confocal images of peritoneal neutrophils stimulated with LPS or curdlan for 6 h.

(**B**) Quantification of IL-1α and CD63 co-localization using ImageJ (each data point represents a single cell).

(**C**) NTA of EV size distribution and concentration.

(**D–G**) Neutrophils were stimulated in the presence of exosome inhibitor GW4869, and IL-1α and IL-1β were quantified by ELISA in isolated EVs following lysis (D and F) and in total cell-free supernatants (**E** and **G**).

(**H**) Inhibition of EV secretion shown by NTA.

(I) Bioactive IL-1 signaling through IL-1R1 reporter cells was measured in isolated exosomes in the absence of detergent lysis (n = 4). Neutralizing antibodies (Abs) to IL-1α, IL-1β, or both cytokines were included in the reporter assay, and bioactive cytokine concentration was calculated based on a standard curve using recombinant IL-1α and IL-1β.

Two-way ANOVA with Tukey's multiple comparisons test. $^{*}p < 0.05$, $^{**}p < 0.01$, $^{***}p < 0.001$, $^{****}p < 0.0001$. Experiments in (**A**) and (**B**) were repeated three times; (**C-G**) are biological replicates from repeat experiments.

DISCUSSION

We and others have reported that neutrophils are an important source of IL-1β during bacterial and fungal infection. In this study, we now show that neutrophils also produce IL-1α. We demonstrated that IL-1α plays an important role in neutrophil recruitment to the peritoneal cavity following injection of *A. fumigatus* conidia expressing surface β-glucan. Initial recruitment of neutrophils following ip injection of casein is likely due to pro-inflammatory and chemotactic cytokines produced by resident macrophages and epithelial cells. However, neutrophils are also a major source of IL-1α, which likely mediate further neutrophil infiltration in a feed-forward mechanism.

Consistent with the response to *A. fumigatus*, we found that particulate β-glucan (curdlan) induced IL-1α secretion by ip neutrophils whereas macrophages and BMDCs (and BM neutrophils) produced more IL-1α in response to LPS/ATP. We and others reported that neutrophils recognize β-glucan by CR3 (CD11b/CD18) (45, 92, 186). Here, we identified a key difference between BM and ip neutrophils where BM neutrophils lack a functional CR3 and do not respond to fungal products.

IL-1α secretion has mostly been studied as an alarmin that is released from non-hematopoietic cells following cell death (136). In contrast, there are relatively few reports on IL-1α secretion by myeloid cells. A recent study showed that *Staphylococcus aureus* can induce GSDMD-dependent IL-1α and IL-1β secretion by macrophages (137). Here, we also found that IL-1α secretion by LPS/ATP-stimulated macrophages (and BMDCs) requires GSDMD. In contrast, IL-1α secretion by β-glucan-stimulated ip neutrophils was independent of GSDMD. We have reported that β-glucan induce caspase-1 and caspase-11 dependent IL-1β secretion in the absence of cell death (Sun

et al., 2018). Similarly, we found in the current study that β-glucan did not induce cell death in any cell type examined despite increased membrane permeability in macrophages and neutrophils.

Further, we show that instead of secretion through GSDMD pores, IL-1α secretion by β-glucan-stimulated neutrophils is mediated by exosomes. Although co-localization of IL-1α with the tetraspanin CD63 measured by Amnis ImageStream^{TM} was only in approximately 20% of neutrophils, this only measures complete localization and might have excluded cells with partial localization. Moreover, neutrophil heterogeneity could account for the differences seen. Taken together with detection of IL-1 in isolated exosomes and that pre-incubating neutrophils with the GW4869 inhibitor blocked exosome production and inhibited IL-1α, but not IL-1β secretion, we conclude that exosomes are an important mechanism of IL-1α secretion by neutrophils. We also demonstrated using IL-1R1 reporter cells that exosomal IL-1α is bioactive.

Although IL-1β secretion was not inhibited by GW4869, it is possible that IL-1β is present in microvesicles given that isolation of exosomes can include other vesicles in the same size range. Consistent with this possibility, ATP activation of the P2X7 receptor on THP-1 monocytes induced secretion of microvesicles containing IL-1β within minutes (187). Further, as cleaved IL-1β in macrophages triggers its relocation to PIP_2-enriched plasma membrane domains (128), it is possible that membrane-associated IL-1β is released in microvesicles.

As IL-1α was not detected on the surface of EVs, it is not clear how IL-1α activate IL-1R1. It is possible that encapsulated cytokines are released when EVs come close to their target cell as liposomes become leaky (188). Alternatively, human

neutrophils secrete phospholipase A_2 in response to fMLP stimulation (189), which could degrade the EVs. Future studies will examine the role of phospholipases in this process.

In conclusion, our data clearly identify EVs as an important mechanism of IL-1α secretion by neutrophils, but EVs are likely not the only mechanism by which this cytokine is secreted. We will continue to examine additional pathways. Nonetheless, results from the current study clearly identified neutrophils as a source of IL-1α following injection of *A. fumigatus* conidia, and adds to our understanding of IL-1α regulation during the inflammatory process.

Supplementary Figures

Supplementary figure 1

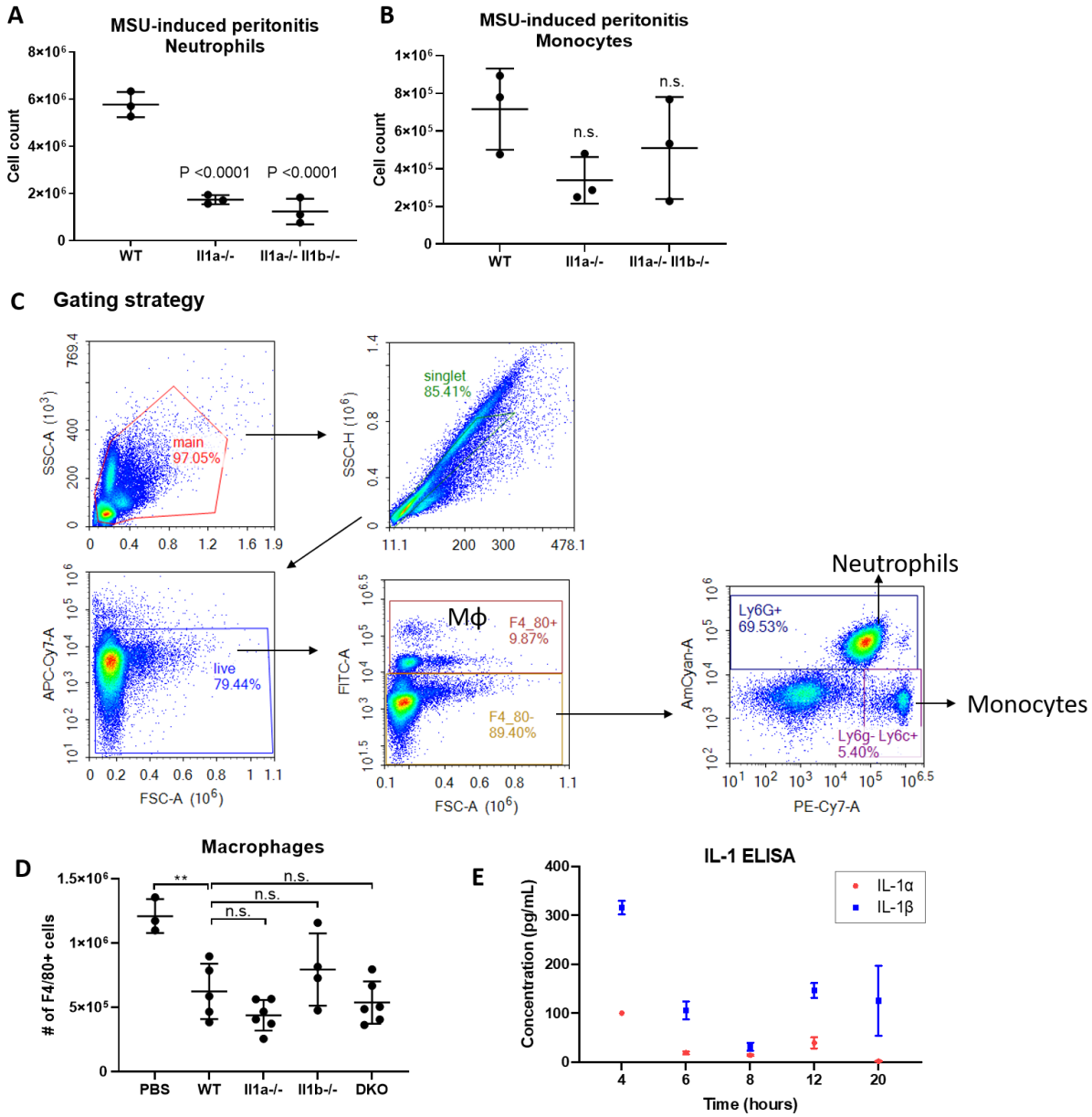

Supplementary Figure 1. IL-1α is important for neutrophil recruitment. Related to Figure 1.
(A, B) Neutrophil and monocyte cell count quantified 4h after intraperitoneal injection of 2 mg/ mouse monosodium urate (MSU) into C57BL/6 (WT), IL-1α$^{-/-}$, and IL-1α$^{-/-}$/IL-1β$^{-/-}$ mice (n=3).
(**C**) Representative flow cytometry plots demonstrating gating strategy for live, singlet F4/80+ macrophages, F4/80- Ly6G+ neutrophils, and F4/80- Ly6G- Ly6C+ monocytes.
(**D**) F4/80+ macrophage cell counts from the peritoneal cavity of mice injected with swollen, heat killed *A. fumigatus* conidia.
(**E**) IL-1α and IL-1β concentration from the peritoneal lavage fluid at multiple time points following injection of heat-killed *A. fumigatus* conidia (n=3).

Supplementary Figure 2

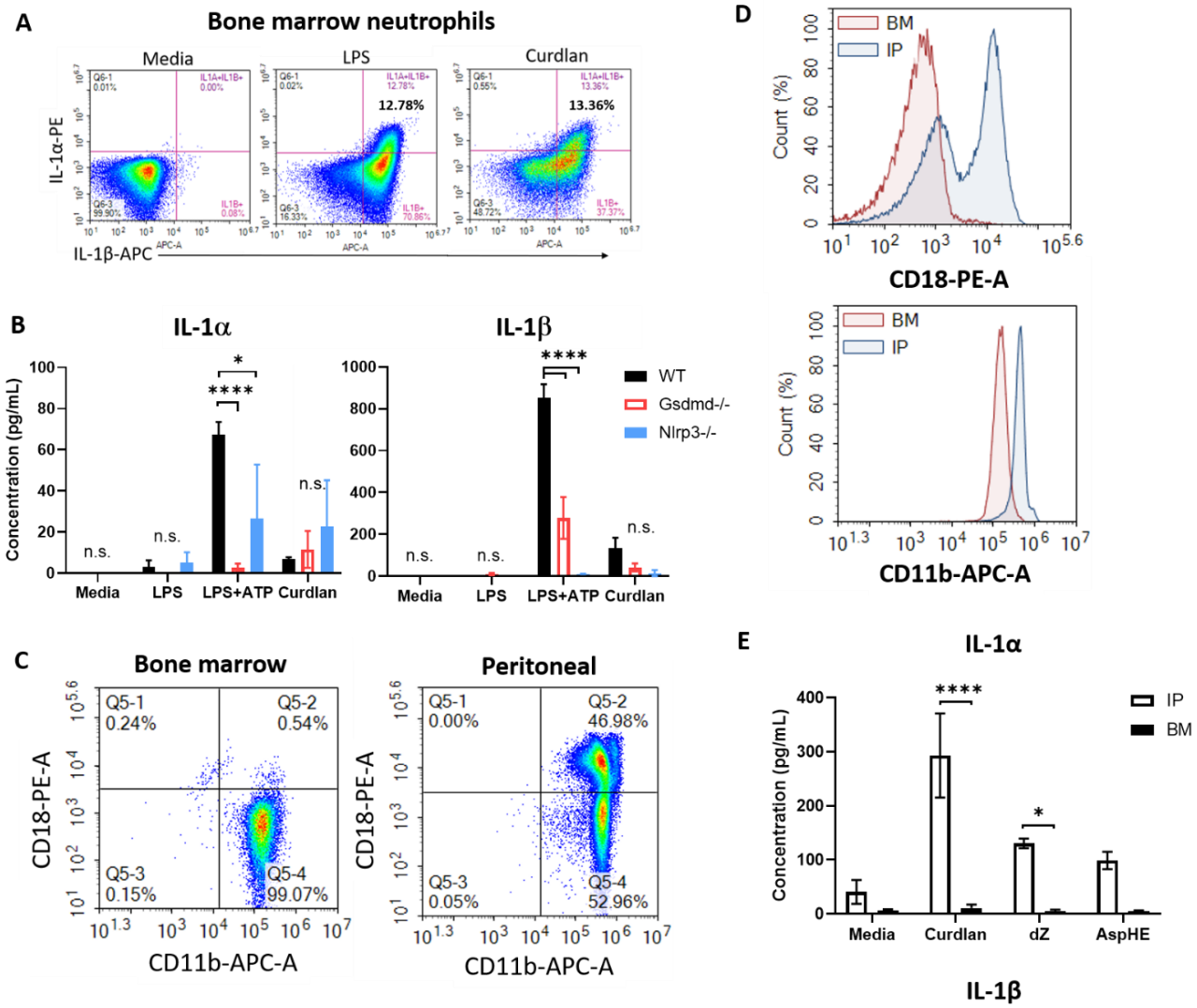

Supplementary Figure 2. IL-1α and IL-1β production by bone marrow neutrophils. Related to Figure 2.

(**A, B**) Intracellular and secreted IL-1α and IL-1β following 6h stimulation with LPS, LPS/ATP (ATP added in the last hour) or β-glucan (curdlan).

(**C, D**) Representative scatter plots and histogram of CD18 and CD11b on the plasma membrane of neutrophils from the peritoneal cavity following casein injection, or bone marrow of naïve mice.

(**E**) β-glucan secretion of IL-1α and IL-1β by BM compared with peritoneal (IP) neutrophils in response to curdlan, depleted zymosan (dZ), or *A. fumigatus* hyphal extract (AspHE).

Supplementary Figure 3

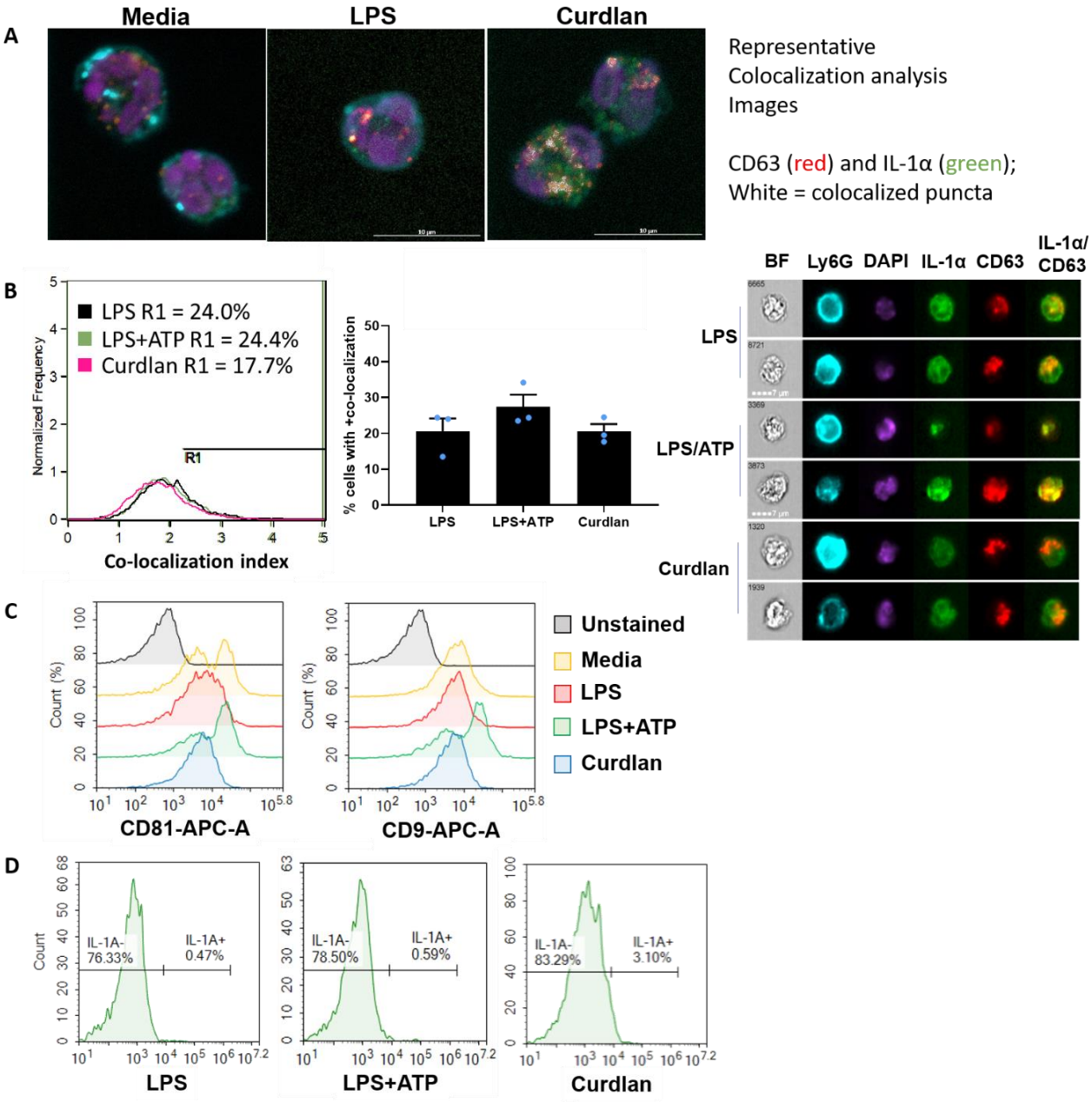

Supplementary Figure 3. Characterization of extracellular vesicles from peritoneal neutrophils. Related to Figure 4.

(**A**) Co-localization analysis by ImageJ of CD63 and IL-1α in unstimulated, LPS- or curdlan-stimulated peritoneal neutrophils. CD63 (red) and IL-1α (green); colocalization of CD63 and IL-1α is shown in white.
(**B**) Representative Amnis ImageStream™ images (left) showing plasma membrane Ly6G and intracellular CD63/IL-1a. Colocalization coefficient of CD63/IL-1a (center panel), and percent co-localization (right panel) of neutrophils stimulated with LPS, LPS/ATP, or curdlan (n=3)
(**C**) Flow cytometry of representative isolated EVs stained with exosome markers CD81 or CD9
(**D**) Representative flow histogram showing no IL-1α on membrane of isolated EVs

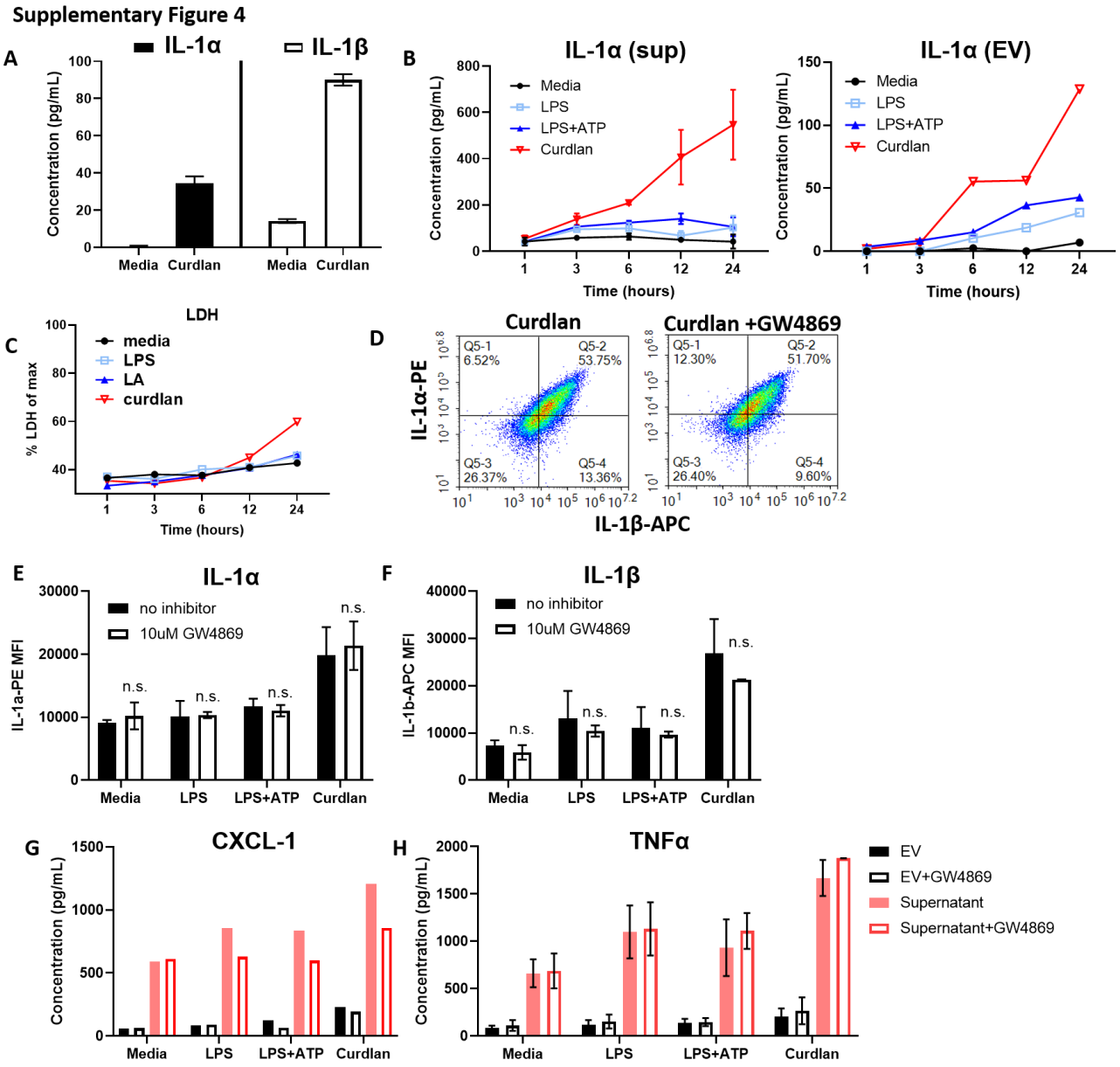

Supplementary Figure 4. IL-1α secretion through EVs increase over time, and GW4869 does not affect intracellular IL-1α or IL-1β production. Related to Figure 4.

(**A**) IL-1α and IL-1β produced by neutrophil exosomes isolated by differential ultracentrifugation (pellet at 100,000xg) and lysed by Triton-X100

(**B**) Total IL-1α (left) and lysed EV IL-1α (right) time course of secretion by neutrophils stimulated with LPS, LPS/ATP, or curdlan for 1, 3, 6, 12, and 24 hours.

(**C**) LDH release time course from neutrophils stimulated for 1, 3, 6, 12, and 24 hours.

(**D**) Representative flow cytometry plots of intracellular IL-1α-PE and IL-1β-APC in GW4869-pre treated neutrophils showing no effect of the inhibitor on intracellular staining.

(**E,F**) MFI quantification of intracellular IL-1α-PE and IL-1β-APC in GW4869-treated neutrophils

(**G, H**) CXCL1 and TNFα is not present in EVs or blocked by the exosome inhibitor GW4869

CHAPTER 4:

CONCLUSION & FUTURE DIRECTIONS

Conclusions & Future Directions

IL-1α and IL-1β are proinflammatory cytokines that are important for amplifying inflammation and recruitment of immune cells. Previous studies from our lab have identified IL-1β as a crucial mediator of neutrophil infiltration and subsequently bacterial killing in the cornea (38). We also found that neutrophils are the main source of IL-1β in our model of microbial keratitis. The studies in this thesis now revealed a non-redundant role for IL-1α compared to IL-1β in regulating inflammation, and identify neutrophils and monocytes as the source of IL-1α in the cornea. Further, we describe a non-canonical mechanism for IL-1α secretion by neutrophils that is distinct from IL-1β (126).

While IL-1β processing and secretion is tightly regulated in a two-step process mediated by inflammasome activation of caspase-1 and GSDMD pore formation (118), IL-1α is passively released through cell death in non-hematopoietic cells (136). However, our observations indicate that β-glucan stimulated neutrophils secrete IL-1α without undergoing cell death. Instead, we described an unconventional secretory pathway for IL-1α release by neutrophils that is mediated by extracellular vesicles in chapter 3. We further show that IL-1α encapsulated in extracellular vesicles are bioactive and able to activate its receptor, IL-1R1. In addition to IL-1α, recent studies have also identified other extracellular vesicle-encapsulated cytokines and complement components that are implicated in inflammatory diseases (190–192). However, it is unclear how encapsulated cytokines are able to signal their receptor extracellularly and what governs whether these cytokines are packaged into exosomes or release through canonical mechanisms. Further studies are necessary to address these questions and improve our understanding of extracellular vesicles signaling.

In addition to dissecting the mechanism of IL-1α secretion, we also explored whether there is a role for IL-1α during bacterial and fungal keratitis. We found no role for IL-1α in our murine model of *Aspergillus fumigatus* keratitis (using strain Af293-RFP, data not shown). However, we uncovered differential roles for IL-1α and IL-1β during *Pseudomonas aeruginosa* keratitis where IL-1β was protective but IL-1α was detrimental. While there were no differences in recruitment of neutrophils or neutrophil effector functions between WT and *Il1a-/-* mice, we found that *Il1a-/-* neutrophils had a more proinflammatory transcriptomic profile. Among the upregulated genes, *C1qb* was of particular interest because of its antimicrobial capabilities. The role of complements in the cornea is not well understood and future directions for this project will examine whether C1q is necessary for protection against microbial keratitis. Moreover, it is unclear whether C1q has a direct antimicrobial role in the cornea or if it is acting indirectly by activating the classical complement pathway. We will also examine other upregulated genes in *Il1a-/-* neutrophils to identify other mechanisms by which *Il1a-/-* mice have enhanced bacterial killing.

Another interesting observation we found comparing *Il1a-/-* to WT mice is that IL-1α is necessary for monocyte recruitment. As previously mentioned, 90% of infiltrating CD45+ cells are neutrophils with <10% being monocytes. Depletion of neutrophils result in severely impaired bacterial killing. However, whether monocytes play a detrimental or protective role during microbial keratitis is unclear.

Studies involving lung infections have shown contradicting effects of monocytes. During *Cryptococcus neoformans* pulmonary infection, depletion of monocytes results in positive disease outcome and better survival indicating that monocytes play a

detrimental role (59). In contrast, infection with Candida albicans require monocytes to effectively control the infection (60, 61). In our model of keratitis, it is possible that monocytes play a detrimental role in the cornea as *Il1a-/-* mice have delayed monocyte recruitment. Therefore, we examined whether monocytes play a role in the cornea.

My preliminary data show that depletion of monocytes with clodronate liposome in the first 24-hours leads to significant decrease in bacterial killing despite no differences in neutrophil recruitment (**Figure 4.1**). Defective bacterial clearance persisted to 48 hours post-infection despite repopulation of monocytes by this time point. We found that IL-1α levels were reduced in the absence of monocytes in the cornea indicating monocytes are the main source of IL-1α *in vivo* (**Figure 4.2**); however, *Il1a-/-* mice do not show impaired bacterial killing (**Figure 2.2**). To examine neutrophil-monocyte cross talk, we will next examine single-cell RNA sequencing data of CD45+ cells from *P. aeruginosa*-infected corneas using CellChat. Further, neutrophils from infected corneas in the presence and absence of monocytes were sorted for bulk RNA sequencing to compare transcriptional changes in neutrophils as a response to communication from monocytes. Future studies will aim at addressing how monocytes regulate bacterial killing in the cornea.

Together, the studies in this thesis describe a novel role for IL-1α and how it is regulated by neutrophils in response to infection. Our findings could provide a new pathway to target for therapeutics. Currently, microbial keratitis is treated by antimicrobials followed by topical corticosteroids. Steroids potently and non-specifically dampen the inflammation to reduce corneal scarring and vascularization (193, 194). However, this allows for the infection to continue if the pathogens are not entirely

cleared with antimicrobials beforehand. Thus, there is a need for a more targeted treatment that can reduce inflammation while still maintaining bacterial and fungal killing.

The IL-1α-IL-1R1 axis could be one of those targets as we found enhanced bacterial killing in the absence of IL-1α. Treatment with anakinra (IL-1Ra) would be more direct compared to corticosteroids. However, anakinra would also affect IL-1β signaling as well. It is unclear whether blocking both IL-1α and IL-1β signaling post-infection would affect bacterial or fungal killing capabilities by neutrophils in the cornea. My preliminary data indicate that IL-1α and IL-1β do not have a direct affect on bacterial killing, and *Il1a-/-* and *Il1b-/-* neutrophils do not have impaired bacterial killing compared to WT. Instead, these cytokines are necessary for myeloid cell recruitment to the corneas. Based on these observations, we predict that blocking IL-1R1 signaling post-infection should not impair bacterial killing as the infiltrating cells have already reached the cornea. Further experiments are required to test this hypothesis.

Our understanding of how IL-1α and IL-1β is regulated allows us to target each cytokine specifically. Further, we add to the growing evidence for non-redundant functions described for IL-1α and IL-1β. Together, the studies described in this thesis improves our understanding of inflammation in the cornea during microbial keratitis and provides potential pathways to target for therapeutics that is more specific than corticosteroids.

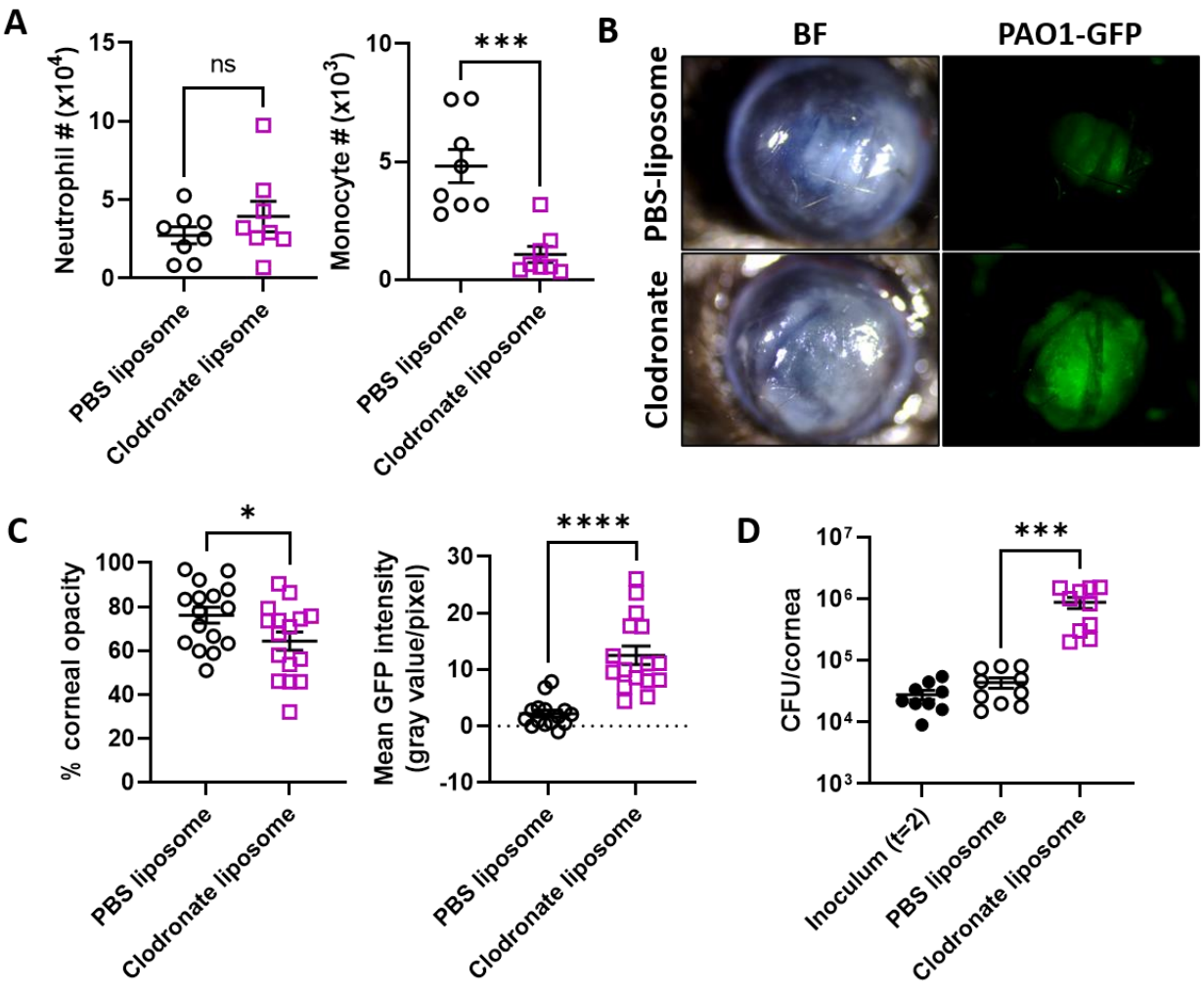

Figure 4.1: Monocytes are essential for protection against *P. aeruginosa* infection of the cornea.

(A) Clodronate liposome depletes monocytes but do not affect neutrophil recruitment to the cornea at 24hpi (n=8). **(B)** Representative brightfield and GFP images of infected corneas with **(C)** quantification of corneal opacity and GFP intensity (n=15). **(D) PAO1** CFU at 24hpi (n=10). Significance was calculated by unpaired T-test. $^{*}p < 0.05$, $^{**}p < 0.01$, $^{***}p < 0.001$, $^{****}p < 0.0001$.

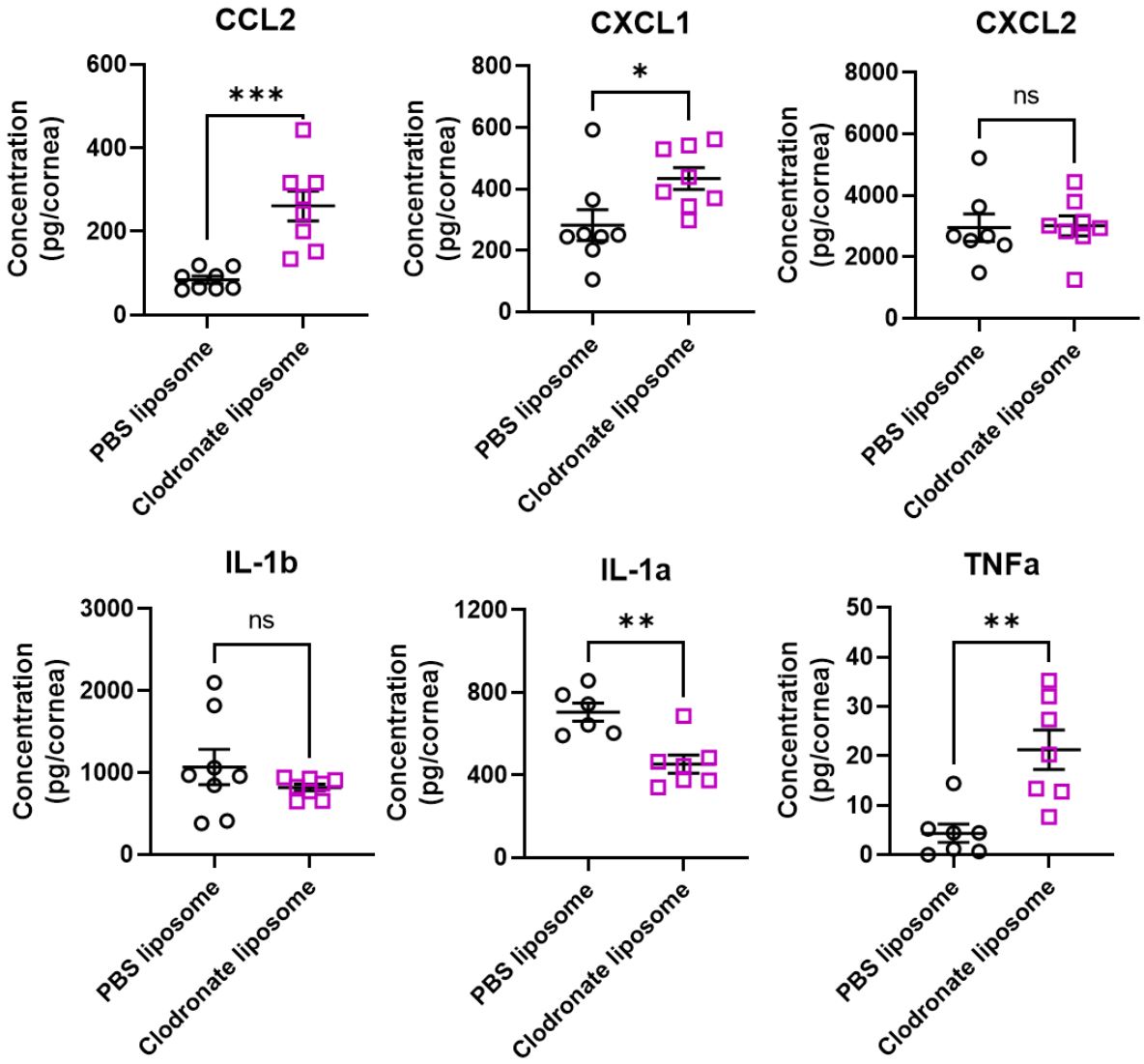

Figure 4.2: Monocytes are an important source of IL-1α but not IL-1β *in vivo*. Whole cornea lysates were collected at 24hpi from PBS liposome or clodronate liposome treated mice. Cytokine levels were determined by ELISA (n=8). Significance was calculated by unpaired T-test. $^{*}p < 0.05$, $^{**}p < 0.01$, $^{***}p < 0.001$, $^{****}p < 0.0001$.

REFERENCE

1. Forrester, J. V., A. D. Dick, P. G. McMenamin, F. Roberts, and E. Pearlman. 2016. *The Eye - Basic Sciences in Practice*, Fourth. Elsevier.

2. Mobaraki, M., R. Abbasi, S. Omidian Vandchali, M. Ghaffari, F. Moztarzadeh, and M. Mozafari. 2019. Corneal Repair and Regeneration: Current Concepts and Future Directions. *Frontiers in Bioengineering and Biotechnology* 7.

3. Castro-Muñozledo, F. 2013. Review: Corneal epithelial stem cells, their niche and wound healing. *Mol Vis* 19: 1600–1613.

4. Pearlman, E., Y. Sun, S. Roy, M. Karmakar, A. G. Hise, L. Szczotka-Flynn, M. Ghannoum, H. R. Chinnery, P. G. McMenamin, and A. Rietsch. 2013. Host defense at the ocular surface. *Int. Rev. Immunol.* 32: 4–18.

5. Clark, H. L., and E. Pearlman. Fungal eye infections - Oxford Medicine. .

6. Al-Mujaini, A., N. Al-Kharusi, A. Thakral, and U. K. Wali. 2009. Bacterial Keratitis: Perspective on Epidemiology, Clinico-Pathogenesis, Diagnosis and Treatment. *Sultan Qaboos Univ Med J* 9: 184–195.

7. Chang, D. C., G. B. Grant, K. O'Donnell, K. A. Wannemuehler, J. Noble-Wang, C. Y. Rao, L. M. Jacobson, C. S. Crowell, R. S. Sneed, F. M. T. Lewis, J. K. Schaffzin, M. A. Kainer, C. A. Genese, E. C. Alfonso, D. B. Jones, A. Srinivasan, S. K. Fridkin, B. J. Park, and for the Fusarium Keratitis Investigation Team. 2006. Multistate Outbreak of Fusarium Keratitis Associated With Use of a Contact Lens Solution. *JAMA* 296: 953–963.

8. McElnea, E., B. Power, and C. Murphy. 2018. Interface Fungal Keratitis After Descemet Stripping Automated Endothelial Keratoplasty: A Review of the Literature With a Focus on Outcomes. *Cornea* 37: 1204–1211.

9. Watson, S. L., M. Cabrera-Aguas, L. Keay, P. Khoo, D. McCall, and M. M. Lahra. 2020. The clinical and microbiological features and outcomes of fungal keratitis over 9 years in Sydney, Australia. *Mycoses* 63: 43–51.

10. Doshi, H., S. Pabon, M. O. Price, M. T. Feng, and F. W. Price. 2018. Overview of Systemic Candida Infections in Hospital Settings and Report of Candida After DMEK Successfully Treated With Antifungals and Partial Graft Excision. *Cornea* 37: 1071–1074.

11. Ung, L., P. J. M. Bispo, S. S. Shanbhag, M. S. Gilmore, and J. Chodosh. 2019. The persistent dilemma of microbial keratitis: Global burden, diagnosis, and antimicrobial resistance. *Surv Ophthalmol* 64: 255–271.

12. Bongomin, F., S. Gago, R. O. Oladele, and D. W. Denning. 2017. Global and Multi-National Prevalence of Fungal Diseases—Estimate Precision. *J Fungi (Basel)* 3.

13. Ung, L., N. R. Acharya, T. Agarwal, E. C. Alfonso, B. Bagga, P. J. Bispo, M. J. Burton, J. K. Dart, T. Doan, S. M. Fleiszig, P. Garg, M. S. Gilmore, D. C. Gritz, L. D. Hazlett, A. Iovieno, V. Jhanji, J. H. Kempen, C. S. Lee, T. M. Lietman, T. P. Margolis, S. D. McLeod, J. S. Mehta, D. Miller, E. Pearlman, L. Prajna, N. V. Prajna, G. D. Seitzman, S. S. Shanbhag, N. Sharma, S. Sharma, M. Srinivasan, F. Stapleton, D. T. Tan, R. Tandon, H. R. Taylor, E. Y. Tu, S. S. Tuli, R. B. Vajpayee, R. N. Van Gelder, S. L. Watson, M. E. Zegans, and J. Chodosh. 2019. Infectious corneal ulceration: a proposal for neglected tropical disease status. *Bull World Health Organ* 97: 854–856.

14. Brown, L., M. J. Burton, M. Gichangi, and D. Denning. 2019. *The Global Incidence of Fungal Keratitis*,. Social Science Research Network, Rochester, NY.

15. Manikandan, P., A. Abdel-hadi, Y. Randhir Babu Singh, R. Revathi, R. Anita, S. Banawas, A. A. Bin Dukhyil, B. Alshehri, C. S. Shobana, K. Panneer Selvam, and V. Narendran. 2019. Fungal Keratitis: Epidemiology, Rapid Detection, and Antifungal Susceptibilities of Fusarium and Aspergillus Isolates from Corneal Scrapings. *BioMed Research International* 2019: e6395840.

16. Spectrum of fungal keratitis in central China - PubMed. .

17. Lalitha, P., N. V. Prajna, G. Manoharan, M. Srinivasan, J. Mascarenhas, M. Das, S. S. D'Silva, T. C. Porco, and J. D. Keenan. 2015. Trends in bacterial and fungal keratitis in South India, 2002-2012. *Br J Ophthalmol* 99: 192–194.

18. Karthikeyan, R. S., S. M. Leal, N. V. Prajna, K. Dharmalingam, D. M. Geiser, E. Pearlman, and P. Lalitha. 2011. Expression of Innate and Adaptive Immune Mediators in Human Corneal Tissue Infected With Aspergillus or Fusarium. *J Infect Dis* 204: 942–950.

19. Ratitong, B., and E. Pearlman. 2021. Pathogenic Aspergillus and Fusarium as important causes of blinding corneal infections — the role of neutrophils in fungal killing, tissue damage and cytokine production. *Current Opinion in Microbiology* 63: 195–203.

20. Ansari, Z., D. Miller, and A. Galor. 2013. Current Thoughts in Fungal Keratitis: Diagnosis and Treatment. *Curr Fungal Infect Rep* 7: 209–218.

21. 1978. Natamycin approved--first U.S. drug for fungal keratitis. *FDA Drug Bull* 8: 37–38.

22. Ting, D. S. J., C. S. Ho, R. Deshmukh, D. G. Said, and H. S. Dua. 2021. Infectious keratitis: an update on epidemiology, causative microorganisms, risk factors, and antimicrobial resistance. *Eye* 35: 1084–1101.

23. Hatami, H., A. Ghaffari Jolfayi, A. Ebrahimi, S. Golmohammadi, M. Zangiabadian, and M. J. Nasiri. 2021. Contact Lens Associated Bacterial Keratitis: Common Organisms, Antibiotic Therapy, and Global Resistance Trends: A Systematic Review. *Frontiers in Ophthalmology* 1.

24. Green, M., A. Apel, and F. Stapleton. 2008. Risk factors and causative organisms in microbial keratitis. *Cornea* 27: 22–27.

25. Hyndiuk, R. A. 1981. Experimental Pseudomonas keratitis. *Trans Am Ophthalmol Soc* 79: 541–624.

26. Karthikeyan, R. S., J. L. Priya, S. M. Leal, J. Toska, A. Rietsch, V. Prajna, E. Pearlman, and P. Lalitha. 2013. Host response and bacterial virulence factor expression in Pseudomonas aeruginosa and Streptococcus pneumoniae corneal ulcers. *PLoS One* 8: e64867.

27. Frontiers | Structural and Functional Characterization of the Type Three Secretion System (T3SS) Needle of Pseudomonas aeruginosa | Microbiology. .

28. Peña, C., G. Cabot, S. Gómez-Zorrilla, L. Zamorano, A. Ocampo-Sosa, J. Murillas, B. Almirante, V. Pomar, M. Aguilar, A. Granados, E. Calbo, J. Rodríguez-Baño, F. Rodríguez-López, F. Tubau, L. Martínez-Martínez, A. Oliver, and Spanish Network for Research in Infectious Diseases (REIPI). 2015. Influence of virulence genotype and resistance profile in the mortality of Pseudomonas aeruginosa bloodstream infections. *Clin Infect Dis* 60: 539–548.

29. El-Solh, A. A., A. Hattemer, A. R. Hauser, A. Alhajhusain, and H. Vora. 2012. Clinical outcomes of type III Pseudomonas aeruginosa bacteremia. *Crit Care Med* 40: 1157–1163.

30. Yang, J. J., K.-S. C. Tsuei, and E. P. Shen. 2022. The role of Type III secretion system in the pathogenesis of Pseudomonas aeruginosa microbial keratitis. *Tzu Chi Med J* 34: 8–14.

31. Sun, Y., M. Karmakar, P. R. Taylor, A. Rietsch, and E. Pearlman. 2012. ExoS and ExoT ADP-ribosyltransferase activities mediate Pseudomonas aeruginosa keratitis by promoting neutrophil apoptosis and bacterial survival. *J Immunol* 188: 1884–1895.

32. Hauser, A. R., and J. N. Engel. 1999. Pseudomonas aeruginosa induces type-III-secretion-mediated apoptosis of macrophages and epithelial cells. *Infect Immun* 67: 5530–5537.

33. Saliba, A. M., A. Filloux, G. Ball, A. S. V. Silva, M.-C. Assis, and M.-C. Plotkowski. 2002. Type III secretion-mediated killing of endothelial cells by Pseudomonas aeruginosa. *Microb Pathog* 33: 153–166.

34. Finck-Barbançon, V., J. Goranson, L. Zhu, T. Sawa, J. P. Wiener-Kronish, S. M. Fleiszig, C. Wu, L. Mende-Mueller, and D. W. Frank. 1997. ExoU expression by Pseudomonas aeruginosa correlates with acute cytotoxicity and epithelial injury. *Mol Microbiol* 25: 547–557.

35. Hauser, A. R. 2009. The Type III Secretion System of Pseudomonas aeruginosa: Infection by Injection. *Nat Rev Microbiol* 7: 654–665.

36. Feltman, H., G. Schulert, S. Khan, M. Jain, L. Peterson, and A. R. Hauser. 2001. Prevalence of type III secretion genes in clinical and environmental isolates of Pseudomonas aeruginosa. *Microbiology (Reading)* 147: 2659–2669.

37. Sun, Y., M. Karmakar, S. Roy, R. T. Ramadan, S. R. Williams, S. Howell, C. L. Shive, Y. Han, C. M. Stopford, A. Rietsch, and E. Pearlman. 2010. TLR4 and TLR5 on Corneal Macrophages Regulate Pseudomonas aeruginosa Keratitis by Signaling through MyD88-Dependent and -Independent Pathways. *The Journal of Immunology* 185: 4272–4283.

38. Karmakar, M., Y. Sun, A. G. Hise, A. Rietsch, and E. Pearlman. 2012. Cutting Edge: IL-1β Processing during Pseudomonas aeruginosa Infection Is Mediated by Neutrophil Serine Proteases and Is Independent of NLRC4 and Caspase-1. *The Journal of Immunology* 189: 4231–4235.

39. Murphy, K., and C. Weaver. 2017. *Janeway's Immunobiology*, 9th ed. Garland Science, Taylor & Francis Group, LLC, New York, NY.

40. Janeway, C. A. 1989. Approaching the asymptote? Evolution and revolution in immunology. *Cold Spring Harb Symp Quant Biol* 54 Pt 1: 1–13.

41. Mogensen, T. H. 2009. Pathogen Recognition and Inflammatory Signaling in Innate Immune Defenses. *Clin Microbiol Rev* 22: 240–273.

42. Park, B. S., and J.-O. Lee. 2013. Recognition of lipopolysaccharide pattern by TLR4 complexes. *Exp Mol Med* 45: e66–e66.

43. Yuan, X., and K. R. Wilhelmus. 2010. Toll-like receptors involved in the pathogenesis of experimental Candida albicans keratitis. *Invest Ophthalmol Vis Sci* 51: 2094–2100.

44. Tarabishy, A. B., B. Aldabagh, Y. Sun, Y. Imamura, P. K. Mukherjee, J. H. Lass, M. A. Ghannoum, and E. Pearlman. 2008. MyD88 regulation of Fusarium keratitis is dependent on TLR4 and IL-1R1 but not TLR2. *J. Immunol.* 181: 593–600.

45. Leal, S. M., S. Cowden, Y.-C. Hsia, M. A. Ghannoum, M. Momany, and E. Pearlman. 2010. Distinct roles for Dectin-1 and TLR4 in the pathogenesis of Aspergillus fumigatus keratitis. *PLoS Pathog.* 6: e1000976.

46. Brown, G. D. 2006. Dectin-1: a signalling non-TLR pattern-recognition receptor. *Nat Rev Immunol* 6: 33–43.

47. Werner, J. L., A. E. Metz, D. Horn, T. R. Schoeb, M. M. Hewitt, L. M. Schwiebert, I. Faro-Trindade, G. D. Brown, and C. Steele. 2009. Requisite role for the dectin-1 beta-glucan receptor in pulmonary defense against Aspergillus fumigatus. *J Immunol* 182: 4938–4946.

48. Liu, T., L. Zhang, D. Joo, and S.-C. Sun. 2017. NF-κB signaling in inflammation. *Signal Transduct Target Ther* 2: 17023.

49. Lionakis, M. S., I. D. Iliev, and T. M. Hohl. 2017. Immunity against fungi. *JCI Insight* 2.

50. Saxena, M., and G. Yeretssian. 2014. NOD-Like Receptors: Master Regulators of Inflammation and Cancer. *Frontiers in Immunology* 5.

51. Galletti, J. G., M. Guzmán, and M. N. Giordano. 2017. Mucosal immune tolerance at the ocular surface in health and disease. *Immunology* 150: 397–407.

52. Liu, J., and Z. Li. 2021. Resident Innate Immune Cells in the Cornea. *Front Immunol* 12: 620284.

53. Lauvau, G., L. Chorro, E. Spaulding, and S. M. Soudja. 2014. Inflammatory Monocyte Effector Mechanisms. *Cell Immunol* 291: 32–40.

54. van Furth, R., and Z. A. Cohn. 1968. THE ORIGIN AND KINETICS OF MONONUCLEAR PHAGOCYTES. *Journal of Experimental Medicine* 128: 415–435.

55. Geissmann, F., S. Jung, and D. R. Littman. 2003. Blood Monocytes Consist of Two Principal Subsets with Distinct Migratory Properties. *Immunity* 19: 71–82.

56. Teh, Y. C., J. L. Ding, L. G. Ng, and S. Z. Chong. 2019. Capturing the Fantastic Voyage of Monocytes Through Time and Space. *Frontiers in Immunology* 10.

57. Tsou, C.-L., W. Peters, Y. Si, S. Slaymaker, A. M. Aslanian, S. P. Weisberg, M. Mack, and I. F. Charo. 2007. Critical roles for CCR2 and MCP-3 in monocyte mobilization from bone marrow and recruitment to inflammatory sites. *J Clin Invest* 117: 902–909.

58. Hoeffel, G., and F. Ginhoux. 2015. Ontogeny of Tissue-Resident Macrophages. *Frontiers in Immunology* 6.

59. Heung, L. J., and T. M. Hohl. 2019. Inflammatory monocytes are detrimental to the host immune response during acute infection with Cryptococcus neoformans. *PLOS Pathogens* 15: e1007627.

60. Domínguez-Andrés, J., L. Feo-Lucas, M. Minguito de la Escalera, L. González, M. López-Bravo, and C. Ardavín. 2017. Inflammatory Ly6Chigh Monocytes Protect against Candidiasis through IL-15-Driven NK Cell/Neutrophil Activation. *Immunity* 46: 1059-1072.e4.

61. Thompson, A., L. C. Davies, C.-T. Liao, D. M. da Fonseca, J. S. Griffiths, R. Andrews, A. V. Jones, M. Clement, G. D. Brown, I. R. Humphreys, P. R. Taylor, and S.

J. Orr. 2019. The protective effect of inflammatory monocytes during systemic C. albicans infection is dependent on collaboration between C-type lectin-like receptors. *PLOS Pathogens* 15: e1007850.

62. Serbina, N. V., T. P. Salazar-Mather, C. A. Biron, W. A. Kuziel, and E. G. Pamer. 2003. TNF/iNOS-Producing Dendritic Cells Mediate Innate Immune Defense against Bacterial Infection. *Immunity* 19: 59–70.

63. Rosen, H., S. Gordon, and R. J. North. 1989. Exacerbation of murine listeriosis by a monoclonal antibody specific for the type 3 complement receptor of myelomonocytic cells. Absence of monocytes at infective foci allows Listeria to multiply in nonphagocytic cells. *Journal of Experimental Medicine* 170: 27–37.

64. Rosales, C. 2018. Neutrophil: A Cell with Many Roles in Inflammation or Several Cell Types? *Frontiers in Physiology* 9.

65. Furze, R. C., and S. M. Rankin. 2008. Neutrophil mobilization and clearance in the bone marrow. *Immunology* 125: 281–288.

66. Casanova-Acebes, M., J. A. Nicolás-Ávila, J. L. Li, S. García-Silva, A. Balachander, A. Rubio-Ponce, L. A. Weiss, J. M. Adrover, K. Burrows, N. A-González, I. Ballesteros, S. Devi, J. A. Quintana, G. Crainiciuc, M. Leiva, M. Gunzer, C. Weber, T. Nagasawa, O. Soehnlein, M. Merad, A. Mortha, L. G. Ng, H. Peinado, and A. Hidalgo. 2018. Neutrophils instruct homeostatic and pathological states in naive tissues. *Journal of Experimental Medicine* 215: 2778–2795.

67. Kolaczkowska, E., and P. Kubes. 2013. Neutrophil recruitment and function in health and inflammation. *Nat Rev Immunol* 13: 159–175.

68. De Filippo, K., and S. M. Rankin. 2020. The Secretive Life of Neutrophils Revealed by Intravital Microscopy. *Frontiers in Cell and Developmental Biology* 8.

69. Adrover, J. M., C. Del Fresno, G. Crainiciuc, M. I. Cuartero, M. Casanova-Acebes, L. A. Weiss, H. Huerga-Encabo, C. Silvestre-Roig, J. Rossaint, I. Cossío, A. V. Lechuga-Vieco, J. García-Prieto, M. Gómez-Parrizas, J. A. Quintana, I. Ballesteros, S. Martin-Salamanca, A. Aroca-Crevillen, S. Z. Chong, M. Evrard, K. Balabanian, J. López, K. Bidzhekov, F. Bachelerie, F. Abad-Santos, C. Muñoz-Calleja, A. Zarbock, O. Soehnlein, C. Weber, L. G. Ng, C. Lopez-Rodriguez, D. Sancho, M. A. Moro, B. Ibáñez, and A. Hidalgo. 2019. A Neutrophil Timer Coordinates Immune Defense and Vascular Protection. *Immunity* 50: 390-402.e10.

70. Scapini, P., and M. A. Cassatella. 2014. Social networking of human neutrophils within the immune system. *Blood* 124: 710–719.

71. Capucetti, A., F. Albano, and R. Bonecchi. 2020. Multiple Roles for Chemokines in Neutrophil Biology. *Frontiers in Immunology* 11.

72. De Filippo, K., and S. M. Rankin. 2018. CXCR4, the master regulator of neutrophil trafficking in homeostasis and disease. *Eur J Clin Invest* 48: e12949.

73. Lawrence, M. B., D. F. Bainton, and T. A. Springer. 1994. Neutrophil tethering to and rolling on E-selectin are separable by requirement for L-selectin. *Immunity* 1: 137–145.

74. McEver, R. P. 2010. Rolling back neutrophil adhesion. *Nat Immunol* 11: 282–284.

75. Muller, W. A. 2013. Getting Leukocytes to the Site of Inflammation. *Vet Pathol* 50: 7–22.

76. Marrazzo, G., L. Bellner, A. Halilovic, G. Li Volti, F. Drago, M. W. Dunn, and M. L. Schwartzman. 2011. The Role of Neutrophils in Corneal Wound Healing in HO-2 Null Mice. *PLoS One* 6: e21180.

77. Wilson, S. E., R. R. Mohan, R. R. Mohan, R. Ambrósio, J. Hong, and J. Lee. 2001. The corneal wound healing response: cytokine-mediated interaction of the epithelium, stroma, and inflammatory cells. *Prog Retin Eye Res* 20: 625–637.

78. Van Acker, H., and T. Coenye. 2017. The Role of Reactive Oxygen Species in Antibiotic-Mediated Killing of Bacteria. *Trends in Microbiology* 25: 456–466.

79. Dinauer, M. C., S. H. Orkin, R. Brown, A. J. Jesaitis, and C. A. Parkos. 1987. The glycoprotein encoded by the X-linked chronic granulomatous disease locus is a component of the neutrophil cytochrome b complex. *Nature* 327: 717–720.

80. Singel, K. L., and B. H. Segal. 2016. NOX2-dependent regulation of inflammation. *Clin Sci (Lond)* 130: 479–490.

81. Kuhns, D. B., W. G. Alvord, T. Heller, J. J. Feld, K. M. Pike, B. E. Marciano, G. Uzel, S. S. DeRavin, D. A. Long Priel, B. P. Soule, K. A. Zarember, H. L. Malech, S. M. Holland, and J. I. Gallin. 2010. Residual NADPH Oxidase and Survival in Chronic Granulomatous Disease. *N Engl J Med* 363: 2600–2610.

82. Li, H., X. Zhou, Y. Huang, B. Liao, L. Cheng, and B. Ren. 2021. Reactive Oxygen Species in Pathogen Clearance: The Killing Mechanisms, the Adaption Response, and the Side Effects. *Frontiers in Microbiology* 11.

83. Vareechon, C., S. E. Zmina, M. Karmakar, E. Pearlman, and A. Rietsch. 2017. Pseudomonas aeruginosa Effector ExoS Inhibits ROS Production in Human Neutrophils. *Cell Host Microbe* 21: 611-618.e5.

84. Leal, S. M., C. Vareechon, S. Cowden, B. A. Cobb, J.-P. Latgé, M. Momany, and E. Pearlman. 2012. Fungal antioxidant pathways promote survival against neutrophils during infection. *J. Clin. Invest.* 122: 2482–2498.

85. Sheshachalam, A., N. Srivastava, T. Mitchell, P. Lacy, and G. Eitzen. 2014. Granule Protein Processing and Regulated Secretion in Neutrophils. *Front. Immunol.* 5.

86. Borregaard, N., O. E. Sørensen, and K. Theilgaard-Mönch. 2007. Neutrophil granules: a library of innate immunity proteins. *Trends Immunol* 28: 340–345.

87. Brinkmann, V., U. Reichard, C. Goosmann, B. Fauler, Y. Uhlemann, D. S. Weiss, Y. Weinrauch, and A. Zychlinsky. 2004. Neutrophil Extracellular Traps Kill Bacteria. *Science* 303: 1532–1535.

88. Papayannopoulos, V. 2018. Neutrophil extracellular traps in immunity and disease. *Nat Rev Immunol* 18: 134–147.

89. Urban, C. F., and J. E. Nett. 2019. Neutrophil extracellular traps in fungal infection. *Semin Cell Dev Biol* 89: 47–57.

90. Thanabalasuriar, A., B. N. V. Scott, M. Peiseler, M. E. Willson, Z. Zeng, P. Warrener, A. E. Keller, B. G. J. Surewaard, E. A. Dozier, J. T. Korhonen, L. I.-T. Cheng, M. Gadjeva, C. K. Stover, A. DiGiandomenico, and P. Kubes. 2019. Neutrophil Extracellular Traps Confine Pseudomonas aeruginosa Ocular Biofilms and Restrict Brain Invasion. *Cell Host Microbe* 25: 526-536.e4.

91. Thiam, H. R., S. L. Wong, R. Qiu, M. Kittisopikul, A. Vahabikashi, A. E. Goldman, R. D. Goldman, D. D. Wagner, and C. M. Waterman. 2020. NETosis proceeds by cytoskeleton and endomembrane disassembly and PAD4-mediated chromatin

decondensation and nuclear envelope rupture. *Proceedings of the National Academy of Sciences* 117: 7326–7337.

92. Clark, H. L., S. Abbondante, M. S. Minns, E. N. Greenberg, Y. Sun, and E. Pearlman. 2018. Protein Deiminase 4 and CR3 Regulate Aspergillus fumigatus and β-Glucan-Induced Neutrophil Extracellular Trap Formation, but Hyphal Killing Is Dependent Only on CR3. *Front Immunol* 9.

93. Khan, M. A., L. M. Philip, G. Cheung, S. Vadakepeedika, H. Grasemann, N. Sweezey, and N. Palaniyar. 2018. Regulating NETosis: Increasing pH Promotes NADPH Oxidase-Dependent NETosis. *Frontiers in Medicine* 5.

94. Rochael, N. C., A. B. Guimarães-Costa, M. T. C. Nascimento, T. S. DeSouza-Vieira, M. P. Oliveira, L. F. Garcia e Souza, M. F. Oliveira, and E. M. Saraiva. 2015. Classical ROS-dependent and early/rapid ROS-independent release of Neutrophil Extracellular Traps triggered by Leishmania parasites. *Sci Rep* 5: 18302.

95. Tatsiy, O., and P. P. McDonald. 2018. Physiological Stimuli Induce PAD4-Dependent, ROS-Independent NETosis, With Early and Late Events Controlled by Discrete Signaling Pathways. *Front Immunol* 9: 2036.

96. Azzouz, D., M. A. Khan, and N. Palaniyar. 2021. ROS induces NETosis by oxidizing DNA and initiating DNA repair. *Cell Death Discov.* 7: 1–10.

97. Metzler, K. D., C. Goosmann, A. Lubojemska, A. Zychlinsky, and V. Papayannopoulos. 2014. A Myeloperoxidase-Containing Complex Regulates Neutrophil Elastase Release and Actin Dynamics during NETosis. *Cell Reports* 8: 883–896.

98. Jin, X., Y. Zhao, F. Zhang, T. Wan, F. Fan, X. Xie, and Z. Lin. 2016. Neutrophil extracellular traps involvement in corneal fungal infection. *Mol Vis* 22: 944–952.

99. Tecchio, C., A. Micheletti, and M. A. Cassatella. 2014. Neutrophil-Derived Cytokines: Facts Beyond Expression. *Front Immunol* 5.

100. Garlanda, C., C. A. Dinarello, and A. Mantovani. 2013. The Interleukin-1 Family: Back to the Future. *Immunity* 39: 1003–1018.

101. Rubartelli, A., F. Cozzolino, M. Talio, and R. Sitia. 1990. A novel secretory pathway for interleukin-1 beta, a protein lacking a signal sequence. *EMBO J* 9: 1503–1510.

102. Fields, J. K., S. Günther, and E. J. Sundberg. 2019. Structural Basis of IL-1 Family Cytokine Signaling. *Frontiers in Immunology* 10.

103. Dinarello, C. A. 1996. Biologic basis for interleukin-1 in disease. *Blood* 87: 2095–2147.

104. Di Paolo, N. C., and D. M. Shayakhmetov. 2016. Interleukin 1α and the inflammatory process. *Nature Immunology* 17: 906–913.

105. Wessendorf, J. H., S. Garfinkel, X. Zhan, S. Brown, and T. Maciag. 1993. Identification of a nuclear localization sequence within the structure of the human interleukin-1 alpha precursor. *J. Biol. Chem.* 268: 22100–22104.

106. Rivers-Auty, J., M. J. D. Daniels, I. Colliver, D. L. Robertson, and D. Brough. 2018. Redefining the ancestral origins of the interleukin-1 superfamily. *Nat Commun* 9: 1156.

107. Goldbach-Mansky, R., and D. L. Kastner. 2009. Autoinflammation: The prominent role of IL-1 in monogenic autoinflammatory diseases and implications for common illnesses. *J Allergy Clin Immunol* 124: 1141–1151.

108. Dinarello, C. A., M. Y. Donath, and T. Mandrup-Poulsen. 2010. Role of IL-1beta in type 2 diabetes. *Curr Opin Endocrinol Diabetes Obes* 17: 314–321.

109. Dinarello, C. A. 2019. The IL-1 family of cytokines and receptors in rheumatic diseases. *Nat Rev Rheumatol* 15: 612–632.

110. Griffiths, J. S., G. Camilli, N. K. Kotowicz, J. Ho, J. P. Richardson, and J. R. Naglik. 2021. Role for IL-1 Family Cytokines in Fungal Infections. *Front. Microbiol.* 12.

111. Sahoo, M., I. Ceballos-Olvera, L. del Barrio, and F. Re. 2011. Role of the Inflammasome, IL-1β, and IL-18 in Bacterial Infections. *ScientificWorldJournal* 11: 2037–2050.

112. Sun, Y., S. Abbondante, M. Karmakar, S. de J. Carrion, C. Che, A. G. Hise, and E. Pearlman. 2018. Neutrophil Caspase-11 Is Required for Cleavage of Caspase-1 and Secretion of IL-1β in Aspergillus fumigatus Infection. *The Journal of Immunology* .

113. Kawai, T., and S. Akira. 2007. Signaling to NF-κB by Toll-like receptors. *Trends in Molecular Medicine* 13: 460–469.

114. Kingeter, L. M., and X. Lin. 2012. C-type lectin receptor-induced NF-κB activation in innate immune and inflammatory responses. *Cell Mol Immunol* 9: 105–112.

115. Agostini, L., F. Martinon, K. Burns, M. F. McDermott, P. N. Hawkins, and J. Tschopp. 2004. NALP3 Forms an IL-1β-Processing Inflammasome with Increased Activity in Muckle-Wells Autoinflammatory Disorder. *Immunity* 20: 319–325.

116. Afonina, I. S., C. Müller, S. J. Martin, and R. Beyaert. 2015. Proteolytic Processing of Interleukin-1 Family Cytokines: Variations on a Common Theme. *Immunity* 42: 991–1004.

117. Broz, P., and V. M. Dixit. 2016. Inflammasomes: mechanism of assembly, regulation and signalling. *Nature Reviews Immunology* 16: 407–420.

118. Franchi, L., T. Eigenbrod, R. Muñoz-Planillo, and G. Nuñez. 2009. The Inflammasome: A Caspase-1 Activation Platform Regulating Immune Responses and Disease Pathogenesis. *Nat Immunol* 10: 241.

119. Zheng, D., T. Liwinski, and E. Elinav. 2020. Inflammasome activation and regulation: toward a better understanding of complex mechanisms. *Cell Discov* 6: 1–22.

120. Kuang, S., J. Zheng, H. Yang, S. Li, S. Duan, Y. Shen, C. Ji, J. Gan, X.-W. Xu, and J. Li. 2017. Structure insight of GSDMD reveals the basis of GSDMD autoinhibition in cell pyroptosis. *PNAS* 201708194.

121. Xia, S., Z. Zhang, V. G. Magupalli, J. L. Pablo, Y. Dong, S. M. Vora, L. Wang, T.-M. Fu, M. P. Jacobson, A. Greka, J. Lieberman, J. Ruan, and H. Wu. 2021. Gasdermin D pore structure reveals preferential release of mature interleukin-1. *Nature* 593: 607–611.

122. Shi, J., Y. Zhao, K. Wang, X. Shi, Y. Wang, H. Huang, Y. Zhuang, T. Cai, F. Wang, and F. Shao. 2015. Cleavage of GSDMD by inflammatory caspases determines pyroptotic cell death. *Nature* 526: 660–665.

123. Shi, J., W. Gao, and F. Shao. 2017. Pyroptosis: Gasdermin-Mediated Programmed Necrotic Cell Death. *Trends Biochem Sci* 42: 245–254.

124. Bergsbaken, T., S. L. Fink, and B. T. Cookson. 2009. Pyroptosis: host cell death and inflammation. *Nat Rev Microbiol* 7: 99–109.

125. Karmakar, M., M. Minns, E. N. Greenberg, J. Diaz-Aponte, K. Pestonjamasp, J. L. Johnson, J. K. Rathkey, D. W. Abbott, K. Wang, F. Shao, S. D. Catz, G. R. Dubyak, and E. Pearlman. 2020. N-GSDMD trafficking to neutrophil organelles facilitates IL-1β

release independently of plasma membrane pores and pyroptosis. *Nature Communications* 11: 1–14.

126. Ratitong, B., M. Marshall, and E. Pearlman. 2021. β-Glucan-stimulated neutrophil secretion of IL-1α is independent of GSDMD and mediated through extracellular vesicles. *Cell Reports* 35: 109139.

127. Sollberger, G. 2022. Approaching Neutrophil Pyroptosis. *Journal of Molecular Biology* 434: 167335.

128. Monteleone, M., A. C. Stanley, K. W. Chen, D. L. Brown, J. S. Bezbradica, J. B. von Pein, C. L. Holley, D. Boucher, M. R. Shakespear, R. Kapetanovic, V. Rolfes, M. J. Sweet, J. L. Stow, and K. Schroder. 2018. Interleukin-1β Maturation Triggers Its Relocation to the Plasma Membrane for Gasdermin-D-Dependent and -Independent Secretion. *Cell Rep* 24: 1425–1433.

129. Son, S., S.-H. Yoon, B. J. Chae, I. Hwang, D.-W. Shim, Y. H. Choe, Y.-M. Hyun, and J.-W. Yu. 2021. Neutrophils Facilitate Prolonged Inflammasome Response in the DAMP-Rich Inflammatory Milieu. *Frontiers in Immunology* 12.

130. Kim, B., Y. Lee, E. Kim, A. Kwak, S. Ryoo, S. Bae, T. Azam, S. Kim, and C. Dinarello. 2013. The Interleukin-1α Precursor is Biologically Active and is Likely a Key Alarmin in the IL-1 Family of Cytokines. *Frontiers in Immunology* 4.

131. Malik, A., and T.-D. Kanneganti. 2018. Function and regulation of IL-1α in inflammatory diseases and cancer. *Immunological Reviews* 281: 124–137.

132. Suzuki, Y., C. Demoliere, D. Kitamura, H. Takeshita, U. Deuschle, and T. Watanabe. 1997. HAX-1, a novel intracellular protein, localized on mitochondria, directly

associates with HS1, a substrate of Src family tyrosine kinases. *J Immunol* 158: 2736–2744.

133. Kawaguchi, Y., E. Nishimagi, A. Tochimoto, M. Kawamoto, Y. Katsumata, M. Soejima, T. Kanno, N. Kamatani, and M. Hara. 2006. Intracellular IL-1alpha-binding proteins contribute to biological functions of endogenous IL-1alpha in systemic sclerosis fibroblasts. *Proc Natl Acad Sci U S A* 103: 14501–14506.

134. Fadeel, B., and E. Grzybowska. 2009. HAX-1: A multifunctional protein with emerging roles in human disease. *Biochimica et Biophysica Acta (BBA) - General Subjects* 1790: 1139–1148.

135. Luheshi, N. M., N. J. Rothwell, and D. Brough. 2008. The Dynamics and Mechanisms of Interleukin-1α and β Nuclear Import. *Traffic* 10: 16–25.

136. England, H., H. R. Summersgill, M. E. Edye, N. J. Rothwell, and D. Brough. 2014. Release of Interleukin-1α or Interleukin-1β Depends on Mechanism of Cell Death. *J Biol Chem* 289: 15942–15950.

137. Evavold, C. L., J. Ruan, Y. Tan, S. Xia, H. Wu, and J. C. Kagan. 2018. The Pore-Forming Protein Gasdermin D Regulates Interleukin-1 Secretion from Living Macrophages. *Immunity* 48: 35-44.e6.

138. Batista, S. J., K. M. Still, D. Johanson, J. A. Thompson, C. A. O'Brien, J. R. Lukens, and T. H. Harris. 2020. Gasdermin-D-dependent IL-1α release from microglia promotes protective immunity during chronic Toxoplasma gondii infection. *Nat Commun* 11: 3687.

139. Gross, O., A. S. Yazdi, C. J. Thomas, M. Masin, L. X. Heinz, G. Guarda, M. Quadroni, S. K. Drexler, and J. Tschopp. 2012. Inflammasome activators induce

interleukin-1α secretion via distinct pathways with differential requirement for the protease function of caspase-1. *Immunity* 36: 388–400.

140. Caffrey, A. K., M. M. Lehmann, J. M. Zickovich, V. Espinosa, K. M. Shepardson, C. P. Watschke, K. M. Hilmer, A. Thammahong, B. M. Barker, A. Rivera, R. A. Cramer, and J. J. Obar. 2015. IL-1α Signaling Is Critical for Leukocyte Recruitment after Pulmonary Aspergillus fumigatus Challenge. *PLOS Pathogens* 11: e1004625.

141. Caffrey-Carr, A. K., C. H. Kowalski, S. R. Beattie, N. A. Blaseg, C. R. Upshaw, A. Thammahong, H. E. Lust, Y.-W. Tang, T. M. Hohl, R. A. Cramer, and J. J. Obar. 2017. Interleukin 1α Is Critical for Resistance against Highly Virulent Aspergillus fumigatus Isolates. *Infect. Immun.* 85: e00661-17.

142. Rider, P., Y. Carmi, O. Guttman, A. Braiman, I. Cohen, E. Voronov, M. R. White, C. A. Dinarello, and R. N. Apte. 2011. IL-1α and IL-1β recruit different myeloid cells and promote different stages of sterile inflammation. *J. Immunol.* 187: 4835–4843.

143. Lee, P. Y., Y. Kumagai, Y. Xu, Y. Li, T. Barker, C. Liu, E. S. Sobel, O. Takeuchi, S. Akira, M. Satoh, and WestleyH. Reeves. 2011. Interleukin-1 alpha modulates neutrophil recruitment in chronic inflammation induced by hydrocarbon oil. *J Immunol* 186: 1747–1754.

144. Rudner, X. L., K. A. Kernacki, R. P. Barrett, and L. D. Hazlett. 2000. Prolonged Elevation of IL-1 in Pseudomonas aeruginosa Ocular Infection Regulates Macrophage-Inflammatory Protein-2 Production, Polymorphonuclear Neutrophil Persistence, and Corneal Perforation. *The Journal of Immunology* 164: 6576–6582.

145. Scarpa, M., S. Kessler, T. Sadler, G. West, C. Homer, C. McDonald, C. de la Motte, C. Fiocchi, and E. Stylianou. 2015. The Epithelial Danger Signal IL-1α Is a Potent

Activator of Fibroblasts and Reactivator of Intestinal Inflammation. *Am J Pathol* 185: 1624–1637.

146. Fukuda, K., W. Ishida, Y. Miura, T. Kishimoto, and A. Fukushima. 2017. Cytokine expression and barrier disruption in human corneal epithelial cells induced by alarmin released from necrotic cells. *Jpn. J. Ophthalmol.* 61: 415–422.

147. Horai, R., M. Asano, K. Sudo, H. Kanuka, M. Suzuki, M. Nishihara, M. Takahashi, and Y. Iwakura. 1998. Production of Mice Deficient in Genes for Interleukin (IL)-1α, IL-1β, IL-1α/β, and IL-1 Receptor Antagonist Shows that IL-1β Is Crucial in Turpentine-induced Fever Development and Glucocorticoid Secretion. *J Exp Med* 187: 1463–1475.

148. Rider, P., Y. Carmi, E. Voronov, and R. N. Apte. 2013. Interleukin-1α. *Seminars in Immunology* 25: 430–438.

149. Zhou, Y., B. Zhou, L. Pache, M. Chang, A. H. Khodabakhshi, O. Tanaseichuk, C. Benner, and S. K. Chanda. 2019. Metascape provides a biologist-oriented resource for the analysis of systems-level datasets. *Nat Commun* 10: 1523.

150. Thielens, N. M., F. Tedesco, S. S. Bohlson, C. Gaboriaud, and A. J. Tenner. 2017. C1q: A fresh look upon an old molecule. *Mol Immunol* 89: 73–83.

151. Thakur, A., R. P. Barrett, S. McClellan, and L. D. Hazlett. 2004. Regulation of Pseudomonas aeruginosa corneal infection in IL-1 beta converting enzyme (ICE, caspase-1) deficient mice. *Curr. Eye Res.* 29: 225–233.

152. Frithz-Lindsten, E., Y. Du, R. Rosqvist, and A. Forsberg. 1997. Intracellular targeting of exoenzyme S of Pseudomonas aeruginosa via type III-dependent translocation induces phagocytosis resistance, cytotoxicity and disruption of actin microfilaments. *Mol Microbiol* 25: 1125–1139.

153. Moussawi, K. A., and B. I. Kazmierczak. 2014. Distinct Contributions of Interleukin-1α (IL-1α) and IL-1β to Innate Immune Recognition of Pseudomonas aeruginosa in the Lung. *Infection and Immunity* .

154. Barry, K. C., M. F. Fontana, J. L. Portman, A. S. Dugan, and R. E. Vance. 2013. IL-1α Signaling Initiates the Inflammatory Response to Virulent Legionella pneumophila In Vivo. *The Journal of Immunology* 190: 6329–6339.

155. Eislmayr, K., A. Bestehorn, L. Morelli, M. Borroni, L. V. Walle, M. Lamkanfi, and P. Kovarik. Nonredundancy of IL-1α and IL-1β is defined by distinct regulation of tissues orchestrating resistance versus tolerance to infection. *Science Advances* 8: eabj7293.

156. Lin, X., T. Twelkmeyer, S.-Y. Wang, R.-N. Xu, F.-S. Wang, C. Zhang, and H. Tang. 2020. An immunopathogenic perspective of interleukin-1 signaling. *Cell Mol Immunol* 17: 892–893.

157. Bersudsky, M., L. Luski, D. Fishman, R. M. White, N. Ziv-Sokolovskaya, S. Dotan, P. Rider, I. Kaplanov, T. Aychek, C. A. Dinarello, R. N. Apte, and E. Voronov. 2014. Non-redundant properties of IL-1α and IL-1β during acute colon inflammation in mice. *Gut* 63: 598–609.

158. Voronov, E., S. Dotan, Y. Krelin, X. Song, M. Elkabets, Y. Carmi, P. Rider, I. Cohen, M. Romzova, I. Kaplanov, and R. Apte. 2013. Unique Versus Redundant Functions of IL-1α and IL-1β in the Tumor Microenvironment. *Frontiers in Immunology* 4.

159. Nazarenko, I., R. Marhaba, E. Reich, E. Voronov, M. Vitacolonna, D. Hildebrand, E. Elter, M. Rajasagi, R. N. Apte, and M. Zöller. 2008. Tumorigenicity of IL-1α- and IL-1β-Deficient Fibrosarcoma Cells. *Neoplasia* 10: 549–562.

160. Benjamin, J. T., D. J. Moore, C. Bennett, R. van der Meer, A. Royce, R. Loveland, and J. L. Wynn. 2018. Cutting Edge: IL-1α and Not IL-1β Drives IL-1R1–Dependent Neonatal Murine Sepsis Lethality. *The Journal of Immunology* 201: 2873–2878.

161. McMahan, C. J., J. L. Slack, B. Mosley, D. Cosman, S. D. Lupton, L. L. Brunton, C. E. Grubin, J. M. Wignall, N. A. Jenkins, and C. I. Brannan. 1991. A novel IL-1 receptor, cloned from B cells by mammalian expression, is expressed in many cell types. *EMBO J* 10: 2821–2832.

162. Peters, V. A., J. J. Joesting, and G. G. Freund. 2013. IL-1 receptor 2 (IL-1R2) and its role in immune regulation. *Brain Behav Immun* 32: 1–8.

163. Bora, N. S., P. Jha, and P. S. Bora. 2008. The role of complement in ocular pathology. *Semin Immunopathol* 30: 85–95.

164. Ricklin, D., E. S. Reis, D. C. Mastellos, P. Gros, and J. D. Lambris. 2016. Complement component C3 - The “Swiss Army Knife” of innate immunity and host defense. *Immunol Rev* 274: 33–58.

165. Bobak, D. A., T. A. Gaither, M. M. Frank, and A. J. Tenner. 1987. Modulation of FcR function by complement: subcomponent C1q enhances the phagocytosis of IgG-opsonized targets by human monocytes and culture-derived macrophages. *J Immunol* 138: 1150–1156.

166. Biswas, R., S. Datta, J. D. Gupta, M. Novotny, J. Tebo, and T. A. Hamilton. 2003. Regulation of chemokine mRNA stability by lipopolysaccharide and IL-10. *J Immunol* 170: 6202–6208.

167. Hamilton, T., X. Li, M. Novotny, P. G. Pavicic, S. Datta, C. Zhao, J. Hartupee, and D. Sun. 2012. Cell type- and stimulus-specific mechanisms for post-transcriptional control of neutrophil chemokine gene expression. *J Leukoc Biol* 91: 377–383.

168. Broz, P., P. Pelegrín, and F. Shao. 2020. The gasdermins, a protein family executing cell death and inflammation. *Nature Reviews Immunology* 20: 143–157.

169. Claude-Taupin, A., B. Bissa, J. Jia, Y. Gu, and V. Deretic. 2018. Role of autophagy in IL-1β export and release from cells. *Semin Cell Dev Biol* 83: 36–41.

170. Kimura, T., J. Jia, S. Kumar, S. W. Choi, Y. Gu, M. Mudd, N. Dupont, S. Jiang, R. Peters, F. Farzam, A. Jain, K. A. Lidke, C. M. Adams, T. Johansen, and V. Deretic. 2017. Dedicated SNAREs and specialized TRIM cargo receptors mediate secretory autophagy. *EMBO J* 36: 42–60.

171. Chen, K. W., C. J. Groß, F. V. Sotomayor, K. J. Stacey, J. Tschopp, M. J. Sweet, and K. Schroder. 2014. The neutrophil NLRC4 inflammasome selectively promotes IL-1β maturation without pyroptosis during acute Salmonella challenge. *Cell Rep* 8: 570–582.

172. Karmakar, M., M. A. Katsnelson, G. R. Dubyak, and E. Pearlman. 2016. Neutrophil P2X7 receptors mediate NLRP3 inflammasome-dependent IL-1β secretion in response to ATP. *Nat Commun* 7: 10555.

173. Kovacs, S. B., C. Oh, V. I. Maltez, B. D. McGlaughon, A. Verma, E. A. Miao, and Y. Aachoui. 2020. Neutrophil Caspase-11 Is Essential to Defend against a Cytosol-Invasive Bacterium. *Cell Reports* 32: 107967.

174. Caffrey-Carr, A. K., C. H. Kowalski, S. R. Beattie, N. A. Blaseg, C. R. Upshaw, A. Thammahong, H. E. Lust, Y.-W. Tang, T. M. Hohl, R. A. Cramer, and J. J. Obar. 2017.

Interleukin 1α Is Critical for Resistance against Highly Virulent Aspergillus fumigatus Isolates. *Infect. Immun.* 85: e00661-17.

175. O'Brien, X. M., and J. S. Reichner. 2016. Neutrophil Integrins and Matrix Ligands and NET Release. *Front. Immunol.* 7.

176. Pegtel, D. M., and S. J. Gould. 2019. Exosomes. *Annu. Rev. Biochem.* 88: 487–514.

177. Raposo, G., and P. D. Stahl. 2019. Extracellular vesicles: a new communication paradigm? *Nat Rev Mol Cell Biol* 20: 509–510.

178. van Niel, G., G. D'Angelo, and G. Raposo. 2018. Shedding light on the cell biology of extracellular vesicles. *Nature Reviews Molecular Cell Biology* 19: 213–228.

179. Fitzgerald, W., M. L. Freeman, M. M. Lederman, E. Vasilieva, R. Romero, and L. Margolis. 2018. A System of Cytokines Encapsulated in ExtraCellular Vesicles. *Sci Rep* 8.

180. Jung, H. H., J.-Y. Kim, J. E. Lim, and Y.-H. Im. 2020. Cytokine profiling in serum-derived exosomes isolated by different methods. *Scientific Reports* 10: 14069.

181. Koritzinsky, E. H., J. M. Street, R. A. Star, and P. S. T. Yuen. 2017. Quantification of Exosomes. *J Cell Physiol* 232: 1587–1590.

182. Shao, H., H. Im, C. M. Castro, X. Breakfield, R. Weissleder, and H. Lee. 2018. New Technologies for Analysis of Extracellular Vesicles | Chemical Reviews. .

183. Essandoh, K., L. Yang, X. Wang, W. Huang, D. Qin, J. Hao, Y. Wang, B. Zingarelli, T. Peng, and G.-C. Fan. 2015. Blockade of Exosome Generation with GW4869 Dampens the Sepsis-Induced Inflammation and Cardiac Dysfunction. *Biochim Biophys Acta* 1852: 2362–2371.

184. Jiang, M., H. Fang, S. Shao, E. Dang, J. Zhang, P. Qiao, A. Yang, and G. Wang. 2019. Keratinocyte exosomes activate neutrophils and enhance skin inflammation in psoriasis. *The FASEB Journal* 33: 13241–13253.

185. Sitrin, R. G., T. M. Sassanella, and H. R. Petty. 2011. An Obligate Role for Membrane-Associated Neutral Sphingomyelinase Activity in Orienting Chemotactic Migration of Human Neutrophils. *Am J Respir Cell Mol Biol* 44: 205–212.

186. O'Brien, X. M., and J. S. Reichner. 2016. Neutrophil Integrins and Matrix Ligands and NET Release. *Front. Immunol.* 7.

187. MacKenzie, A., H. L. Wilson, E. Kiss-Toth, S. K. Dower, R. A. North, and A. Surprenant. 2001. Rapid secretion of interleukin-1beta by microvesicle shedding. *Immunity* 15: 825–835.

188. Yang, S.-T., E. Zaitseva, L. V. Chernomordik, and K. Melikov. 2010. Cell-penetrating peptide induces leaky fusion of liposomes containing late endosome-specific anionic lipid. *Biophys. J.* 99: 2525–2533.

189. Degousee, N., F. Ghomashchi, E. Stefanski, A. Singer, B. P. Smart, N. Borregaard, R. Reithmeier, T. F. Lindsay, C. Lichtenberger, W. Reinisch, G. Lambeau, J. Arm, J. Tischfield, M. H. Gelb, and B. B. Rubin. 2002. Groups IV, V, and X Phospholipases A2s in Human Neutrophils ROLE IN EICOSANOID PRODUCTION AND GRAM-NEGATIVE BACTERIAL PHOSPHOLIPID HYDROLYSIS. *J. Biol. Chem.* 277: 5061–5073.

190. Chan, L., C.-C. Chung, J.-H. Chen, R.-C. Yu, and C.-T. Hong. 2021. Cytokine Profile in Plasma Extracellular Vesicles of Parkinson's Disease and the Association with Cognitive Function. *Cells* 10.

191. Pieters, B. C. H., A. Cappariello, M. H. J. van den Bosch, P. L. E. M. van Lent, A. Teti, and F. A. J. van de Loo. 2019. Macrophage-Derived Extracellular Vesicles as Carriers of Alarmins and Their Potential Involvement in Bone Homeostasis. *Front. Immunol.* 10.

192. Kumar, S., M. G. Frid, H. Zhang, M. Li, S. Riddle, R. D. Brown, S. C. Yadav, M. K. Roy, M. E. Dzieciatkowska, A. D'Alessandro, K. C. Hansen, and K. R. Stenmark. 2021. Complement-containing small extracellular vesicles from adventitial fibroblasts induce proinflammatory and metabolic reprogramming in macrophages. *JCI Insight* 6.

193. Palioura, S., C. R. Henry, G. Amescua, and E. C. Alfonso. 2016. Role of steroids in the treatment of bacterial keratitis. *Clin Ophthalmol* 10: 179–186.

194. Knutsson, K. A., A. Iovieno, S. Matuska, L. Fontana, and P. Rama. 2021. Topical Corticosteroids and Fungal Keratitis: A Review of the Literature and Case Series. *J Clin Med* 10.